

博士論文

HYBRID ENERGY STORAGE SYSTEM FOR ELECTRICAL
VEHICLES USING BATTERY AND SUPER CAPACITOR

(電池とスーパーキャパシタを用いた電気自動車用
ハイブリッドエネルギー貯蔵システムの研究)

HUANG XIAOLIANG

黄 孝亮

**HYBRID ENERGY STORAGE SYSTEM FOR ELECTRICAL VEHICLES
USING BATTERY AND SUPER CAPACITOR**

by

Huang Xiaoliang

A dissertation submitted in partial satisfaction of the
requirements for the degree of
Doctor of Philosophy
in Advanced Energy

in the

Graduate School of Frontier Sciences

of

The University of Tokyo

Supervisor:

Professor Yoichi Hori

June 2014

**HYBRID ENERGY STORAGE SYSTEM FOR ELECTRICAL VEHICLES
USING BATTERY AND SUPER CAPACITOR**

© Copyright 2014
by
Huang Xiaoliang

ACKNOWLEDGMENTS

I would like to express my deep gratitude to my supervisor, Professor Yoichi Hori. There are too many words I would like to write here. His always supporting and encouragement gave me the power to go ahead during the past four years. I think there is no need to explain more about the help from his insight, wisdom and knowledge for my research. There are more others he offered to me, which are invaluable I can see when I look back. He provided strong supporting every time when I was lost, took me to industry, trained me as a team leader... Also the attitude to life and to work, the philosophy of making choices and decisions, the intuition as an engineer, these are much more precious I learnt from him. It is my real fortune to be as his student.

I also would like to thank Professor Hiroshi Fujimoto for his encouragement and guidance during these years. I take him as the excellent model of young age with full of passion, talent, ambition and diligence.

I truly appreciate all the supervising committee members, Professor Hiroyuki Ohsaki, Professor Takafumi Koseki, and Professor Baba Shuntaira. Their guidance and kind comments led me to improve and complete this work.

I would like to thank all of my colleagues in Hori- Fujimoto laboratory. I remind all bits and pieces of supporting from each of you. Specially, I would like to give thanks to Capacitor EV team members, Minaki, Marcus, Hiramatsu, Hata. It is my honor to have worked together with you. For the supporting from Dr. Imura, Wireless Power Transfer team, and Mr. Uchida, I would like to say thanks deeply.

Finally, I would like to thank my father and mother. Their supporting gave me the condition and courage to try what I really like. I will never be able to express my feelings enough. Only I love you!

NOTE: This dissertation was submitted to the supervising committee on June, 2014.

ABSTRACT

This thesis focuses on the application of super capacitor to the energy storage system of electric vehicles (EV). The aim of battery and super capacitor (SC) hybrid energy storage system (HESS) is to realize high power density and high energy density in one system to satisfy the requirement from EV powertrain system. By applying HESS to EV, the battery life can be extended, and acceleration performance can be improved. More importantly, efficiency of energy recovery from regenerative brake can be increased based on the characteristic of SC charging. Several aspects of HESS applied to EV are researched in the thesis.

Firstly, the topologies of the two energy sources, combined with power interfaces, are introduced and analyzed for EV application. Three types of converter topologies, bidirectional half-bridge converter, half-controlled converter, three-level converter, operated as power interface for SC linked to DC bus, are compared and analyzed. The operation conditions and advantages are given for different DC bus voltage classes, considering the converter scales, efficiency and available operation ranges of state of charge of SC banks.

Then, the current control of power interface is proposed for controlling power flow from HESS to the motor system and recovering energy to SC banks in different EV driving stages. The current controller design principles are given, and the dynamic response of the system is analyzed. The control method is applied to the converter systems of the mentioned HESS topologies. A three-layer control system is proposed as the energy management system of HESS after the power interface design. Variable frequency decoupling method is applied as the basic power sharing strategy between battery and super capacitor. The efficiency of the whole energy management strategy is discussed, and the state of charge of SC bank is considered for vehicular system operation.

Lastly a laboratory-scale test platform of HESS with WPT charging, especially

considering the power interface section, is developed. The system design aspect of the electric vehicle prototype powered by HESS is given in detail. The proposed methods are verified through experiments using the designed platform and prototypes.

Furthermore, Wireless Power Transfer (WPT) is a promising solution for charging future electric vehicles. The principle of wireless charging to EV HESS is introduced. The relationship between the capacity of HESS and wireless charging power pattern is analyzed. The HESS capacity design method considering WPT charging is stated in appendix.

CONTENTS

1	Introduction.....	1
1.1	Introduction of hybrid energy storage for EV	1
1.2	Survey of current research trends	3
1.2.1	Review of super capacitor based hybrid electric vehicle prototypes	3
1.2.2	Review of super capacitor application in current vehicle industry	4
1.2.3	Review of power interface for super capacitor energy bank	7
1.3	Motivation and dissertation outline	8
2	Modeling and Topologies of HESS for Electric Vehicles	12
2.1	EV energy problems and new energy devices.....	12
2.2	Modeling and characteristics of super capacitor and battery as energy units	13
2.2.1	Modeling of super capacitor bank	15
2.2.2	Modeling of EV battery	17
2.3	HESS topology analysis for EV application	18
2.4	Capacity design of HESS for EV power train.....	26
2.5	Summary.....	27
3	Analysis and Control of Power Interface for Super Capacitor and Battery	29
3.1	Introduction of converters as the power interface of EV HESS	29
3.2	The optimized topology of converter for EV HESS.....	32
3.3	Converter control of HESS for EV.....	36
3.3.1	Basic control method for bidirectional dc-dc converter.....	36
3.3.2	Current control method of half-controlled converter	39
3.3.3	Current control method of three-level converter	43
3.4	Experimental verification of HC converter and analysis	48
3.5	Summary.....	53
4	Power Control and Energy Management of HESS	54
4.1	Three-layer energy management system for EV HESS.....	54

4.2 Power sharing control strategy with variable-frequency filter	56
4.3 Super capacitor state of charge control	61
4.4 Experimental setup and analysis	62
4.5 Summary	67
5 Design of EV Prototype with HESS and Onboard Experiment Results	69
5.1 Introduction of experimental platform	69
5.2 Prototype design and experiments of converters for HESS	71
6 Conclusions and Future Works	78
Appendix Advanced Charging System for HESS using Wireless Power Transfer	80
A.1 Requirement analysis HESS charging using WPT	80
A.2 HESS Capacity design method with WPT charging	81
Bibliography	86
Publications	92

LIST OF FIGURES

Figure 1.1 EV prototype powered by pure super capacitor modules of Hori Lab.	2
Figure 1.2 Structure of EV with ZEBRA battery and super capacitor hybrid system	3
Figure 1.3 Prototypes of super capacitor based hybrid electric vehicles	4
Figure 1.4 System structure of Mazda i-ELOOP system	5
Figure 1.5 Honda Fit3 start-stop system configuration	6
Figure 1.6 Toyota TS040 HYBRID with super capacitor models	6
Figure 1.7 HESS for EV COMS	8
Figure 1.8 Proposed EV frame of HESS with WPT charger	9
Figure 1.9 Outline of this thesis	11
Figure 2.1 The representative model of super capacitor	14
Figure 2.2 SC production trend, provide by Nippon Chemi-Con	15
Figure 2.3 Super capacitor modules	15
Figure 2.4 Simple dynamic model of SC bank	16
Figure 2.5 Nonlinear and linear model of SC bank	17
Figure 2.6 Simple dynamic model of battery	18
Figure 2.7 Serial structure	19
Figure 2.8 Passive cascaded structure	19
Figure 2.9 Battery active cascaded structure	20
Figure 2.10 SC active cascaded structure	21
Figure 2.11 Bi-active cascaded structure	21
Figure 2.12 Parallel active structure	22
Figure 2.13 Direct parallel hybrid energy system	24
Figure 2.14 Two-converter parallel hybrid energy system	24
Figure 2.15 One-converter parallel hybrid energy system	24
Figure 3.1 Power flow of bidirectional converter	30
Figure 3.2 Relationship between bidirectional and Buck/Boost converter	30
Figure 3.3 Three-phase interleaved converter for battery power interphase	31

Figure 3.4 Converter topologies for SC interface	33
Figure 3.5 HC's voltage balance gets disturbed	34
Figure 3.6 SC banks voltage in HC topology without balance.....	35
Figure 3.7 Balance circuits for HC converter	36
Figure 3.8 Modeling for bidirectional converter with two-side voltage sources	37
Figure 3.9 Operation modes of bidirectional converter	37
Figure 3.10 Q1 on stage of bidirectional converter	38
Figure 3.11 Q1 off stage of bidirectional converter	38
Figure 3.12 The basic bidirectional structure in half-bridge converter	40
Figure 3.13 The basic bidirectional structure in half-controlled converter	40
Figure 3.14 Current control block for HC converter	41
Figure 3.15 Current control block for HC converter power sharing strategy	42
Figure 3.16 Balance current control block for HC converter	42
Figure 3.17 Framework of current control algorithm with HC converter	43
Figure 3.18 PWM signal principle of TL converter	44
Figure 3.19 Different stages in one action period	45
Figure 3.20 Actions of Three-level converter prototype	47
Figure 3.21 Large-signal average model of three-level converter	47
Figure 3.22 Current control of three-level converter	48
Figure 3.23 Prototype of half-controlled converter	49
Figure 3.24 Inertial torque generator	50
Figure 3.25 Structure of inertial control	50
Figure 3.26 HESS power sharing experiment	51
Figure 3.27 Experiments of recovering energy to HESS	51
Figure 3.28 Speed control, and load torque control with increased inertia	52
Figure 3.29 No regenerative current	52
Figure 3.30 Max regenerative current 1.4 A	52
Figure 4.1 HESS management structure	54
Figure 4.2 Control strategy block diagram	57
Figure 4.3 Power filter strategy block	59

Figure 4.4 Power filter strategy description	59
Figure 4.5 NEDC speed profiles from reference	60
Figure 4.6 Frequency-varying filter for power sharing	60
Figure 4.7 SC bank state of charge control	61
Figure 4.8 Reduced scale test platform for hybrid energy system	65
Figure 4.9 Power sharing and regenerative brake in simulated ECE15 driving cycle	66
Figure 4.10 Test of HESS with variable frequency decoupling strategy	67
Figure 5.1 Sections of hybrid energy EV COMS	69
Figure 5.2 System structure of our EV with HESS	71
Figure 5.3 Arranged hybrid energy systems for EV prototype	72
Figure 5.4 Converter structure setup to vehicle prototype	73
Figure 5.5 ADC sampling period and PWM period in converter controller DSP	73
Figure 5.6 Simple flow chart of DSP program with high level controller communication ...	74
Figure 5.7 Experiment result in simulated urban drive cycle	75
Figure 5.8 Experiment results in simulated highway driving cycle	76
Figure 5.9 Relationship between decoupling frequency and output energy proportion from batter and SC	77
Figure A.1 Characteristics of battery, SC, and WPT as EV energy sources	80
Figure A.2 Conception of Choco-Choco charging to EV	81
Figure A.3 WPT charging system with converter interface for HESS	81
Figure A.4 EV prototype with HESS and WPT charger	82
Figure A.5 Energy system topology of Hybrid CMOS with WPT charger	82
Figure A.6 WPT charging mode for HESS in one driving cycle	83
Figure A.7 Optimization constraints for HESS charging using WPT	84
Figure A.8 Example of HESS capacity design with WPT charging	85

LIST OF TABLES

Table 2.1 Performance comparison of storage devices for EV and HEV	13
Table 2.2 Comparison among different HESS structures	23
Table 3.1 Comparison between different converters for SC	33
Table 3.2 Parameters of converter and HESS platform	49
Table 4.1 Drive and load motor specification	62
Table 4.2 Half-controlled converter specification	64
Table 5.1 Main parameters of Hybrid EV	70
Table 5.2 Analysis of Energy sharing and decoupling frequency.....	77
Table A.1 Performance parameters for EV HESS	83
Table A.2 Parameters for EV HESS in driving test	84
Table A.3 Parameters for WPT charging system	84

1 Introduction

1.1 Introduction of hybrid energy storage for EV

In recent years Electric Vehicles (EV) appear as one solution for the world's environmental and economic problems, as renewable energy can be used to charge the vehicle. However, other issues of EV reduce the attractiveness to consumers.

The energy supply, for example, is one of the major problems of EV because it does not achieve the same autonomy comparing with the internal combustion engine (ICE) vehicles. Energy Storage Systems (ESS) have been a major research area in electric, hybrid electric and plug-in Hybrid Electrical Vehicles (EVs, HEVs, and PHEVs) since 1990s [1, 2].

Among all the energy storage devices, battery is one of the most widely used. However, using battery as the sole energy storage system has several disadvantages, such as limited energy density, short battery lifetime, and low effectiveness when recovering regenerative energy. In order to solve the problems above, several aspects which can provide solutions of performance improvement for batteries have been suggested, including fly-wheels, superconducting magnetic energy storage, and others. One of the popular methods is adding an auxiliary energy storage system, as the battery works as the main energy system. They compose the Hybrid Energy Storage System (HESS). Hybrid energy storage system, which is based on the combination with more than two different energy sources, includes batteries, fuel cells, and super capacitors, interfaced by DC/DC power converters, in order to achieve better performance of the storage system. Power interface between the battery and super capacitor plays a key role in the energy efficiency and dynamic performance.

On the other hand, the future electric vehicle will be driven by motor, powered by capacitor, and charged by wireless transfer technology [3]. New approaches for energy storage and transformation system are needed for the future EV systems. Hori laboratory has developed an EV that is able to run for 20 minutes with mere 30 seconds charging. This EV is powered solely by Super Capacitors (SC) [4, 5]. The inverter system and powertrain system are designed especially for the huge voltage range of energy bank without DC/DC converter interface [4]. Although a small size

EV powered by SC is realizable, a commercial EV that is fully powered by SC is difficult to realize, due to low energy density and high price of the SC bank.

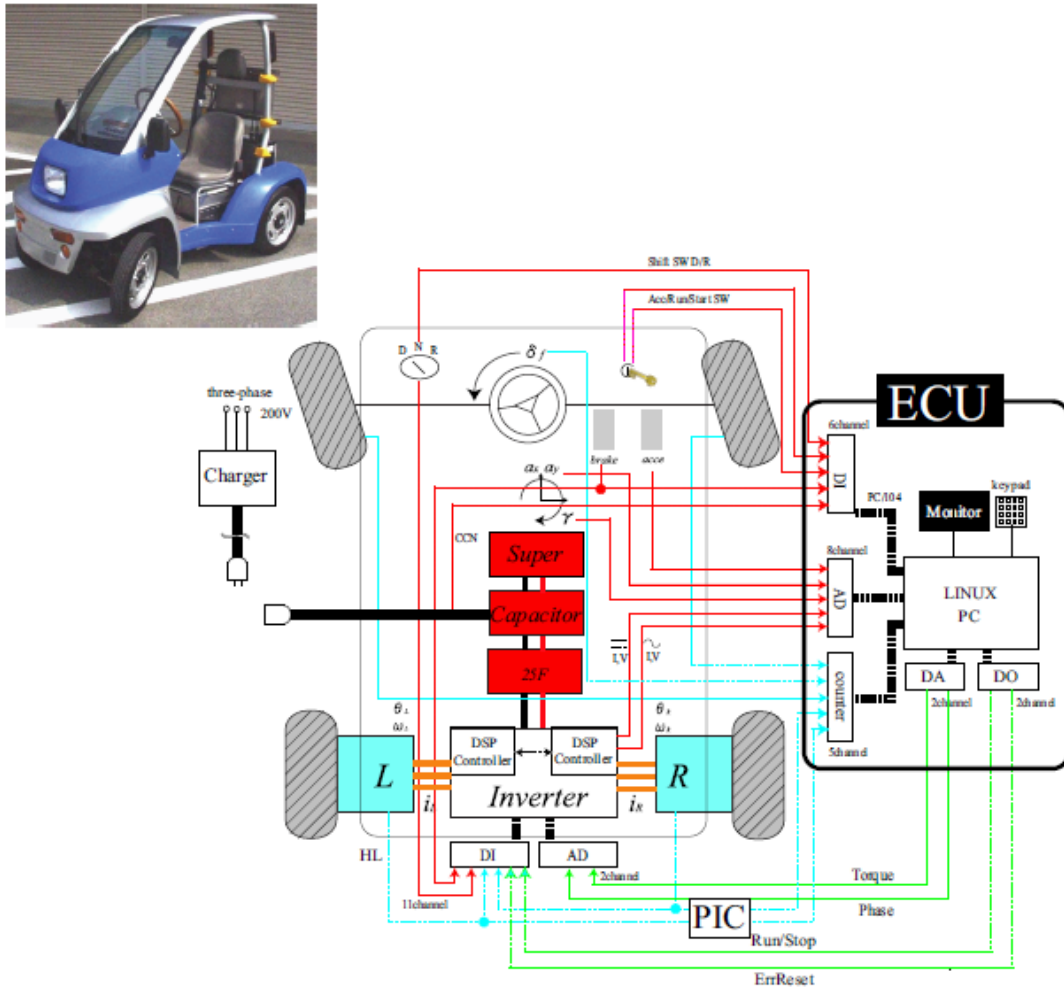


Figure 1.1 EV prototype powered by pure super capacitor modules of Hori Lab. [4]

The aim of battery and super capacitor hybrid system is to realize high power density and high energy density in one system to satisfy the requirement of EV powertrain system. Based on the combination of two energy devices, the aim of hybrid system, is to realize a high-efficacy, high-performance, controllable, easy charging ESS for future EV application. By applying HESS to EV, the battery life can be extended, and acceleration performance can be improved. More importantly, efficiency of energy recovery from regenerative brake can be increased based on the characteristics of SC charging.

1.2 Survey of current research trends

Many researches on hybrid energy storage system have been published in past several years, following the improvements of new energy storage devices, super capacitor, fuel cell, high performance battery, and the requirements from industrials. Considering the application of HESS to vehicles, three main aspects were explored by researchers:

- Topologies of multi-sources and power interface combination;
- Power sharing and energy management strategies for electric vehicle powertrain;
- Converter technology for high power application.

1.2.1 Review of super capacitor based hybrid electric vehicle prototypes

Several hybrid energy system experiment platform of laboratory-scale was setup, and electric vehicles prototypes powered by hybrid energy system are setup. Figure 1 shows the first electric vehicle prototype powered by battery and super capacitor energy system [6, 7, 8]. The super capacitor and ZEBRA battery combination is realized for electric vehicle driving. Two energy management strategies are applied, the first strategy is based on heuristic, and the second is based on an optimization model with neural networks. The conclusion is that the ZEBRA battery life is extended by 50% using the energy management strategy. One of the issues of this system is the bidirectional boost converter, functioning as the interface of super capacitor bank needs specially designed large inductor and heat sink system.



Figure 1.2 Structure of EV with ZEBRA battery and super capacitor hybrid system [6, 7, 8]

The EV hybrid energy system with battery, fuel cell, and super capacitor is

demonstrated in [9]. A test bed and hybrid energy simulation system is also setup in [9]. The practical control structure and fuzzy logic controller is proposed for arranging the State of Charge (SoC) of SC. Many driving cycle simulation based analysis is given for evaluate the efficiency of the whole system. This whole project still have no special consideration of DC bus voltage stability and response speed of power interface from the viewpoint of power electronics application.

More hybrid energy systems are applied in different electric vehicle systems, including electric bicycle, educational mobile system, power assistant elevator, racing vehicle [9, 10, 11, 12, 13]. Meanwhile, many reduced scale HESS experiment platform is set up, based on different research objectives [14, 15, 16, 17].

Among these research, topologies and system structures are widely discussed for vehicle operation. Advanced system evaluation, control and optimization methods are applied to energy management, such as model predictive control [14], flatness control [15], slide mode control [16], adaptive control [17], and strategies based on vehicular information fusions [8]. The final aim is to generate the optimized principle for energy application and s improving system efficiency.



Figure 1.3 Prototypes of super capacitor based hybrid electric vehicles [9, 10, 11, 12, 13]

1.2.2 Review of super capacitor application in current vehicle industry

With the development of material for super capacitor, higher energy density

capacitor modules can be realized in the coming decades. However, recent super capacitor energy system is already used by car maker for low voltage vehicular energy system by recovering energy from regenerative braking, and improving the efficiency of starting stage.

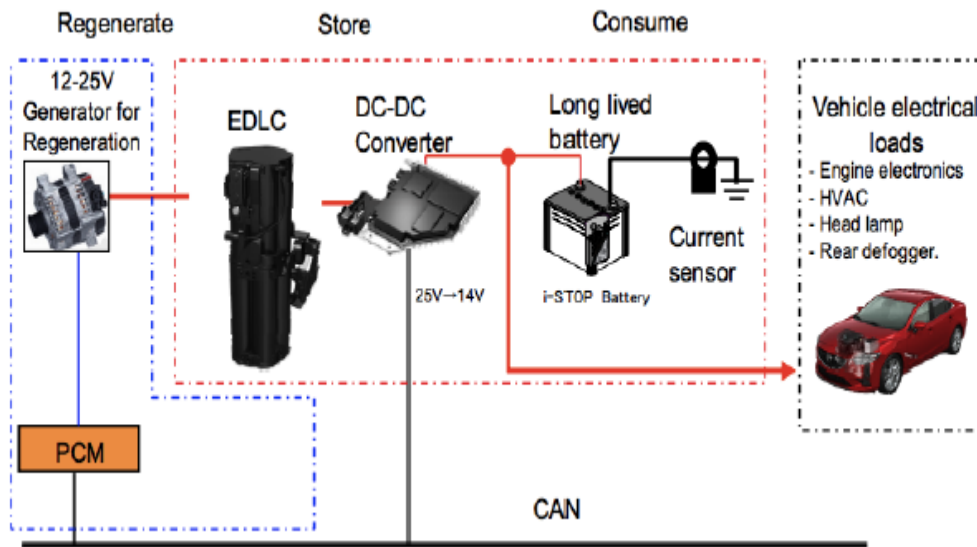


Figure 1.4 System structure of Mazda i-ELOOP system [18]

Mazda i-ELOOP system is the first super capacitor based micro hybrid energy system in the world for vehicle application [18]. Super capacitor, provided by Nippon Chemi-Con Co, Ltd.[19], and low cost lead acid battery is a good option for the balance of cost and system life. However, the energy stored in super capacitor is applied for low power vehicle electrical load, such as head lamps and engine electronics. The DC bus voltage is less than 24V, the system is therefore easy to realize, considering high frequency low power class DC/DC converter and special designed compact super capacitor modules. The efficiency of the electric system can be improved around 10%. The output efficiency of main powertrain system, however, cannot be improved. The next generation of i-ELOOP system will be considered as power assistance for main power system, and the SoC usability will be improved based on new converter topology.

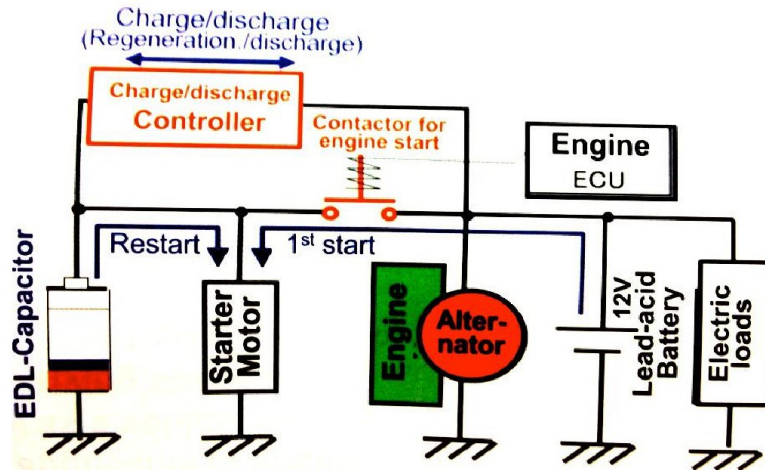


Figure 1.5 Honda Fit3 start-stop system configuration [20]



Figure 1.6 Toyota TS040 HYBRID with super capacitor models [21]

Super capacitor and lead acid battery system is also applied to Honda Fit3 powertrain system [20]. Different from i-ELOOP system, a starter motor is used to improve the performance of the start and stop stage of engine. The system DC bus voltage is 12V, which does not belong to strong hybrid system that is directly linked to high voltage DC bus for the main power system like Toyota Prius. High power hybrid system equipped by super capacitor modules, named TS040 HYBRID was developed by Toyota for FIA world endurance championship [21]. Compact super capacitor modules, provided by Nisshimbo, are used for recovering energy directly.

In summary, super capacitor application to hybrid system for vehicle application is increasing in recent years. If charging strategies can be improved in the future transportation system, it will be a promising solution for future EV energy system and

will change the energy storage structure of EV system. For example, the super capacitor bus is now implemented in large scale in public transportation of Shanghai.

1.2.3 Review of power interface for super capacitor energy bank

From university laboratory level research to vehicle industrial application, there are many of valuable and interesting points need to be considered. The power interface of super capacitor linked to energy system for EV is a key section for hybrid system.

Huge temporary power will flow into and out from super capacitor bank during operation. Due to the limitation of the power devices, the system capacity and cost for vehicular application, the power interface should be considered from devices selection, topology optimization and control algorithms aspects.

The high power class interface should be realized for super capacitor application in vehicular system. Considering optimization of different aspects, such as cost, control ability and stability, many researches have been proposed. The multi-phase interleaved converters are considered for hung current holding ability [22, 23]. Multi-level topology is suitable for high voltage application without changing chopper devices [24, 25]. Also zero current/voltage soft switch and discontinues mode control is applied for decreasing switch components loss [26, 27, 28]. Advanced converter control method and response analysis method is proposed for high performance application of HESS [27, 28, 29]. On the other hand, from the viewpoint of control of EV, PM motor's quick speed response is rarely discussed. Although there are researches on the DC bus stability for constant power load [30, 31], especially for the EV motor powertrain with different drive considerations, the cooperated control strategy with EV motor inverter and DC bus voltage boost system is absolutely needed for future high power vehicles.

In [32, 33], the approach of converter for SC bank, half-controlled (HC) converter is applied to HV HESS for super capacitor application, which is proposed and researched in our laboratory. The idea is based on the structure of the super capacitor modules. The objective is to decrease the converter size, with the cost of letting parts of capacitor modules under passive condition [34]. We will try to improve the control principle, apply HC converter topologies to electric vehicle prototypes. This aspect will be discussed in detail in Chapter 3.

The recent trends of the super capacitor application in hybrid energy storage system in vehicle systems are summarized below:

- Hybrid powertrain for EV is widely researched in recent 5-6 years;
- Super capacitor hybrid with fuel cell is also accepted as a promising solution;
- Multi-layer control strategy is necessary for multi-source hybrid powertrain;
- Advanced control and optimization methods to be applied in this research topic has just begun;
- High performance converter is needed based on the characteristics of energy source is needed.

1.3 Motivation and dissertation outline

This thesis focuses on the application of super capacitor to the energy storage system to electric vehicles (EV). The aim of battery and super capacitor (SC) hybrid energy storage system (HESS) is to realize high power density and high energy density in one system to satisfy the requirement from EV powertrain system. By applying HESS to EV, the battery life can be extended, and acceleration performance can be improved. Efficiency of energy recovery from regenerative brake can be increased. Several aspects of HESS applied to EV are researched in this thesis.

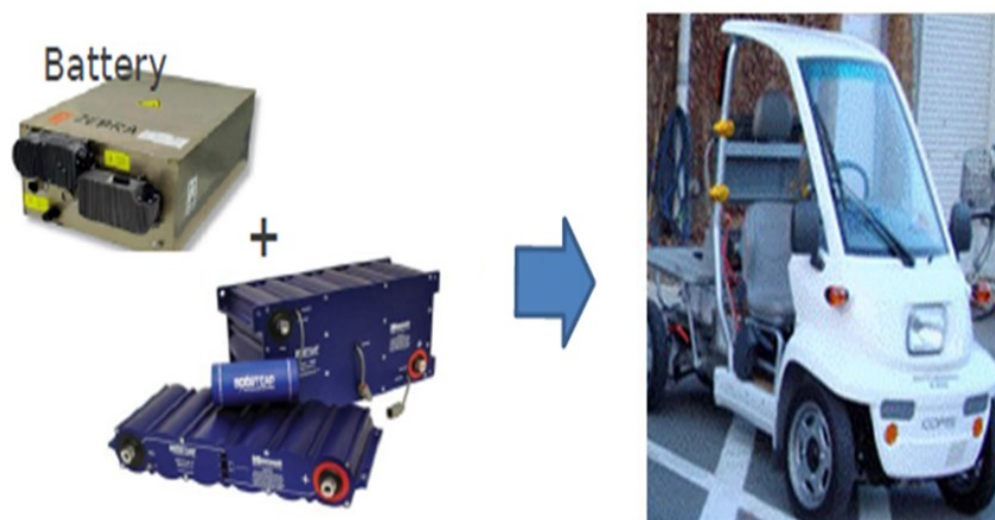


Figure 1.7 HESS for EV COMS

In order to realize high efficiency and high performance super capacitor hybrid energy system for EV application, considering also the effort of new charging strategy, using wireless power transfer, is one motivation of this thesis. The structure of the electric vehicle prototype is shown in Figure 1.8. The vehicle prototype is based on

COMS manufactured by Toyota Auto body Co., Ltd. The hybrid energy system is equipped together with in-wheel motor driving system. Also wireless charging system is considered as a new approach for hybrid energy charging.

The power interface for super capacitor, power flow control method, energy management strategy, and the capacity design principle is discussed. The possibility and principle of HESS charging with wireless power transfer is also analyzed and proved discussed reduced-scale demonstration system. Motor, wireless power transfer technology, capacitor, will play key roles in the electric vehicle development in coming decades [3]. This thesis shows an exploration for this idea application, from the aspect of energy utilization of EV system.

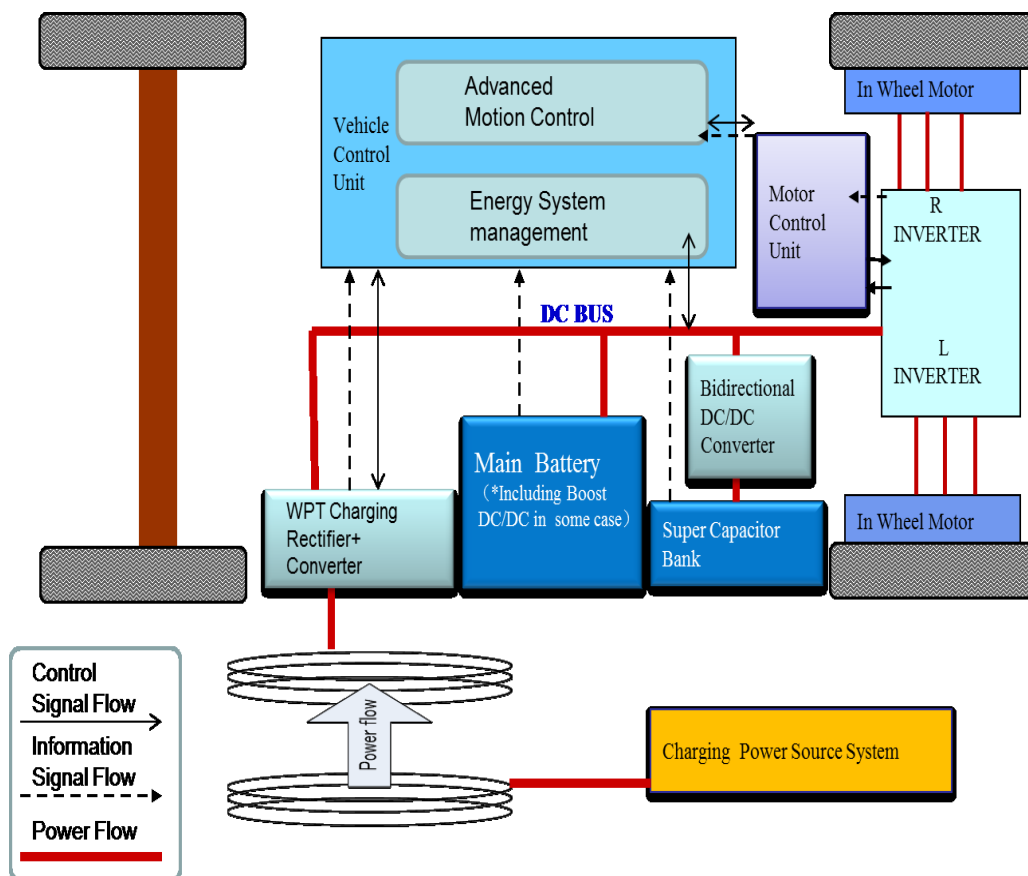


Figure 1.8 Proposed EV frame of HESS with WPT charger

In Chapter 1 [Introduction], the framework of thesis is introduced. The background and the motivation of this research are analyzed. The super capacitor based hybrid energy storage system, proposed from universities, and developed by industrial is surveyed and analyzed. The issues and the objective of this research are introduced briefly.

In Chapter 2 [Modeling and Topologies of HESS for Electric Vehicles], the topologies of the two energy sources combination with power interfaces are introduced and analyzed for EV application.

In Chapter 3 [Analysis and Control of Power Interface for Super Capacitor and Battery], three types of converter topologies, bidirectional half-bridge converter, half-controlled converter, three-level converter, operated as power interface for SC linked to DC bus, are compared and analyzed. The operation conditions and topology advantages are given for different dc bus voltage classes, considering the converter scales, efficiency and available operation ranges of state of charge of SC banks.

In Chapter 4 [Power Control and Energy Management of HESS], a three-layer control system is proposed as the energy management system of HESS after the power interface design. Variable frequency decoupling method is applied as the basic power sharing strategy between battery and super capacitor. The efficiency of the whole energy management strategy is discussed, and the state of charge of SC bank is considered for vehicular system operation.

In Chapter 5 [Design of EV Prototype with HESS and Onboard Experiment Results], a laboratory-scale test platform of HESS with WPT charging, especially considering the power interface section, is developed. The system design of the electric vehicle prototype powered by HESS is given in detail. All the proposed methods are verified and analyzed by the experiment results using the designed platform and prototypes.

In Chapter 6 [Conclusions and Future Works], the conclusion and future works are given.

In Appendix [Advanced Charging System for HESS using Wireless Power Transfer], the principle of wireless charging to HESS is analyzed. The relationship between the optimal size of HESS and wireless charging power is stated. The control method for WPT charging to HESS, considering charging efficiency and power demand, will be considered for the next step.

The framework and the relations among chapters are explained in Figure 1.9. The system design detail, and control system program developed for this research is also given in the appendix.

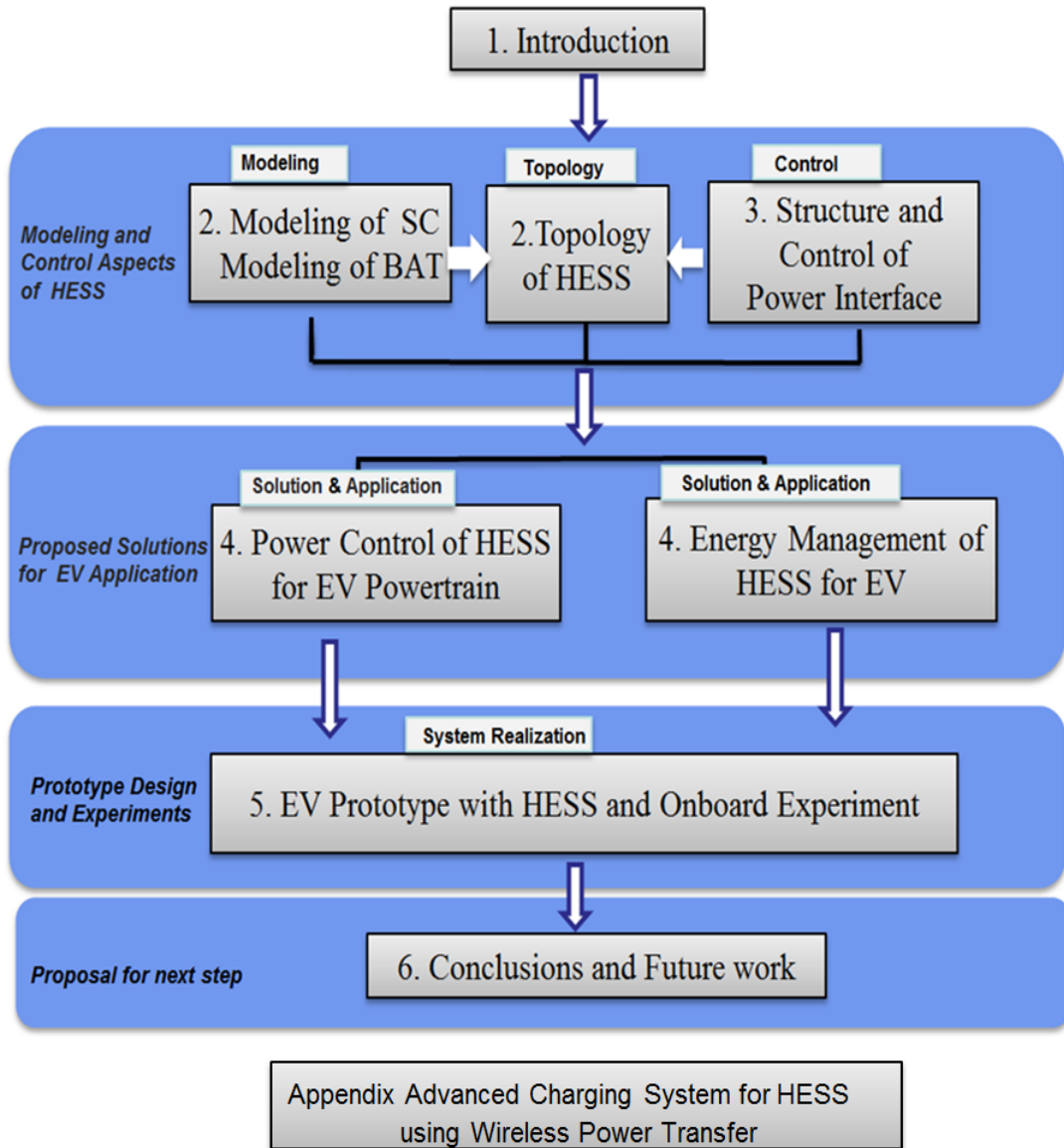


Figure 1.9 Outline of this thesis

2 Modeling and Topologies of HESS for Electric Vehicles

2.1 EV energy problems and new energy devices

Electric vehicles powered by battery still have not achieved the cruising range that is comparable to gas-powered conventional vehicles. This problem, caused by the low-energy density and specific energy in most batteries in comparison to ICE vehicles, can be solved in hybrid vehicles by combining high power density energy source with the high power density one. High ratios with peak to average power usually happen in vehicle driving cycles. Therefore limiting the load dynamic effects can improve the battery performances and extend its life. From this point of view, many applications such as vehicular, batteries should not be used alone. Other suitable sources should provide the fast power demand, allowing regenerative energy recovery.

For fast power demands, storage devices as super capacitors may be the best choice. In order to achieve this kind of hybridization, the following requirements should be considered:

- Fulfill load performance ,
- Extend battery life time,
- Maximize the global energy efficiency.

In order to achieve these goals, many hybrid energy system configurations have been studied and documented. Hybrid power sources topologies and proper related energy management controllers are designed. Fuel cells, capacitor modules, batteries are combined to this system. For electric vehicle application, there are also some extra requirements:

- Simple energy management,
- Less component constraints,
- Good reliability,
- Acceptable cost.

Table 2.1 Performance comparison of storage devices for EV and HEV [35]

	Capasitor		Lithium-ion batteries		Nickel-metal hydride bateries		Lead-acid storage batteries	
type	Electric double layer		HEV application		HEV application		Vent type	
Energy density(Wh/kg)	x	5~10	O	100~200	O	50~80	O	30~40
Voltage(V)	Δ	2.5	O	3~3.7	Δ	1.2	Δ	2
Maximum Output(W/kg)	O	10,000>	O	4,000	Δ	1,000~2,000	x	200
Resistance(mΩ)	O	1	Δ	2.5	Δ	3	Δ	5
Operating temperature(°C)	O	-30~70	Δ	-30~60	Δ	-30~60	O	-30~80
Cycle life (soc 0 ⇄ 100% @25°C)	O	1,000,000>	Δ	3,000>	Δ	1,000>	x	300>
Safety	O	—	Δ	—	O	—	O	—
Environmental load	O	—	x	Li,Co,Ni,Mn	x	Ni	x	Pb

Table 2.1 shows the performance of super capacitor modules, types of batteries, for the electric vehicle application.

2.2 Modeling and characteristics of super capacitor and battery as energy units

The basic principles of SC rely on the EDL effect, which was firstly described by Helmholtz in 1861 [36]. The EDL (Electric Double Layer) is formed when a charged solid gets in contact with an electrolyte, creating two layers of opposite charges. In order to increase the capacitance of EDL capacitor, carbon based materials are commonly used. Those layers are formed in order to neutralize the charged surface, but it also causes a very small potential between the two layers [36]. The potential is proportional to the charged surface area. The carbon layers can highly increase the surface, so they increase its capacitance, called by super or ultra capacitor.

Following this concept, the SC is composed of two carbon layers, immersed in an electrolyte solution and separated by a thin layer. The representative model is shown in Figure 2.1[4].

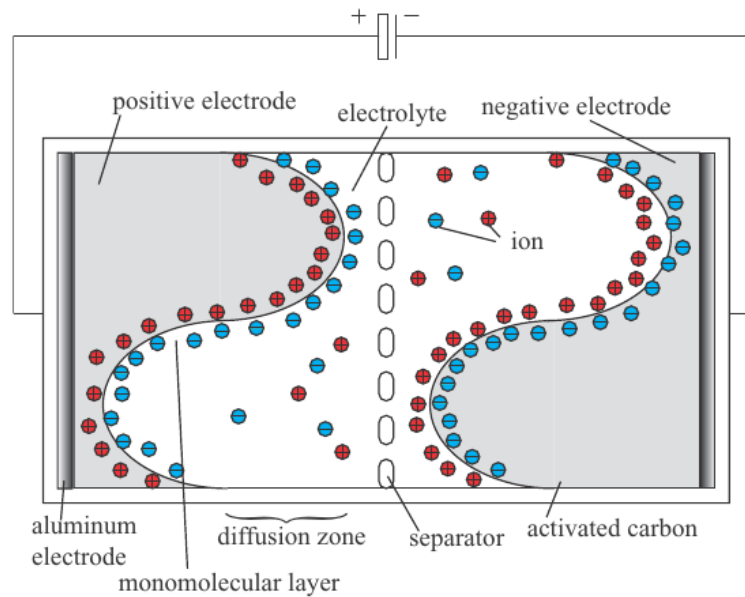


Figure 2.1 The representative model of super capacitor [4]

The main difference between a normal electrolytic capacitor and the SC other than the much higher capacitance is that the SC cells have a very small equivalent serial resistance (ESR). While the electrolytic capacitor can deal with very high voltages and usual SC cell voltage is less than 3V; and therefore must be connected in series to achieve higher voltage rate [37, 38].

As presented, the SC's principal advantages are the following:

- High power density;
- Charged and discharged nearly unlimited times;
- Rapidly charged and discharged;
- Energy level can be easily estimated;
- No danger of overcharge;
- No heavy metal for its manufacturing.

However, SC's also present some disadvantages:

- Low energy density;
- Low voltage range per cell;
- High self-discharge rate.

Figure 2.2 shows the production trend of the super capacitor modules, it is clearly shown that the next generation will be at the same class of energy density, comparing with batteries as the main power supply. So it is available for high voltage and high energy density energy bank with super capacitor modules to power the electric motor system in the coming decades.

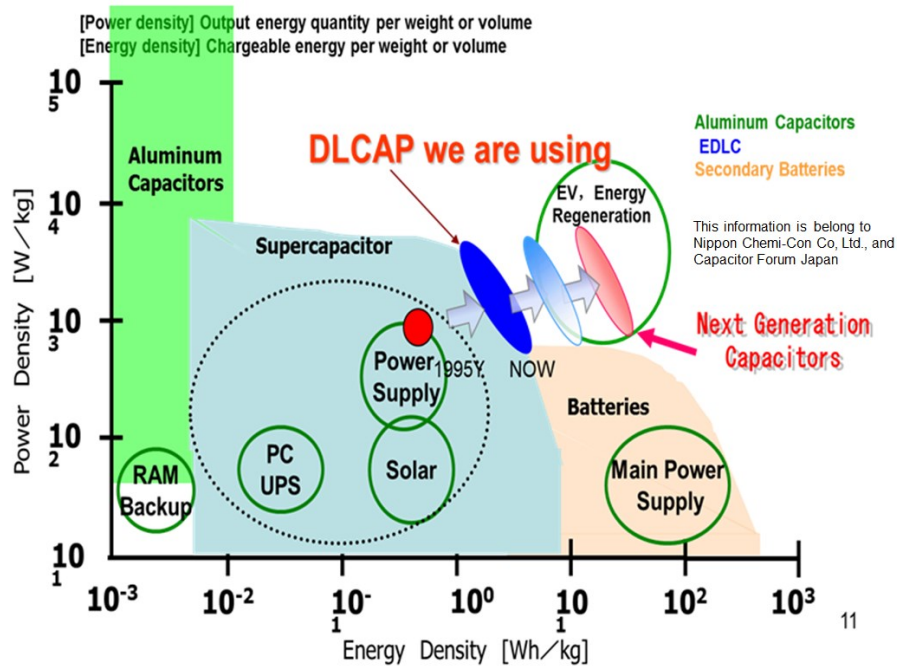


Figure 2.2 SC production trend, provide by Nippon Chemi-Con [39]

2.2.1 Modeling of super capacitor bank

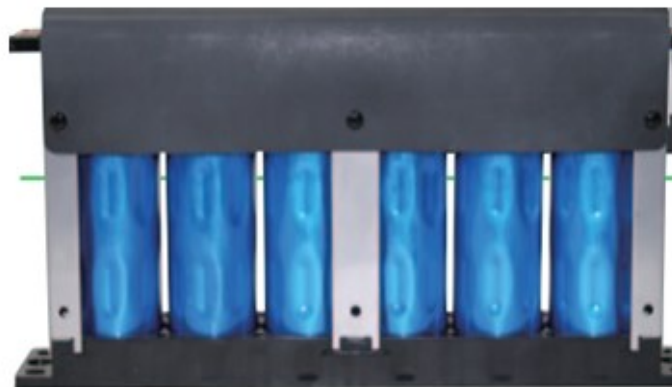


Figure 2.3 Super capacitor modules [39]

There are many mathematics modeling methods for super capacitor [40]. Here, we would like to confirm the electrical performance of SC. So power charging /discharging modeling is necessary for super capacitor application.

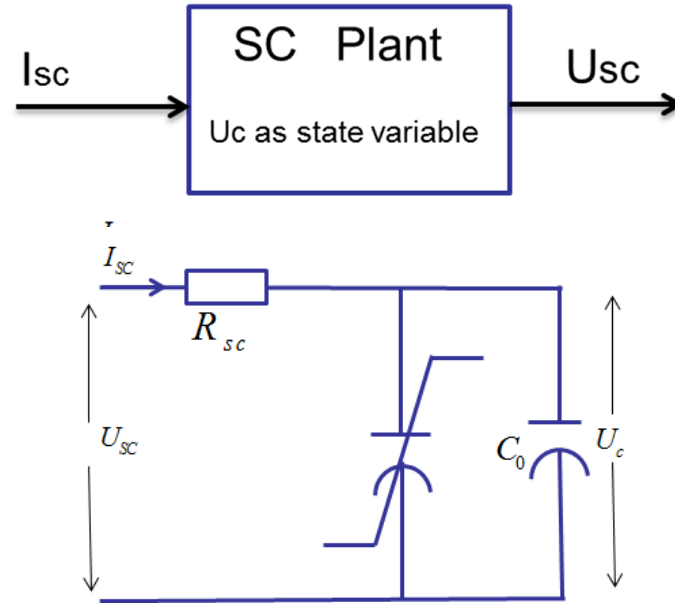


Figure 2.4 Simple dynamic model of SC bank [40]

Figure 2.4 is a simple RC model of SC; there are also the nonlinear sections because the total capacitance of SC is of the voltage controlled capacitance [40].

$$C_{sc} = C_0 + k_c \cdot U_c \quad (2.1)$$

C_0 is the initial capacitance that represents the electrostatic capacitance of the capacitor. k_c is a coefficient that represents effects of the diffused layer of the SC. The electrical performance of SC bank is shown in Equation 2.2. It shows the relationship between the input I_{sc} and output U_{sc} .

$$I_{sc} = (C_0 + 2k_c U_c) \frac{dU_c}{dt} \quad (2.2)$$

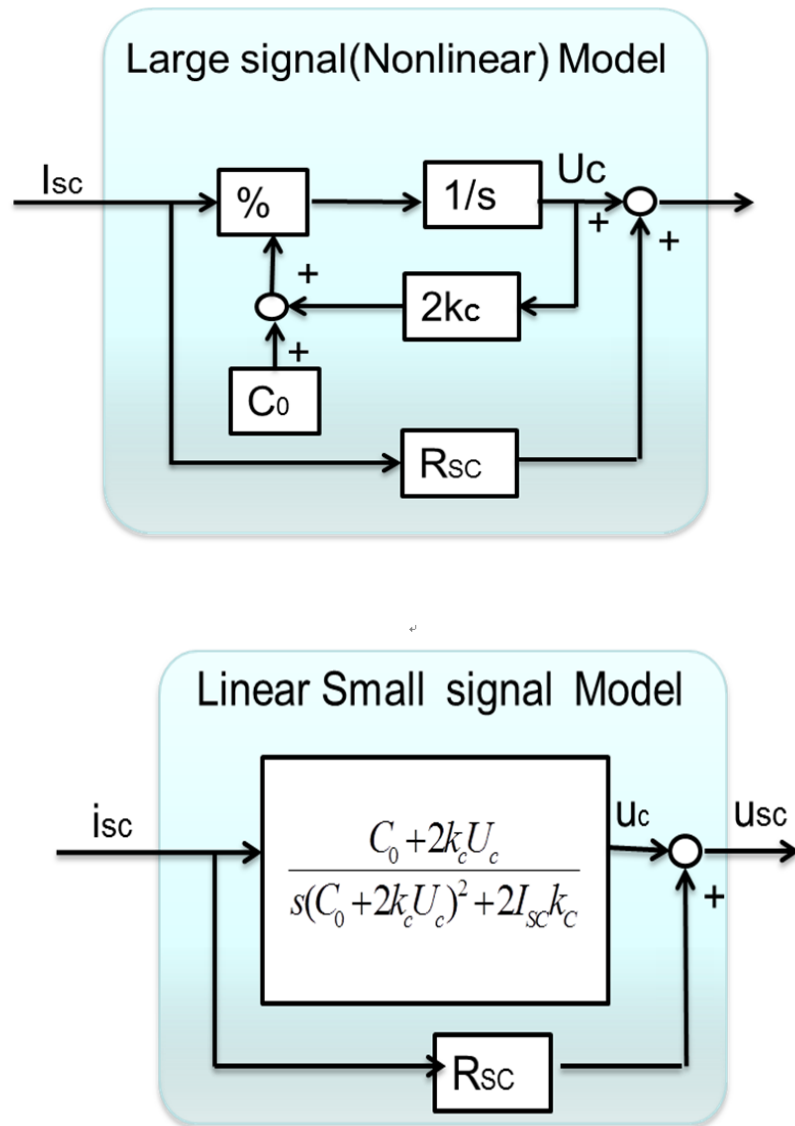


Figure 2.5 Nonlinear and linear model of SC bank [38]

2.2.2 Modeling of EV battery

The battery modeling in Figure 2.6 is a constant voltage source in series with battery internal resistant. The battery is used as the DC bus voltage holder and parallel linked by DC bus filter in our system.

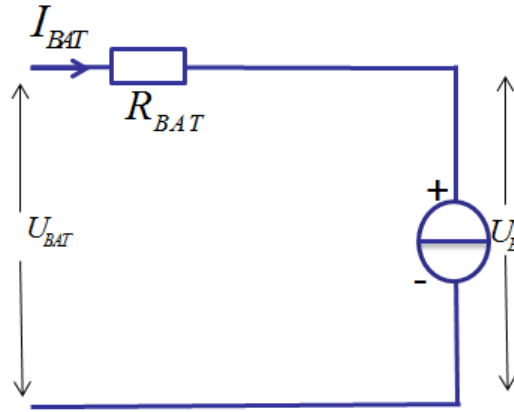


Figure 2.6 Simple dynamic model of battery

$$U_{BAT} = U_B + I_{BAT}R_{BAT} \quad (2.3)$$

As noticed, SC has the internal resistances lower than that of batteries, and this allows the SC to supply very large currents to the load. There is no chemical reaction involved in the SC's operation, and as a result, the SC can provide high torque acceleration with quick response. Despite of those advantages, creating a commercial EV fully powered by SC is not yet possible due to the very low energy density. Regarding this fact, it is reasonable to think that a system which could allow EV to reach further distances is needed. A good solution for such problem is the combination of SC's and batteries.

The main qualities of each battery type could be performed in a hybrid based system by using bidirectional DC/DC converter. Assuring controllable power flow, it provides widely variable input voltage as well as a virtually constant voltage output. Therefore, an efficient and costless topology for the DC/DC converter could provide means to enhance the HESS, and consequently, increase EV's autonomy.

2.3 HESS topology analysis for EV application

One important aspect about the HESS refers to its topology, which can be chosen among several types. There are six basic topological structures used for the SC-Battery Hybrid System. Mostly all the current researches upon DC/DC converters, for the HESS, are implementing different modification on those six topologies.

The SC voltage can be independent from the voltage of the DC link, and it can also achieve a wider range. In addition, the battery is connected directly to the DC link.

Consequently, the DC link voltage can be maintained relatively constant.

A. Serial structure

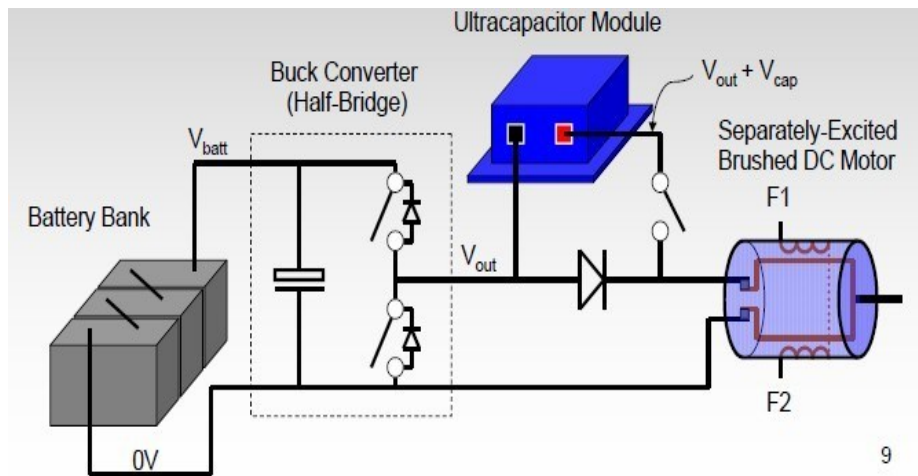


Figure 2.7 Serial structure [13]

The battery and SC is linked in a simple serial structure, but the SC is not able to absorb the peak of power by itself as shown in Figure 2.7. There is no power transfer path between battery and SC, so the prototype with this structure just for educational demonstration [13].

B. Passive cascaded structure

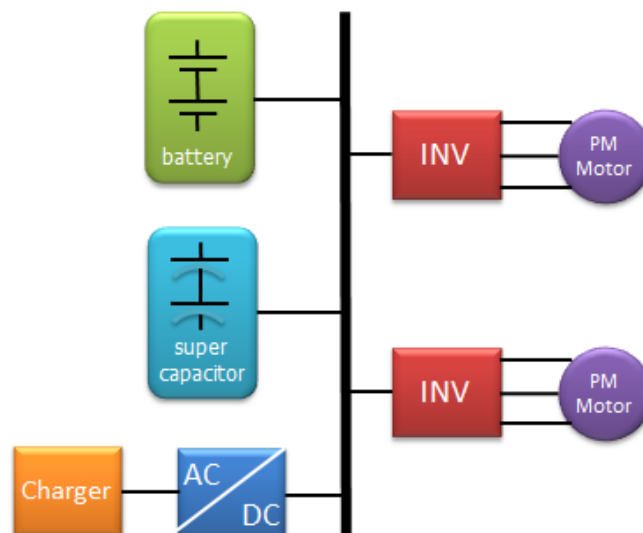


Figure 2.8 Passive cascaded structure

The two electric sources, batteries and SC, are directly connected in parallel without converter interface as shown in Figure 2.8. This configuration is also simple because DC/DC converter is not needed. However, this coupling needs the same voltage for both energy sources, and the power flow is not able to control or arrangement. The power or current output distribution needs to be fixed by the internal resistors and voltage.

In this topology, the working range of the SC is very small, due to the voltage constraint of the stiff DC voltage. Moreover, just a small part of the energy is available in the SC buffer, which can be used by the load, as presented in [41].

C. Battery active cascaded structure

In this configuration, there is a bi-directional converter between the battery and the SC as shown in Figure 2.9. It allows the battery's voltage to be different than that of the SC, so the voltage of the battery can be maintained lower. Also, the SC is directly connected to the DC link.

Advantage of setting the battery on the input side of converter is the current control is available and the freedom of battery size design is obtained. However, there is a large voltage swing on the input to the DC link since the voltage of the SC is relative to the energy in SC bank, as described in [42].

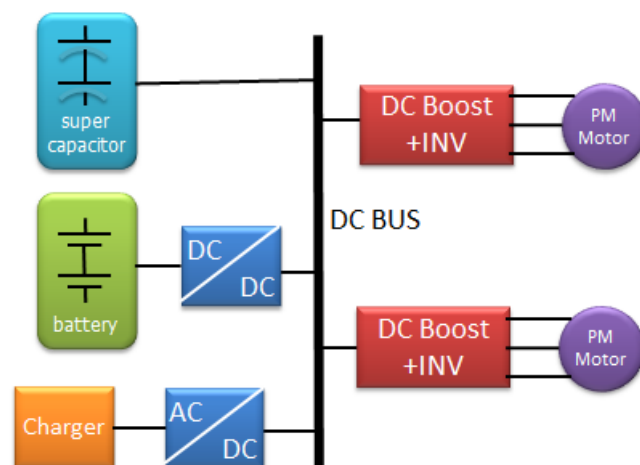


Figure 2.9 Battery active cascaded structure [41, 42]

D. SC active cascaded structure

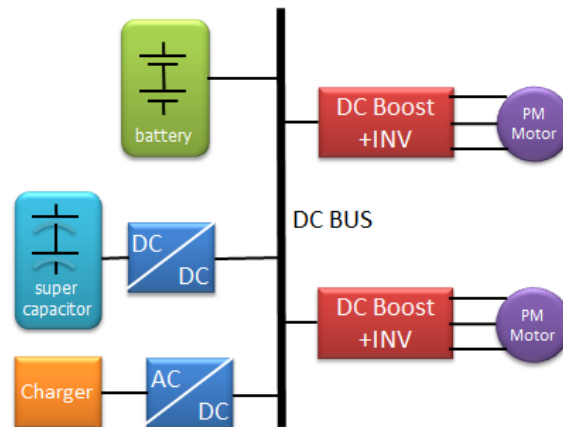


Figure 2.10 SC active cascaded structure

This configuration as shown in Figure 2.10, previously studied in [43, 44], is the most studied and researched HESS. The DC/DC converter is between the ultra-capacitors and the DC bus, allowing the current from the SC to be controlled directly. The SC voltage can be independent from the voltage of the DC link, and it can also achieve a wider range.

The battery is connected directly to the DC link, and the DC link voltage can be relatively constant. This topology also allows using a full voltage range of the SC, and the energy provided by regenerative braking can be effectively controlled or absorbed only by the SC. Furthermore, the bi-directional converter needs to be designed, in order to handle the power transfer of the super capacitor bank.

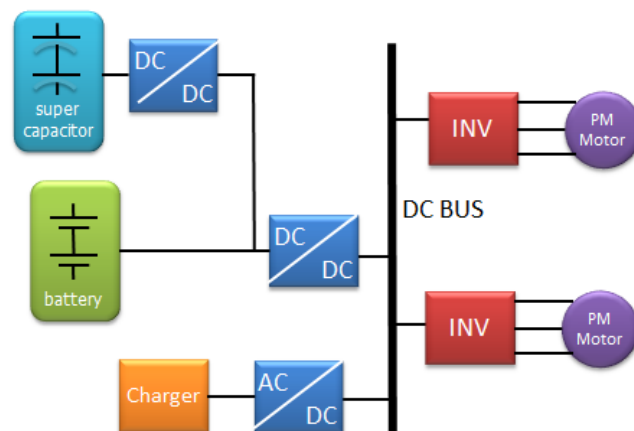


Figure 2.11 Bi-active cascaded structure [45, 46]

E. Bi-active cascaded structure

Based on the structure above, added another bi-directional DC/DC converter is added between energy bank and the DC link as shown in Figure 2.11. Both the voltage of super capacitor and battery can achieve a wide range. However due to the additional one converter in this topology, the cost and complexity of the system is highly increased.

F. Parallel active structure

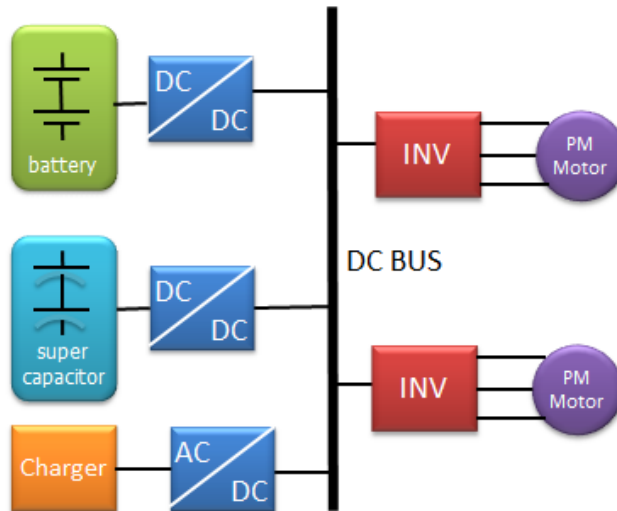


Figure 2.12 Parallel active structure [47]

This topology applies two input bi-directional DC/DC converters as shown in Figure 2.12, which is able to determine the current that each source should supply. The two currents are fully controlled, and the voltage of DC link is not necessarily the same as the voltage of the super capacitors or the one from the battery. Those voltages can be maintained lower than the DC link voltage.

In this topology, the voltages of SC and battery both can be defined freely, so that the energy bank SoC can be fully used. The stability and robustness is also improved, since a failure of one source still allows the operation of the other. The disadvantage of this method is increasing the cost and complexity.

The summarized evaluation is given by Table 2.2 as below. We can see that the SC active cascaded and parallel active structure is the best choice than others with comprehensive consideration for low voltage compact DC bus of the EV system.

Table 2.2 Comparison among different HESS structures

Structure	Controllable ability	Redundancy	Efficiency	Stability	Cost/ Complexity
Serial structure	N	N	N	G	G
Passive cascaded structure	N	A	N	G	G
Battery active cascaded	M	M	A	M	M
SC active cascaded	M	M	G	M	M
Bi-active cascaded	G	G	A	M	A
Parallel active	G	G	M	M	A

G=Good; M=Marginal; A= Acceptable; N= No Acceptable

Many power structure have been associated to hybrid energy sources in parallel topologies, and three hybrid power-source structures are mainly used, including the two-converter, direct, and one-converter structures.

The two-converter structure consists in associating a static converter and a control loop to each energy source, as shown in Figure 2.14. This control strategy generates a large number of degrees of freedom in the control design. However, the drawback lies in the inevitable losses in converter.

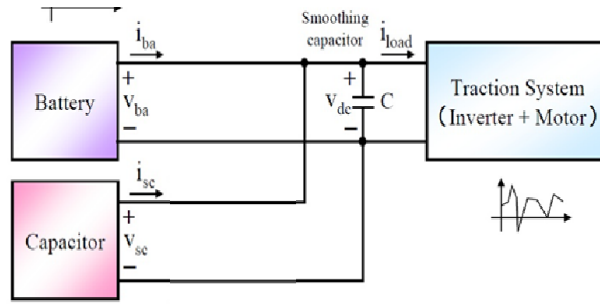


Figure 2.13 Direct parallel hybrid energy system

The direct parallel structure consists of connecting the battery directly to the load, as shown in Figure 2.13. The main drawback is SC size is fixed by DC bus voltage, and SC output power is limited. Although the system is low cost, battery controllability is also low.

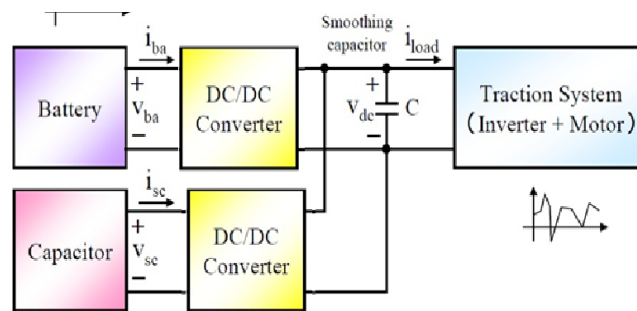


Figure 2.14 Two-converter parallel hybrid energy system

The one-converter structure consists of adjusting the power flow (Figure 2.15). The main advantages are simplicity and reduction of both losses and costs of the power management interfaces and a good controllability. Therefore the structure in Figure 2.15 is the best option for the low DC bus suitability.

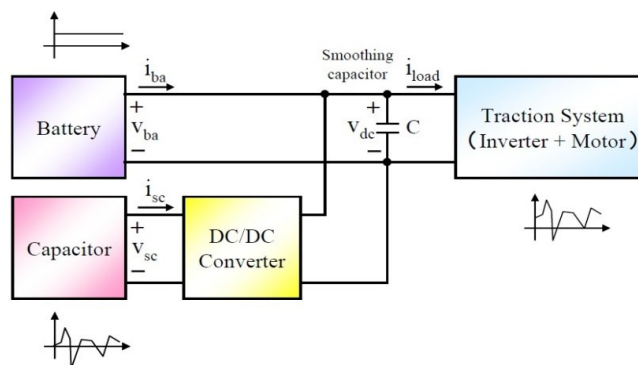


Figure 2.15 One-converter parallel hybrid energy system

The topologies must be defined to allow a continuous functioning of the hybrid source with good performances and limited component deteriorations. Hence, the hybridization purpose is to perform the following:

- 1) Using the advantage of the SC bank to compensate the low battery dynamics.
- 2) Recover the power generated by the load in generative mode and recover the power by the battery during load power decrease.

Thus, the studied hybrid structure has several modes of operation.

- Normal mode. The main source supplies the electric load and maintains the auxiliary source current;
- Discharge mode. Both energy sources supply the electric load simultaneously;
- Regenerative mode. The electric load supplies the storage devices;
- Charge mode. The SC bank should be charged by battery when the energy of the SCs is in low level and the load output power is relatively smooth.

Also we should pay attention that if the SCs are completely charged, the extra energy will be transferred into a dissipative safety device. So the SOC of the SC should be considered real-time and controlled to maintain at a suitable level.

The hybrid energy source is generally composed of different specific energy sources, such as batteries and SCs, which enable to provide both the permanent and transient powers demanded by the load.

Many power electronic architectures have been associated to hybrid energy sources. And the hybrid power-source structures mainly used, including serial, passive cascaded, one source cascaded; bi-active structure are compared in the Table 2.2, based on different requirements for EV application.

The one-converter structure consists in adjusting the power fluxes. Its main advantages are simplicity and reduction of both losses and costs of the power management interfaces and a good controllability. So the structure in Figure 2.13 is the best choice for our system. Simply speaking, the SC is linked by one bidirectional DC/DC converter as the power interface to the DC bus of the vehicle energy system. The battery hold the DC bus voltage by linked to the DC bus directly.

In our energy system design for our EV prototype, the dc bus is 72V linked with charger, HESS and power train system. It gives us a flexible structure for many kinds of converter tests, not only for the super capacitor interface, also the interface for charger system for the next step.

The next chapter is analyzing which kind of converter is most suitable in different voltage class as the power interface, especially for SC banks.

2.4 Capacity design of HESS for EV power train

For design the capacity of HESS with battery and super capacitor combination for electric vehicle power train, there are two aspects should be considered. The total energy size of the whole HESS system is the one aspect to consider. The other aspect is the proportion of the two energy banks.

The total energy size based on the requirement of EV prototype, such as the cursing range of the vehicle, the power rate of the traction motor, and the efficiency of the energy system. The proportion of battery and super capacitor bank should be designed based on the size and weight of the HESS, the power sharing principle and the efficiency desired by the whole system.

The performance parameters of battery and super capacitor for EV HESS are shown in' Table A1 in appendix. The total capacity of HESS should satisfy the requirement form EV power train system in the whole driving period between two times of charging. Table A.2 shows the energy state of HESS before and after the desired driving cycle.

HESS capacity design principle should satisfy the requirements as below.

- Energy stored in ESS should be over than the consumption in designed driving range.
- The maximum power from HESS should satisfy the peak power to traction motor.
- The weight and size of HESS should be acceptable than auto body design.

Based on the parameters in Table A1, and Table A2, the total available energy before driving cycle is E_0 , and the consumption of energy in the desired driving range

E_r , which is decided by the power class and efficiency of power train system. The relationship for total energy consumption is as below.

$$E_0 = ((1-\alpha)e_{Bat} + \alpha e_{SC})M_{HESS} \geq E_r \quad (2.4)$$

$$M_{HESS} \geq \frac{E_r}{(1-\alpha)e_{Bat} + \alpha e_{SC}} \quad (2.5)$$

HESS maximum discharge power is P_{dis} , and the power required by traction system is P_D . Their relationship can be explained as below.

$$P_{dis} = ((1-\alpha)p_{Bdis} + \alpha p_{sc})M_{HESS} \geq P_D \quad (2.6)$$

$$M_{HESS} \geq \frac{P_D}{(1-\alpha)p_{Bdis} + \alpha p_{sc}} \quad (2.7)$$

The maximum available weight of HESS is M_{max} , which is based on vehicle auto body design.

$$M_{MAX} \geq M_{HI} \quad (2.8)$$

The Equations (2.5), (2.7), (2.8) shows the basic principle of HESS capacity design to satisfy the requirement of EV power train system. The available ranges of M_{HESS} , α can be obtained by fixing system parameters and design requirements. In the next step, the converter efficiency as power interface and the volume size of HESS will be considered as vehicular equipment.

2.5 Summary

In this chapter, three aspects of HESS for EV application are introduced.

The modeling of batteries and super capacitor as energy banks is necessary for power control and SoC monitor of energy banks. Simple model of battery is selected in our HESS system. The nonlinear large signal modeling of super capacitor and the small signal normalized model is given, which can be used for analyzing the dynamic response of HESS system, and the SoC observer of SC bank. All possibilities of the

topologies of battery SC linked with converter are analyzed, the optimal SC active topologies for EV system are considered in detailed. The capacity design principle is proposed, for the whole HESS size and the proportion between battery and SC banks. In the next chapter, the converter structure and control method will be considered for SC active topology.

3 Analysis and Control of Power Interface for Super Capacitor and Battery

3.1 Introduction of converters as the power interface of EV HESS

The high power class interface should be realized for pure electric powertrain system, and super capacitor application. Considering optimization of different aspects, such as cost, control ability and stability, many researches are proposed. The multi-phase interleaved converters are considered for hung current holding ability. Multi-level topology is suitable for high voltage application without changing current chopper devices. Also zero current soft switch and discontinues mode control is applied for decreasing switch components loss. Advanced converter control method and response analysis method is proposed for high performance application of HESS. Nevertheless, control method for EV PM motor high speed response is rarely discussed. Although there are some researches on the DC bus stability for constant power load, especially for the EV motor power train with different driving considerations, the cooperated control strategy with EV motor inverter and DC bus voltage boost system is still needed for future high power vehicles.

The DC/DC converter functioning as the interface for the SC bank to the DC bus must have the characteristics below:

- Bidirectional power flow;
- Wide variable voltage on one side;
- Relatively constant voltage on the other side;
- Wide response bandwidth of output current is needed.

In order to realize bidirectional power flow dc-dc converters, the switch cell should carry the current on both directions.

Power MOSFET and IGBT with diode in parallel usually works as basic switch for the bidirectional converter. In Figure 3.2, the basic boost and buck converter, which is signal directional converter, can be combined together for bidirectional power flow.

The operation model of this topology works in boost model in one direction of power flow, another direction will be buck model, depending on the voltages of two sides.

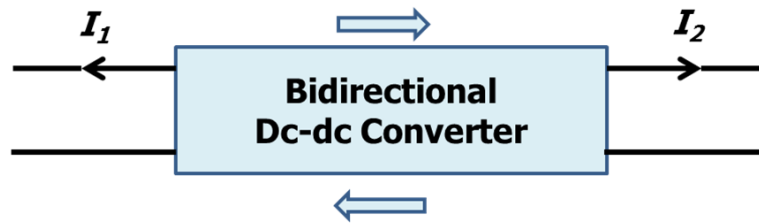


Figure 3.1 Power flow of bidirectional converter

Lots topologies are developed for bidirectional dc-dc converter application [22-29]. Non-isolated and isolated converters are the basic two types. The selection is based on actual system and voltage class of two sides.

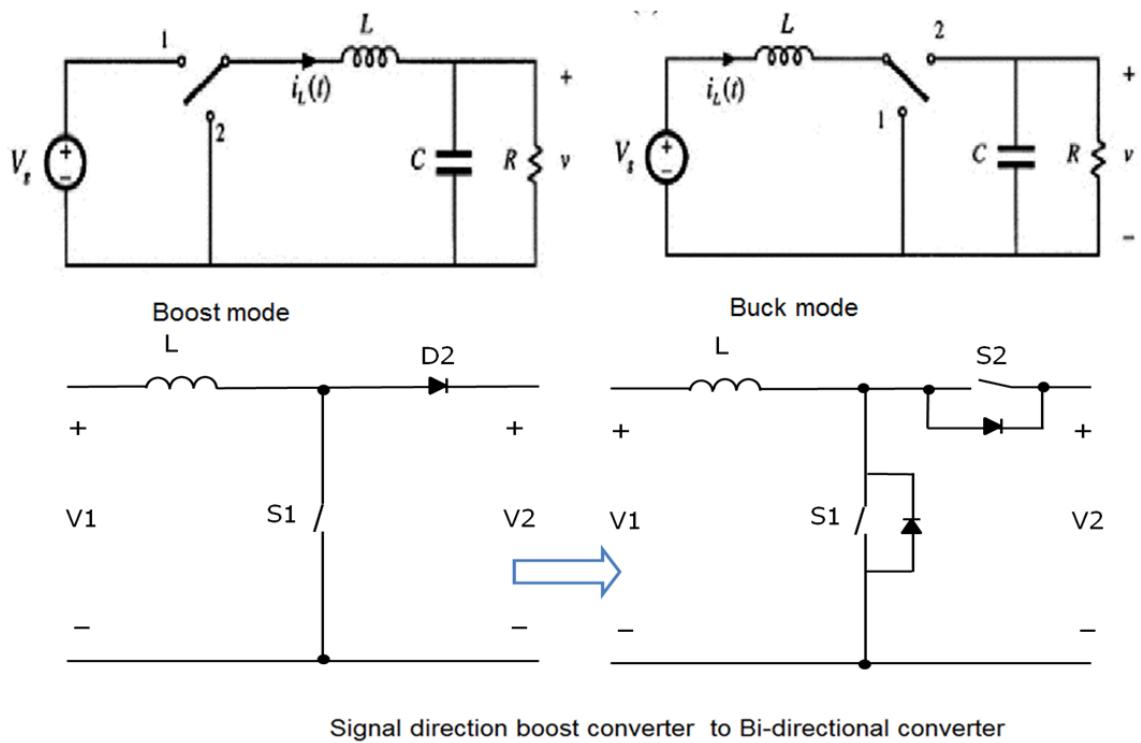


Figure 3.2 Relationship between bidirectional and Buck/Boost converter

For EV application, the energy system requires high efficiency, and small size. Also cost and stability are both important aspects for consideration. The EV dc bus is usually less than 1000V, and the output power is lower than 100KW, the transformer-less non-isolated boost type and buck type dc-dc converter is preferred.

Also the bidirectional type is necessary, because the energy recovery from break is one important aspect for EV system.

The basic non-isolated bidirectional dc-dc converter topology is shown in Figure 3.2. In fact, it is the combination of signal directional boost and buck converter, which use on inductance commonly. The power train side is high voltage size because the high voltage motor system will improve the system efficiency remarkably. The energy banks usually stay in the low voltage side, caused by the battery module and SC module size limitation in the high voltage situation. So the boost stage will be used for the energy to the powertrain system when EV cursing. And the buck stage will be used as energy recovery when vehicle break.

Multiphase current interleaving technology with minimized inductance is a good option for the increase the maximum power of the power output [23, 46]. A three-phase bidirectional dc-dc converter is shown in Figure 3.3, where the phase switch is controlled with 120-degree phase shift from each other. The control system will be the same class complexity if the three phase signal generator is available in the control unit.

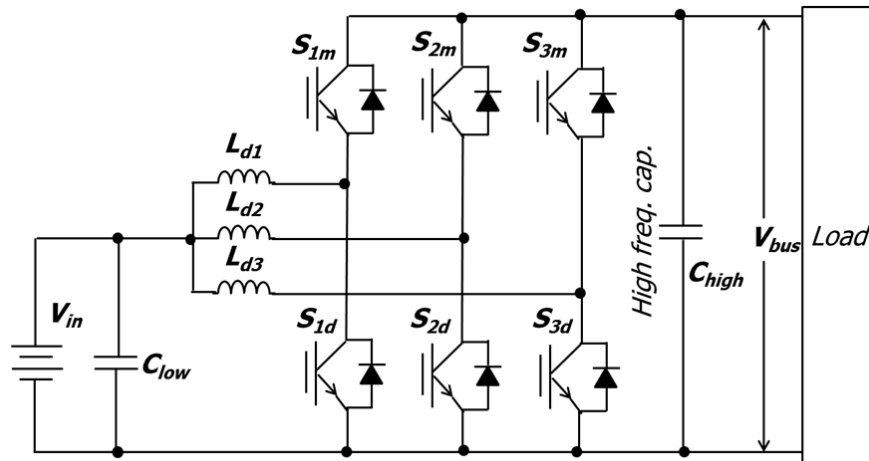


Figure 3.3 Three-phase interleaved converter [46]

In the battery and super capacitor hybrid energy system, as the battery will hold the main average power and the SC will provide the peak power, the inter-leaved structure will not be one good option when the output current requirement is satisfied in the fixed voltage by one group chopper system, such as low voltage small scale EV system. Also in the high voltage condition, single group of chopper will be selected, as the current is can be limited in the out power is fixed.

On the other hand, for future super capacitor powered electric vehicles, if the stable power interface is needed for constant huge current to traction side, the three-phase inter-leaved system may be a good option.

The next section presents the discussion of optimal converter topologies for battery and super capacitor hybrid system.

3.2 The optimized topology of converter for EV HESS

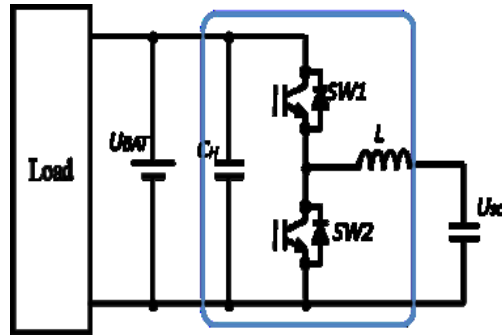
As mentioned previously, SC active cascade topology is able to achieve desirable performance with only one dc-dc converter and therefore is the more preferable topology. Based on the performance and the role of SC bank in HESS for EV, non-isolated DC/DC converters are good options for super capacitor interface.

Considering the non-isolated dc-dc converter, there are several choices available. Therefore, it is also necessary to have an ideal converter that can be applied to the HESS.

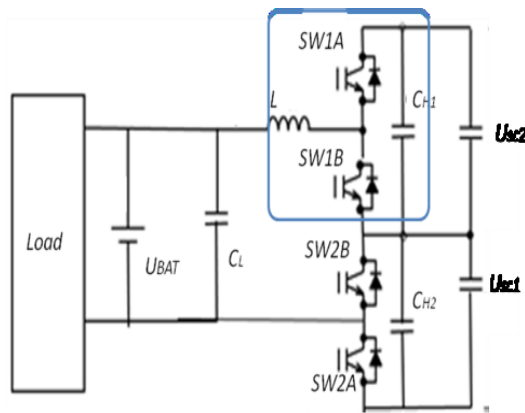
However, the HB converter has several disadvantages. The silicon utilization is relatively poor due to the wide voltage ratio range between SC bank and DC bus. The inductance size should be considered, due to the huge output current under relative wide voltage range.

3.2.1 Analysis of Half-controlled converter and Three-level converter as SC interface

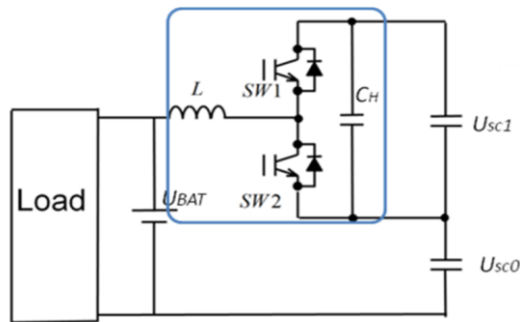
Two improved topologies are introduced here. First is the three-level converter topology for SC application as shown in Figure 3.4 (b). Another topological approach first presented in our lab under the name of half-controlled (HC) converter, shown in Figure 3.4 (c) [32, 33, 34]. The aims of both improved topologies are size reduction and efficiency improvement of the power interface. Both of these two improved topologies set the SC to high voltage level to increase the efficiency. The utilization of state of charge of the SC bank should be first considered in the system design. For our design, 25% of SoC remains after every deep discharge for SC bank is acceptable, considering the size of SC energy bank and the SC modules protection.



(a) Bidirectional half-bridge (HB) converter



(b) Three-level (TL) converter



(c) Half-controlled (HC) converter

Figure 3.4 Converter topologies for SC interface

Considering battery and super capacitor bank voltages for TL converter and HC converter, we set the voltage rate of Battery and SC is p , and the voltage rate between SC

modules is k , So For HB converter, $p = \frac{U_{BAT}}{U_{SC}}$; for TL converter, $p = \frac{U_{BAT}}{U_{SC1} + U_{SC2}}$,

$$k = \frac{U_{SC2}}{U_{SC1}}; \text{ for HB converter, } p = \frac{U_{BAT}}{U_{SC0} + U_{SC1}}, \quad k = \frac{U_{SC1}}{U_{SC0}}.$$

Base on the working condition of voltages of two sides of converters, the operation range of this three converter topologies is as below,

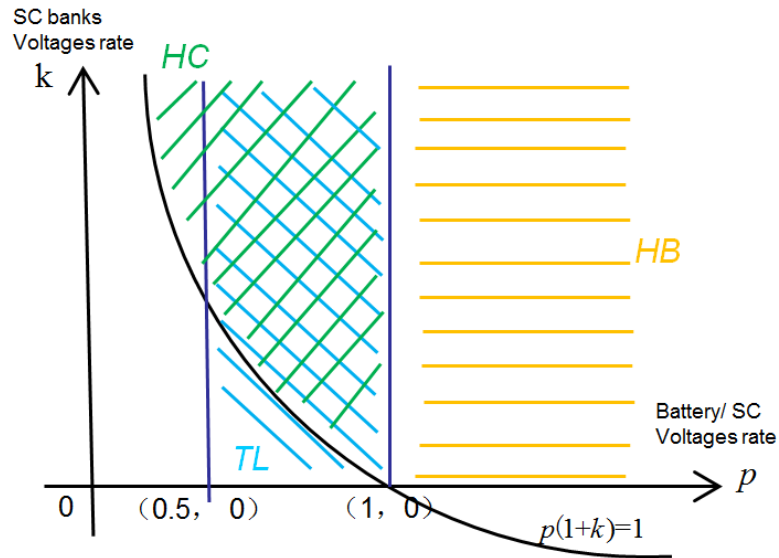


Figure 3.5 Operation voltage range of HB TL HC converter

As shown in Figure 3.5, the blue section is TL convert operation range, and the green section is HC converter operation range. For Battery in high voltage, we can select conditional half bridge converter, as shown the operate range in the yellow section

Table 3.1 Comparison between different converters for SC

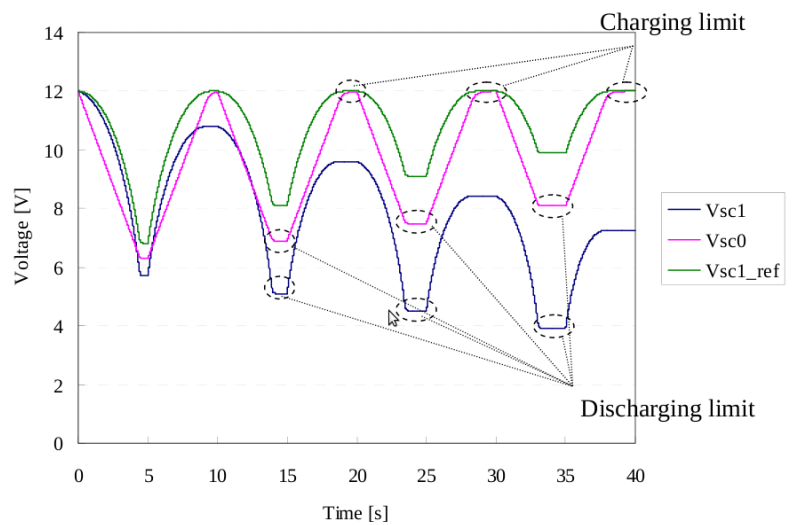
Bidirectional Converters For SC interface	Bidirectional Boost Converter	Three Level converter	Half-Controlled Converter
Operation Condition	$0 < U_{sc} < U_{BAT}$	$(U_{SC1} + U_{SC2})/2 < U_{BAT}$ $U_{BAT} < U_{SC1} + U_{SC2}$	$U_{sc0} < U_{BAT}$ $U_{BAT} < U_{SC0} + U_{SC1}$
Minimum SC Storage Energy	0	> 25% SoC	25% SoC
Switching Elements	2	2 (+ 2)	4
Designed Inductance Size	100%	50%	25%
SC banks Voltages balance	No	Need	Need

The comparison among different converters for SC interface is given in Table 3.1. The three-level converter uses four switching elements for the output power from SC [35]. The upper group switch has 180 degree phase error with the lower group. Consequently, the switching frequency of the whole chopper system is twice as the chopper using two switch elements. Naturally, if the requirement of the output ripple is the same, the inductance can be decreased to 25%, compared to the conventional design. Therefore three-level converter is very suitable for the high voltage EV powertrain system. The disadvantage is that the number of switching elements is increased.

The advantages of HC converter are as below; the ratio between the volt-ampere ratings of the switches in the HC converter can be decreased to half compared to half-bridge system. The inductor of the HC converter can be decreased nearly 50% [34]. The half-controlled converter has smaller inductance than the conventional one, and the switching elements are reduced. We applied this topology to our system, and the current control method mentioned in the next chapter will be based on this topology.

3.2.2 SC bank voltage balance for HC converter and TL converter

One issue of half-controlled converter is that, the voltage balance system is needed, which adds to the complexity of the system. As the SC banks are separated to controlled section and passive section. The voltage relationship between SC0 and SC1 for system operation will be broken by the unbalance charge and discharge of the two banks.



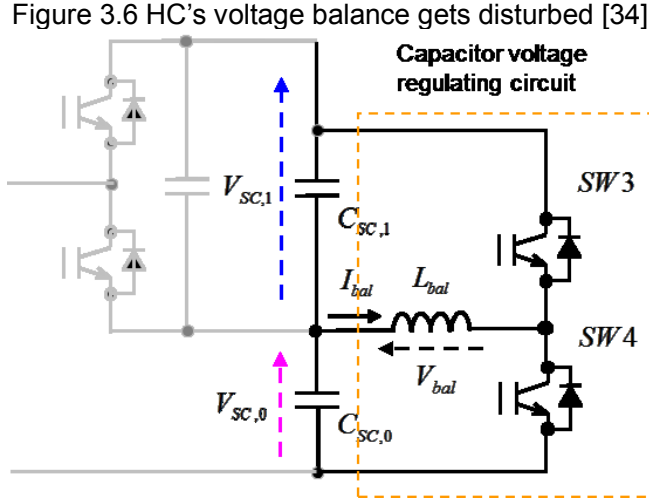


Figure 3.7 Balance circuits for HC converter [33]

The optimized voltage balance principle is researched in [33]. The size of the balance circuit is very small if the voltage balance works dynamically and continuously. By controlling the small scale chopper system, the relationship of VSC1 and VSC0 can be arranged to optimized rate, using the equation [33], as below.

$$V_{sc,1}(t) = \sqrt{V_{sc,1}^2(0) + \frac{C_{sc,0}}{C_{sc,1}} \left(2(V_{DC} - V_{sc,0}(0)) \cdot (V_{sc,0}(t) - V_{sc,0}(0)) - (V_{sc,0}(t) - V_{sc,0}(0))^2 \right)} \quad (3.1)$$

The three level converter can realized voltage balance of two capacitor banks without extra structure. As shown in Figure 3.21, balance voltage v_C can be controlled by Equation 3.19, and the input signal is the duty error of the duty d_1 and d_2 . This method is explained in [50] in detail.

3.3 Converter control of HESS for EV

3.3.1 Basic control method for bidirectional dc-dc converter

As shown in the previous section, the basic of the three topologies of power interface of super capacitor bank is the section marked by the blue line. The difference between bidirectional converter interface for HESS and buck/boost converter is that, the two sides of the converter can seem as voltage sources if we do not consider the extremely low frequency response of the super capacitor voltage shown in Chapter 2. Also voltage and current information can be obtained using current sensors and voltage sensors, so this can be considered in the control system design.

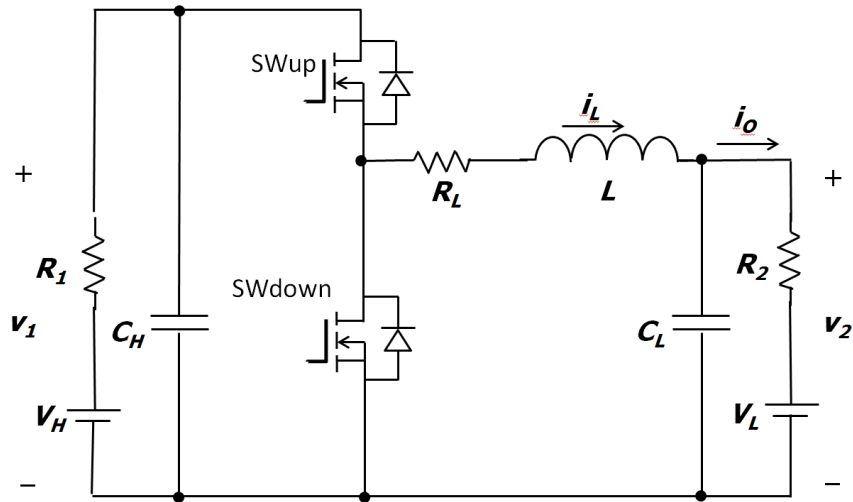


Figure 3.8 Modeling for bidirectional converter with sources on two-side

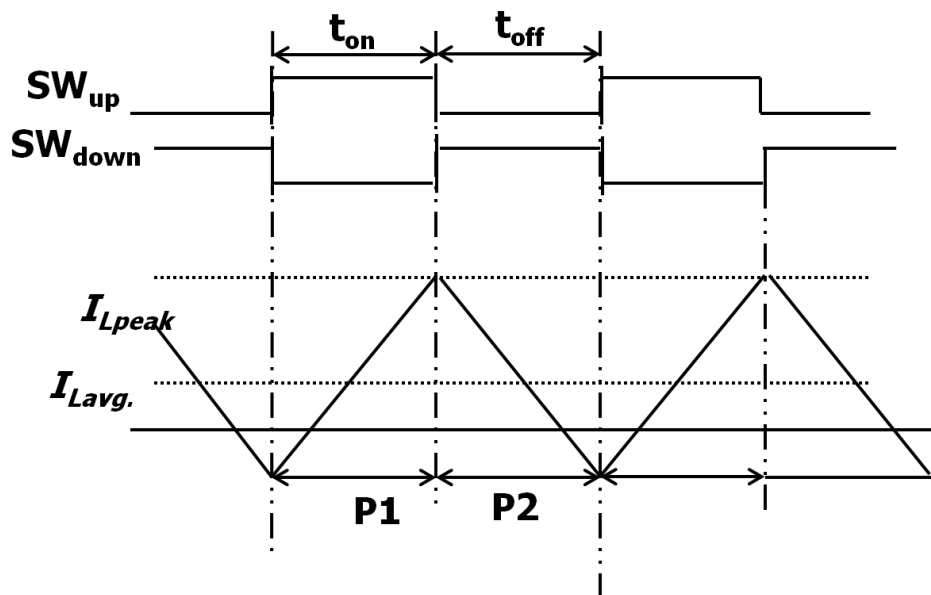


Figure 3.9 Operation modes of bidirectional converter

During On stage, SWup turns on and SWdown turns off, the system equivalent circuit can be represented in Figure 3.9.

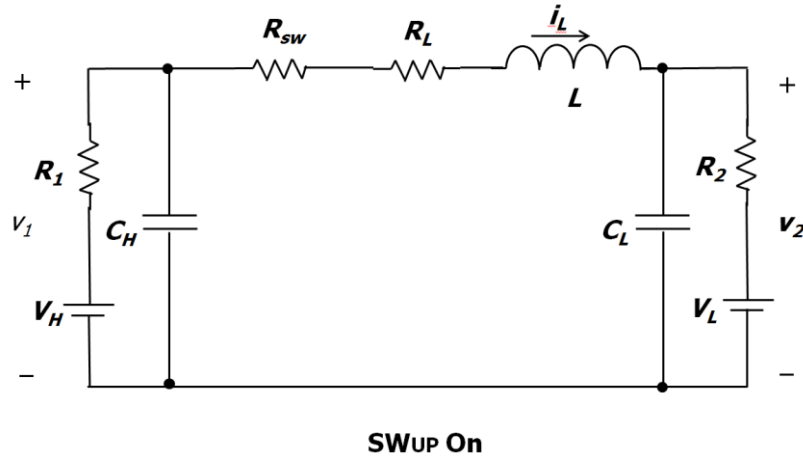


Figure 3.10 SWup on stage of bidirectional converter

The inductor current is i_L , the low side capacitor voltage is v_2 and the high side capacitor voltage is v_1 . Inductor voltage across the inductor L is given by Equation (3.2) and the capacitor current is given by Equation (3.3).

$$L \frac{di_L}{dt} + i_L \cdot (R_{sw} + R_L) = -v_2 + v_1 \quad (3.2)$$

$$\begin{cases} C_H \frac{dv_1}{dt} = -\frac{v_1 - V_H}{R_1} \\ C_L \frac{dv_2}{dt} = i_L - \frac{v_2 - V_L}{R_2} \end{cases} \quad (3.3)$$

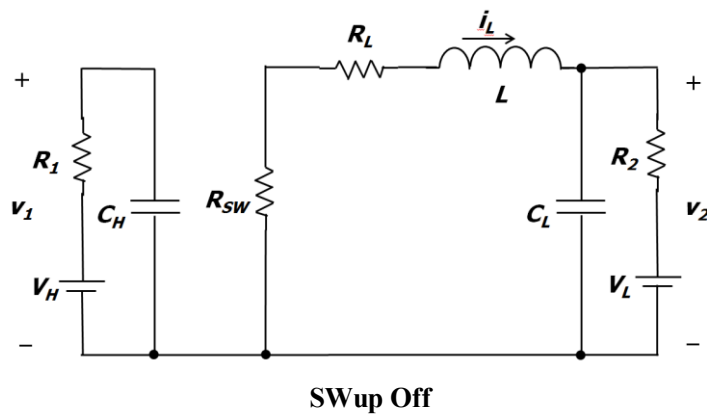


Figure 3.11 SWup off stage of bidirectional converter

System model can be obtained by the relationship for current passing capacitor and the voltage hold by the inductance, shown by Equation (3.4) and Equation (3.5).

$$L \frac{di_L}{dt} + i_L \cdot (R_{sw} + R_L) = -v_2 \quad (3.4)$$

$$\begin{cases} C_H \frac{dv_1}{dt} = -\frac{v_1 - V_H}{R_1} \\ C_L \frac{dv_2}{dt} = i_L - \frac{v_2 - V_L}{R_1} \end{cases} \quad (3.5)$$

So we can get the state-space averaging equations using Equation (3.5), and here D is the duty of SW1; all the parameters is the average vale in one PWM duty.

$$\begin{cases} L \frac{d\bar{i}_L}{dt} = D(\bar{v}_1 - \bar{v}_2) - \bar{i}_L \cdot (R_{sw} + R_L) + (1-D)(-\bar{v}_2) \\ C_H \frac{d\bar{v}_1}{dt} = -D(\bar{i}_L + \frac{\bar{v}_1 - V_H}{R_1}) - (1-D)\frac{\bar{v}_1 - V_H}{R_1} \\ C_L \frac{d\bar{v}_2}{dt} = \bar{i}_L - \frac{\bar{v}_2 - V_L}{R_2} \end{cases} \quad (3.6)$$

Easily to know, these the relationship of the control variable, inductor current i_L , low side capacitor voltage v_2 , and high side capacitor voltage v_1 can be measured in real-time by current sensors and voltage sensors.

The conventional control method of this kind of converter structure is based on the state average model and the small signal analysis. Nonlinear system is considered usually for control one side voltage to a constant range.

3.3.2 Current control method of half-controlled converter

Here we use the decoupling method based on real-time voltage signal feed forward to obtain the transfer function for continuous current model of bidirectional converter.

From Figure 3.13, we can see that the sections in the blue block of the half controlled bi-directional converters are the same structure of the basic half-bridge, shown in the Figure 3.12.

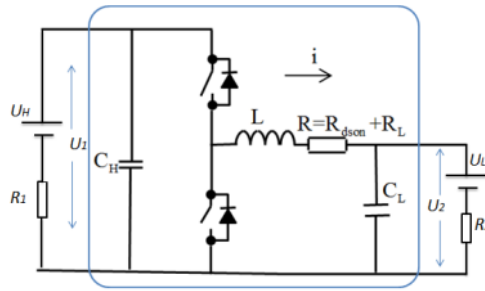


Figure 3.12 The basic bidirectional structure in half-bridge converter

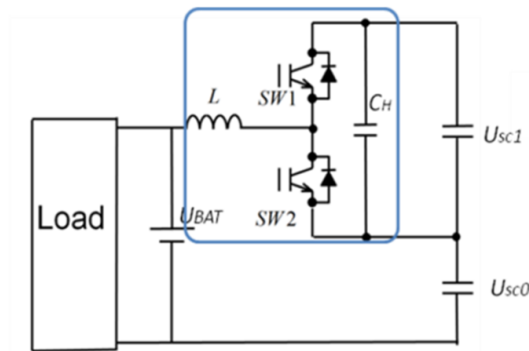


Figure 3.13 The basic bidirectional structure in half-controlled converter

$$\begin{cases} L \frac{di}{dt} = dU_1 - U_2 - iR \\ C_H \frac{dU_1}{dt} = -di - \frac{U_1 - U_H}{R_1} \\ C_L \frac{dU_2}{dt} = i - \frac{U_2 - U_L}{R_2} \end{cases} \quad (3.7)$$

Using the state space average method, the system can be described as above,

Here d is the PWM duty of the chopper system.

Usually, the system is considered as nonlinear system due to the dU_1 in the Equation (3.7). Term d is input, and U_1 is one of the outputs. Then the small signal modeling is done at system operation point, and linear model is realized. The controller can be designed based on the small signal model [47].

Only current control is considered and the voltages U_1 and U_2 are measurable by

using voltage sensors in real-time.

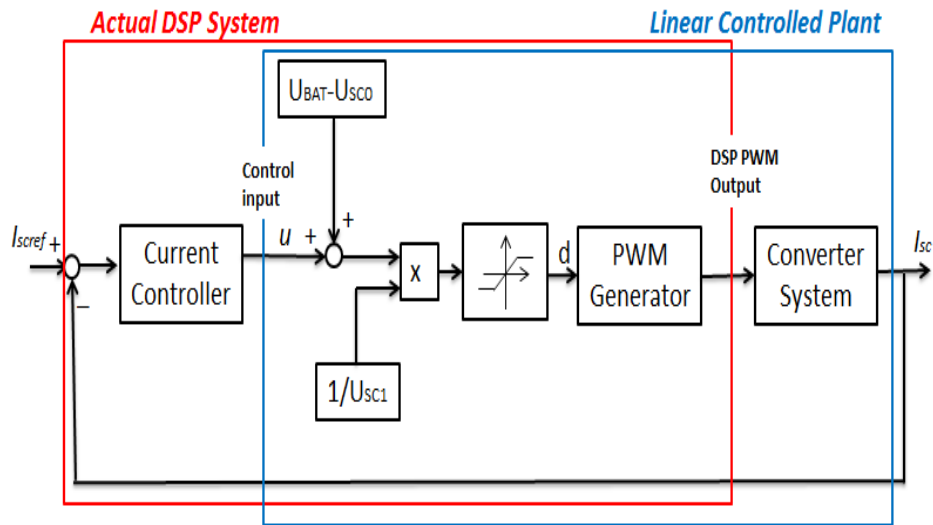


Figure 3.14 Current control block for HC converter

The relationship between the current and input is given in Equation (3.8).

$$L \frac{di}{dt} = u - iR \quad (3.8)$$

Setting u as the system input, and i as the output. The current control system is one order linear system.

The transfer function is:

$$\frac{i(s)}{u(s)} = \frac{1}{L + Rs} \quad (3.9)$$

It means that, considering only the current control loop, if the voltage signal can be measured and feedback in real time, the system is one order system.

PI controller is designed as current controller, shown in Figure 3.14.

The system open loop transfer function is

$$\frac{I(s)}{I_{ref}(s)} = \frac{K_p K_f s + 1}{K_f s(L + Rs)} \quad (3.10)$$

The current controller can be designed using the classic control method without

small signal analysis.

A conventional PI controller is applied for the current tracking control. In order to improve the dynamic response, the feed forward loop to the control duty is generated with the measurement of the voltages of V_{dc} , V_{SC0} and V_{SC1} . Also the duty output limitation is set in real-time control system as shown in the Figure 3.15.

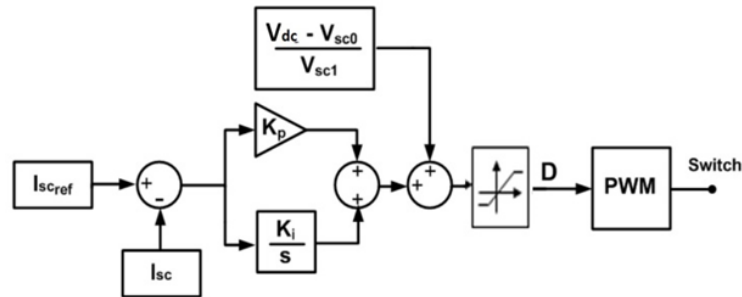


Figure 3.15 Current control block for HC converter power sharing strategy [51]

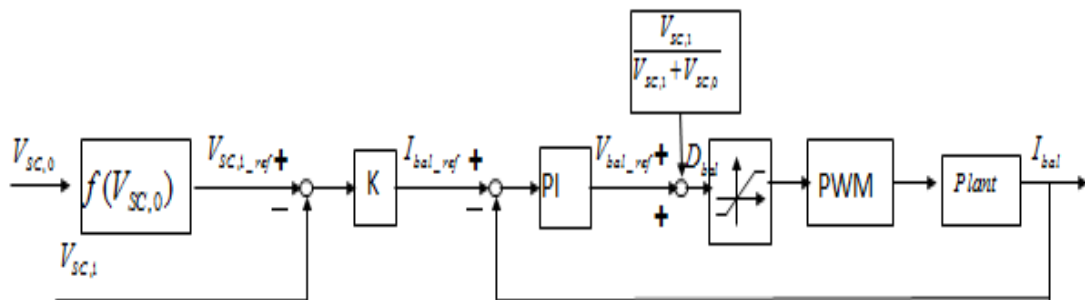


Figure 3.16 Balance current control block for HC converter [51,52]

Based on the same principle, the current control loop of the HC converter can be designed as below.

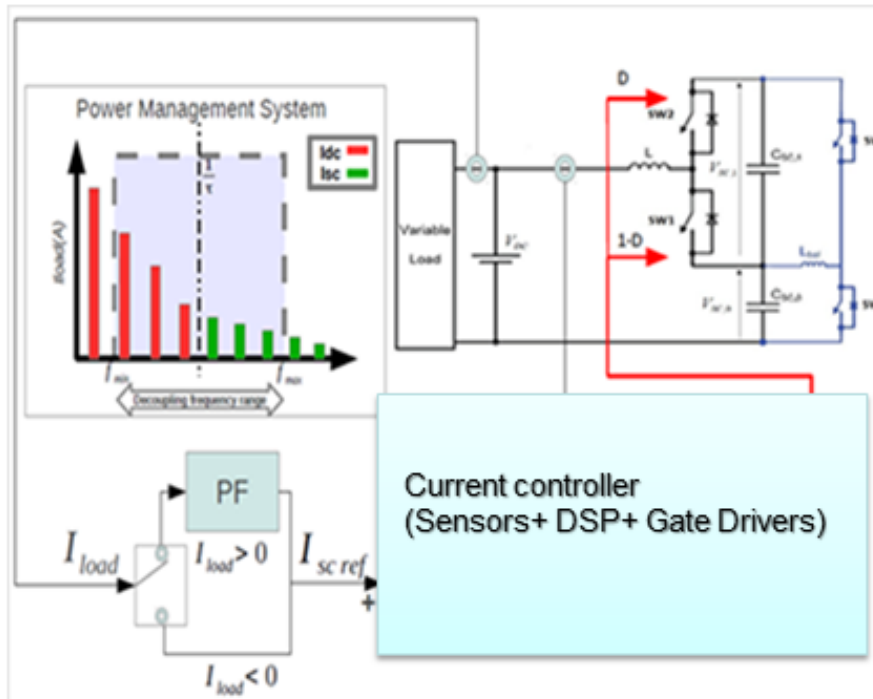


Figure 3.17 Framework of current control algorithm with HC converter

3.3.3 Current control method of three-level converter

From the proposal of half-controlled converter, we can naturally deduce that, the super capacitor energy bank can be separated to different banks inside the topology. The fundamental reason is that, the rated voltage of the super capacitor cell is determined by the voltage of the electrolyte. The typical cell voltage is 1–2.8 V, depending on the electrolyte technology [40]. In order to obtain a higher working voltage that is determined by the application, elementary cells are series connected into one capacitor module.

Three-level converters are a well-adopted solution in applications with high input voltage and high switching frequency [48, 49, 50]. The voltage stress of the switches is only half of the total dc bus voltage. This allows us to use lower-voltage-rated switches and still having better switching and conduction performance compared to the switches rated on the full blocking voltage. Therefore, the converter cost and efficiency can be significantly improved compared to two-level converters, such as half-bridge and Cuk converter, particularly when the switching frequency is above 20 kHz.

The capacitors are series connected and serve as a capacitive voltage divider to split

the dc bus voltage SC_{12} into two equal voltages SC_1 and SC_2 , when considering the basic condition that the two separated super capacitor bank is strictly equal with the same filter capacitor linked to the chopper.

As shown in Figure 3.18, the states of the switches SW1B and SW1A are determined by a switching function s_1 and the complementary function, while the states of switches SW2B and SW2A are determined by a switching function s_2 and the complementary function. The switching functions s_1 and s_2 are generated by pulse width modulators PWM1 and PWM2. The phase between the triangle signal for the PWM 1 and PWM 2 will be 180 degree.

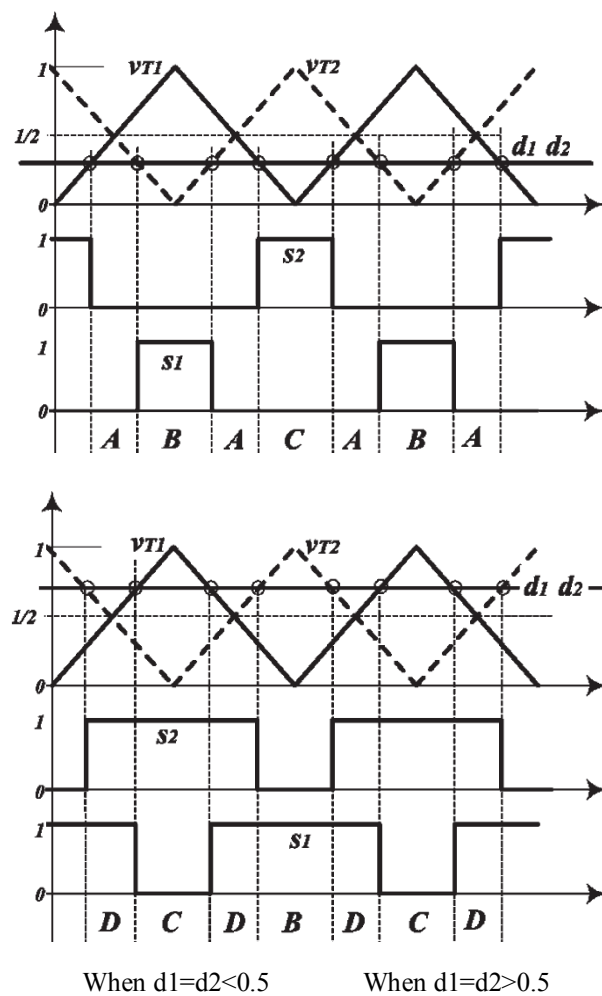


Figure 3.18 PWM signal principle of TL converter [50]

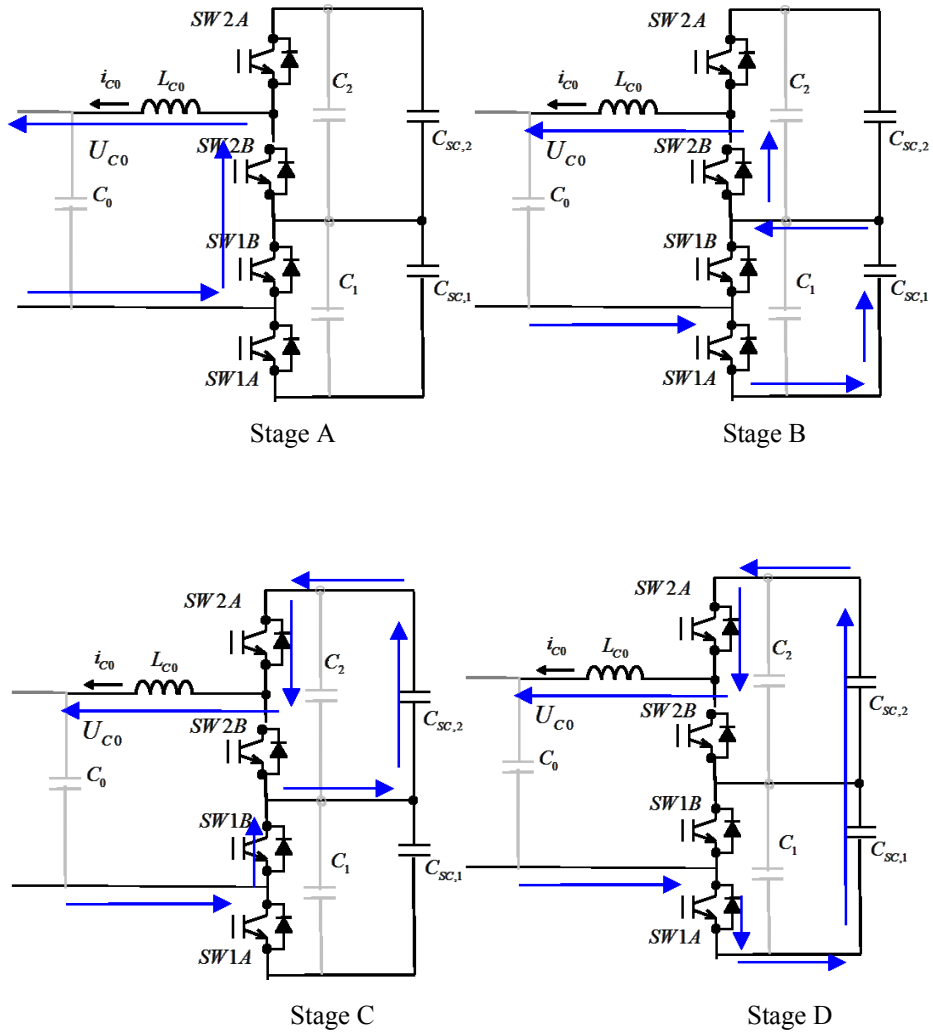


Figure 3.19 Different stages in one action period

We can see clearly that in stage A, B, C and D, the inductance current is

$$\frac{di_{C_0}}{dt} = \left(-\frac{u_{C_0}}{L_{C_0}} \right) \quad \text{Stage A}$$

$$\frac{di_{C_0}}{dt} = \left(\frac{u_{C_2} - u_{C_0}}{L_{C_0}} \right) \quad \text{Stage B}$$

$$\frac{di_{C_0}}{dt} = \left(\frac{u_{C_1} - u_{C_0}}{L_{C_0}} \right) \quad \text{Stage C}$$

$$\frac{di_{C_0}}{dt} = \left(\frac{u_{C_1} + u_{C_2} - u_{C_0}}{L_{C_0}} \right) \quad \text{Stage D}$$

The action of SW1 and SW2 can be explained clearly by Equation (3.11) and Equation (3.12) [50].

$$s_1(t) = \begin{cases} 1, & kT_{SW} \leq t \leq T_{SW}(k + \frac{d_1}{2}) \\ 1, & kT_{SW}(k + 1 - \frac{d_1}{2}) \leq t \leq T_{SW}(k + 1) \\ 0, & T_{SW}(k + \frac{d_1}{2}) < t < T_{SW}(k + 1 - \frac{d_1}{2}) \end{cases} \quad (3.11)$$

$$s_2(t) = \begin{cases} 1, & kT_{SW} + \frac{T_{SW}}{2} \leq t \leq T_{SW}(k + \frac{d_2}{2}) + \frac{T_{SW}}{2} \\ 1, & kT_{SW}(k + 1 - \frac{d_2}{2}) + \frac{T_{SW}}{2} \leq t \leq T_{SW}(k + 1) + \frac{T_{SW}}{2} \\ 0, & T_{SW}(k + \frac{d_2}{2}) + \frac{T_{SW}}{2} < t < \frac{T_{SW}}{2} + T_{SW}(k + 1 - \frac{d_2}{2}) \end{cases} \quad (3.12)$$

The instantaneous output voltage V_{OUT} can be expressed as:

$$u_{C0}(t) = (u_{C1} + u_{C2})s_1(t) + u_{C1}(s_1(t) - s_2(t))$$

$$u_{C0}(t) = u_{C0}\left(t + \frac{T_{SW}}{2}\right)$$

$$\overline{u_{C0}} = \frac{1}{T_{SW}} \int_0^{T_{SW}} u_{C0}(t) dt = (u_{C1} + u_{C2})d$$

It means that the output voltage is a periodic function with the half period of PWM driver signal.

It is easy to calculate the peak to peak current ripple [50].

$$\Delta i_{C0}(d) = \begin{cases} \frac{u_{C12}}{L_{C0} 2f_{sw}} (1 - 2d)d & d \leq 0.5 \\ \frac{u_{C12}}{L_{C0} 2f_{sw}} (2d - 1)(1 - d) & d \geq 0.5 \end{cases} \quad (3.13)$$

$$\Delta i_{C0\max} = \frac{u_{C12}}{16L_{C0}f_{sw}} \quad (3.14)$$

The inductance is 25% of the inductance of the half-bridge dc-dc converter for the same current ripple and the same switching frequency [50].

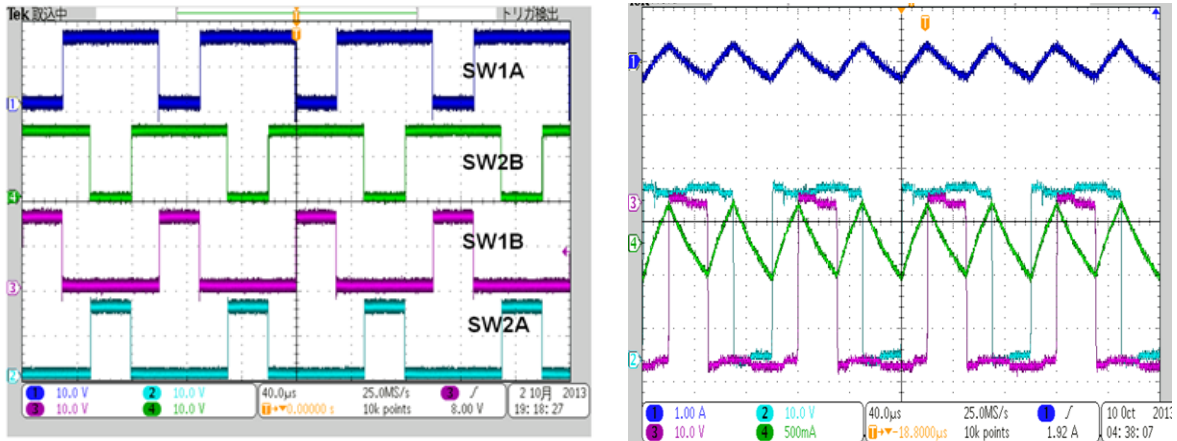


Figure 3.20 Actions of three-level converter prototype

Figure 3.20 shows the action of three-level converter prototype designed for super capacitor bank interface. The test voltage of SC_1 and SC_2 is 30 V respectively.

The blue signal and the pink signal show the voltages hold by SW_{2B} , and negative voltage by SW_{1B} respectively. Green current signal means output current i_{c0} .

In the condition as shown in Figure 3.20, the output current is equal to 0, when

$$(u_{C1} + u_{C2})d = u_{C0} \quad (3.15)$$

The ripple of the output current is nearly 0.75A, which is the same as the calculation result based on Equation (3.14).

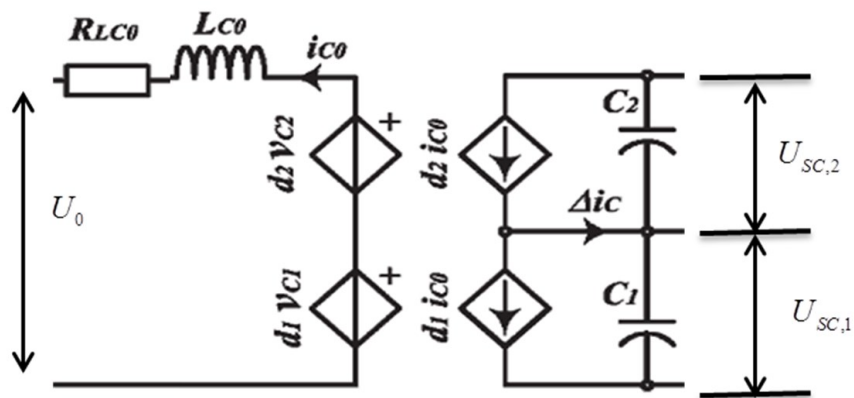


Figure 3.21 Large-signal average model of three-level converter [50]

By simplified the conclusion of [50], the transfer functions of input voltage and output current will be :

Let
$$d_1 = \frac{u_0 + u_{C0}}{u_{C12}} + \Delta d, \quad (3.16)$$

$$d_2 = \frac{u_0 + u_{C0}}{u_{C12}} - \Delta d \quad (3.17)$$

$$G_{i_c u_0} = \frac{i_{C0}}{u_0} = \frac{1}{sL_{C0} + R_{L_{C0}}} \quad (3.18)$$

$$G_{v_{C0} \Delta d} = \frac{V_c}{\Delta d} = -2 \frac{I_{C0}}{sC} \quad (3.19)$$

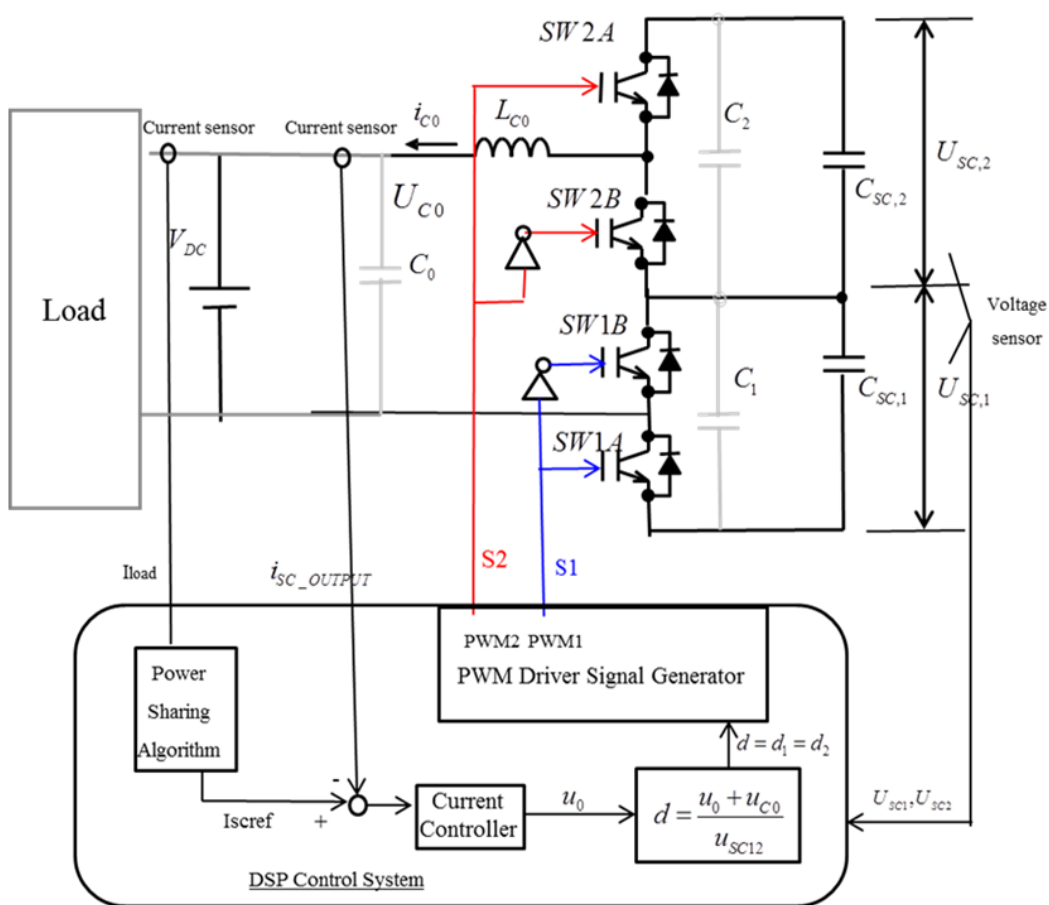


Figure 3.22 Current control of three-level converter

3.4 Experimental verification of HC converter and analysis

In our experiments, the basic parameters for the half-controlled converter control for HESS is as below.

Table 3.2 Parameters of converter and HESS platform

Inductance	0.5 mH
R	20 m Ω
SC0	45 V
SC1	35 V
DC bus voltage	60 V
Load DC motor power	MAX 400 W
Controller DSP	150 MHz
PWM frequency	10 kHz, 20kHz, 25kHz, available

The design of a HESS test platform, especially for the converter section, is introduced in [51, 52] in detail. The system is tested before EV prototype setup.



Figure 3.23 Prototype of half-controlled converter

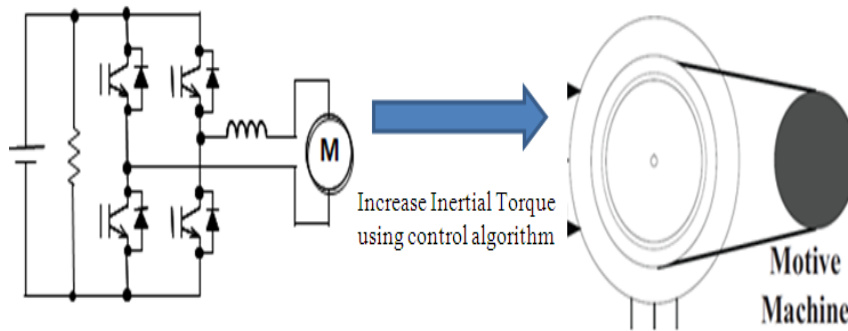


Figure 3.24 Inertial torque generator system

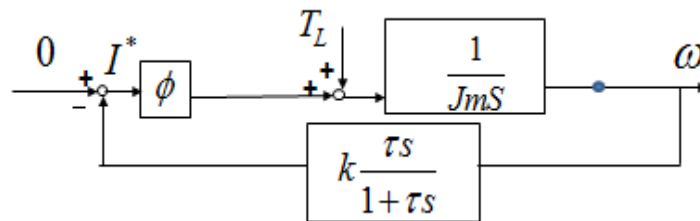


Figure 3.25 Structure of inertial control

Figures 3.22 and Figures 3.23 show the hybrid energy system operation with the current control of SC converter. In experiment of Figure 3.26, the load is variable resistance. The frequency decoupling method is applied to the power sharing between two energy sources. In the experiment of Figure 3.27, DC motor is the load of HESS with constant acceleration in every seven seconds.

Based on the analysis of output response and the experiment results, we can clearly see that the SC output current tracking ability using the current control method can satisfy the requirement of power sharing strategy for HESS operation. Also all the regenerative energy can be recovered to SC bank based on current control and the application of bidirectional half-controlled converter.

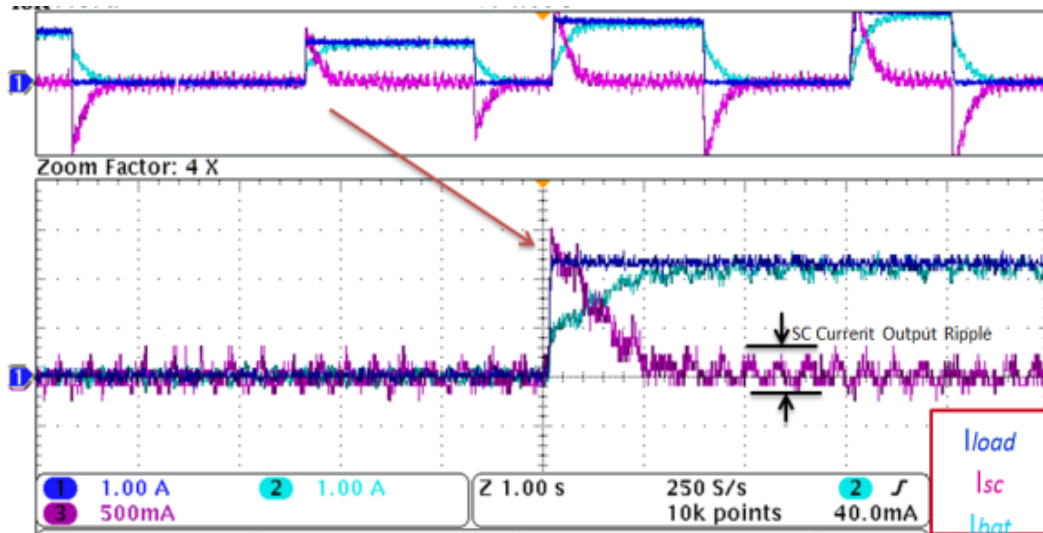


Figure 3.26 HESS power sharing experiment

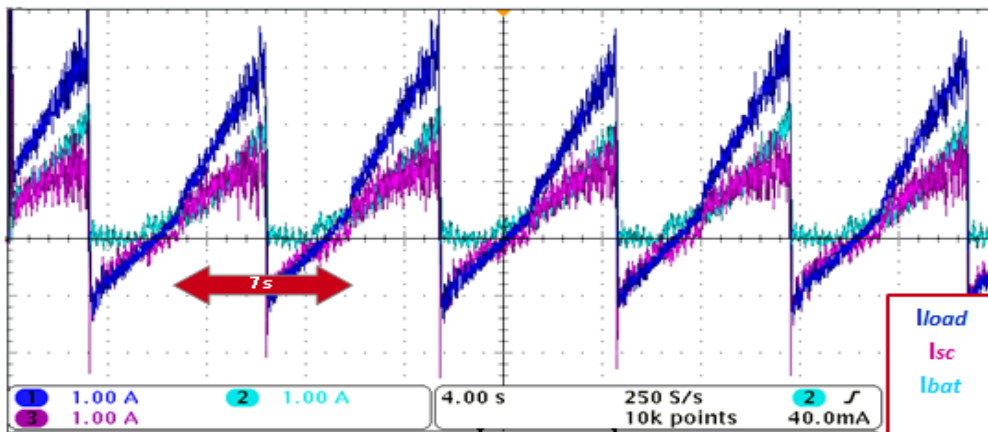


Figure 3.27 Experiments of recovering energy to HESS

Increasing the energy which can be regenerative to simulate a considerable amount of energy in the regenerative brake experiment, the inertia control is applied to the load motor. The control method is given in the block diagram above Figure 3.27. In this system the total inertial force can be adjusted by the gain k . The maximum inertial in our experiment is obtained when k is set to 5 because the limitation of the current of load motor is 6 A, and the maximum regenerative current achieved is 1.4 A.

- Dark blue line represents total load current;
- Pink line represents capacitor current;
- Blue line represents battery current;
- Green line represents current to motor torque.

It can be seen in the picture that the filter strategy is effective and the power is distributed between the super capacitor and battery.

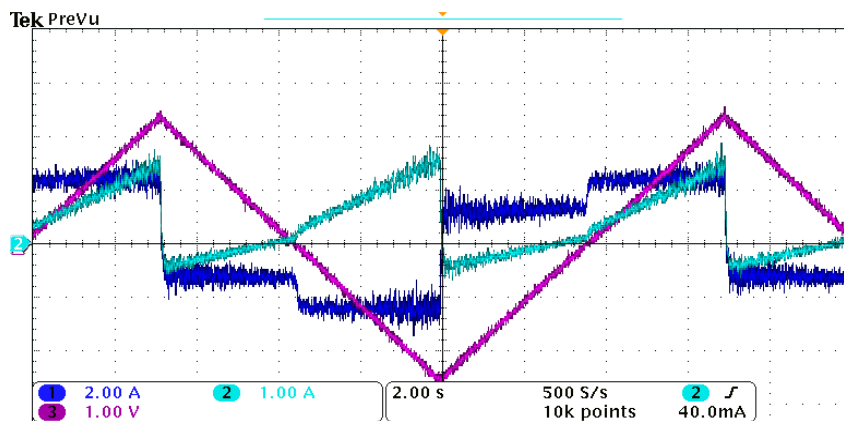


Figure 3.28 Speed control, and load torque control with increased inertia

Figure 3.28 shows the motor rolling under the speed control, and driving the load with increased inertia, speeding up and down. We can see clearly that there are regenerative beaks when the speed slows down.

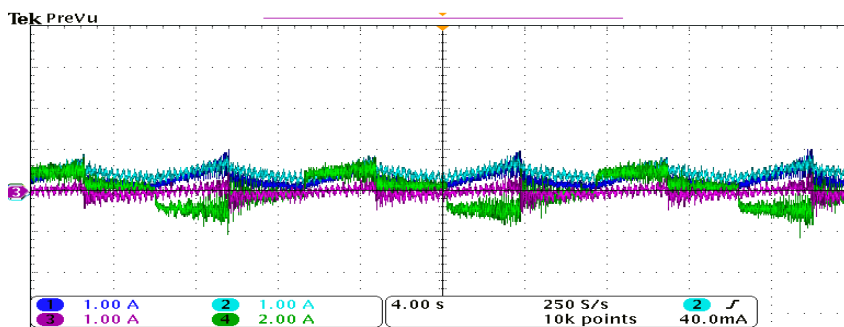


Figure 3.29 No regenerative current

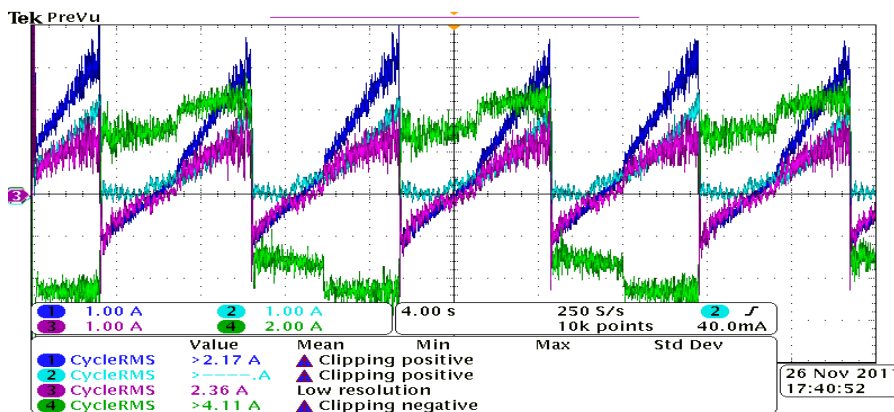


Figure 3.30 Max regenerative current 1.4 A

The filter strategy is used when the load current is positive. All the current is absorbed by the super capacitor during regenerative brake. The value of regenerative current is depending on the value of the inertia and the acceleration.

3.5 Summary

The battery and super capacitor hybrid energy system with optimized topology is analyzed. Half-controlled converter, and three-level converter topologies, operated as power interface for SC linked to DC bus, are compared and analyzed.

The controller design is introduced and the dynamic response is analyzed. HESS power sharing experiments using variable resistance load, and energy recovery experiment using motor generator system, show the efficiency of the proposed method. The next step is HESS power control and energy management strategy verification using the ground test of our EV prototype.

4 Power Control and Energy Management of HESS

4.1 Three-layer energy management system for EV HESS

In order to implement HESS, proper HESS management and power control is required. Researches in this topic can be divided into three areas. For simplification, the division is demonstrated in Figure 4.1.

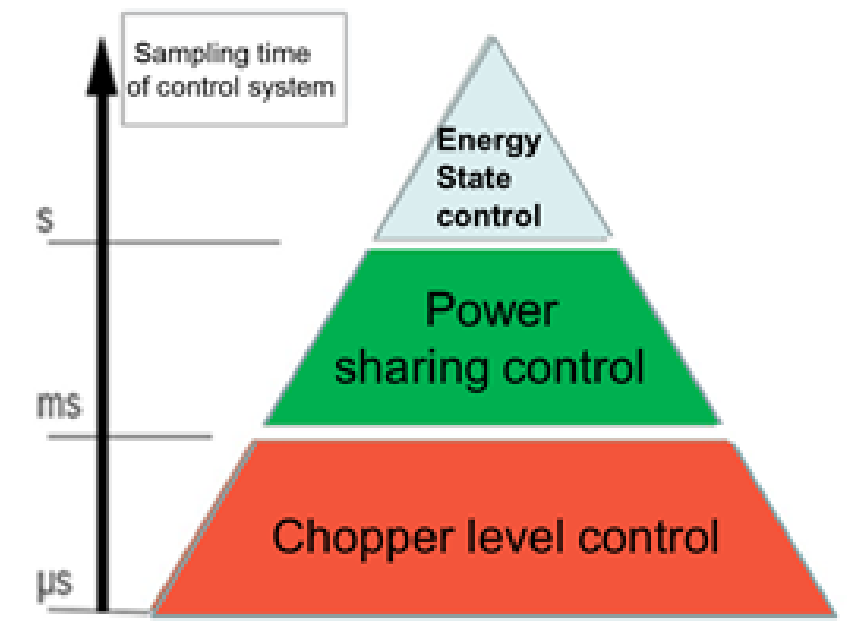


Figure 4.1 HESS management structure

The objective of the energy and power management strategy is to enhance HESS. The performance should be obtained from the power flow control among different energy sources.

In our system as shown in the Figure 4.2, the battery holds the DC bus voltage and the bidirectional DC/DC converter controls the output current from the super capacitor. This means that the power flow distribution will be decided by the load current requirement and output current from super capacitor bank. The power from battery bank will be controlled passively.

Here we proposed the three-layer control strategy for HESS as shown in the Figure 4.2.

Chopper level control

The objective of this section is controlling the output current from the converter to track the current reference. Different from the conventional converter control, here the wide range of output current response is needed as the output voltage is already suppressed by the battery bank. The control method is given in the previous chapter. Usually, this control loop is operated at up to 25 kHz, to realize the high speed response for the current tracking in high frequency domain

Power sharing control

This section realizes the power distribution control between the two energy banks. In other words, the output power from one source is controlled, the remaining part of the power will be provided by the energy bank. Here, we use the simple method as proposed before [52]. A simple filter is used to spate the power between the two energy sources as shown in Figure 4.2.

The high frequency part of the load power will be provided by the SC, and the low frequency part will be provided from the battery.

During regenerative braking, all the power will be recovered to the SC bank to increase the efficiency of the energy recovery. The decoupling frequency for the power filter can be changed according to different driving condition. The higher level controller will decide the decoupling frequency in real-time. This control loop is operated at 1 kHz to satisfy the dynamic requirement from the load power requirement for the motion of the EV.

Energy state control

This section will realize the energy management function considering the State of Charge of the SC, load current information and the State of health of the battery. The fuzzy logic algorithm is used for the decision of the operation model selection. The state of charge of SC will be considered for the continuous working of the system. The decoupling frequency for the power sharing will be decided based on different driving condition. The protection of the peak current for the SC bank will be set. This layer represents the long term goal of HESS; the control loop can be defined in 10 Hz.

In order to realize the three-layer control system, the lowest level chopper controlled is designed together with converter system, using DSP for high speed PWM signal output. The other two level controllers, for power sharing and SC State of charge control, the control algorithm will be realized by dSPACE with Simulink. The current reference signal will be transferred to the DSP from dSPACE with CAN bus in real-time.

Considering the sampling time of digital control system, the lowest control loop is operated at higher than 20 kHz, to achieve the high speed response and good performance of the current tracking in the high frequency domain. The power sharing level works at 1 kHz, to meet the requirements of the instantaneous power output for the advanced motion control of electric vehicle dynamics. The energy state control level will be the slowest. The processing can be done in second layer, because the objective of this level is long term optimization of HESS, and state of charge of SC and battery will be changed slowly.

In the system design, the chopper level controller can be designed together with the converter system. The floating-point DSP with high speed sampling time and PWM signal output is applied in this system. For the other two layer controllers, which are power sharing and energy state control, the control algorithm will be realized by dSPACE with Matlab Simulink. The advantages of this selection are that the complex advanced energy management strategy can be realized easily with Simulink for future work. On the other hand, the low level controller with DSP satisfies the high speed response with simple control algorithms.

The communication between DSP and dSPACE is realized by CAN bus, for transferring current reference signal and the state information of converter.

4.2 Power sharing control strategy with variable-frequency filter

Our control strategy includes three layer control structure, as shown in Figure 4.2, with the following:

- 1) The current class controlling the SC current;
- 2) The power distribution class controlling the power distributing in the DC bus;

3) The SoC adjustment layer controlling the SoC of SC bank.

Finally, the three-layer control structure drive the duty cycle of the dc chopper pulse width modulation to control the current from or into the SC bank. On the other hand, the current from the battery is passively controlled base on the three terminal network relationships among SC bank, battery, and load requirement.

We have successfully developed a vehicular motor traction system powered by Battery/Super capacitor Hybrid Energy System as shown below, which is used as our experiment platform in our research on HESS control strategy.

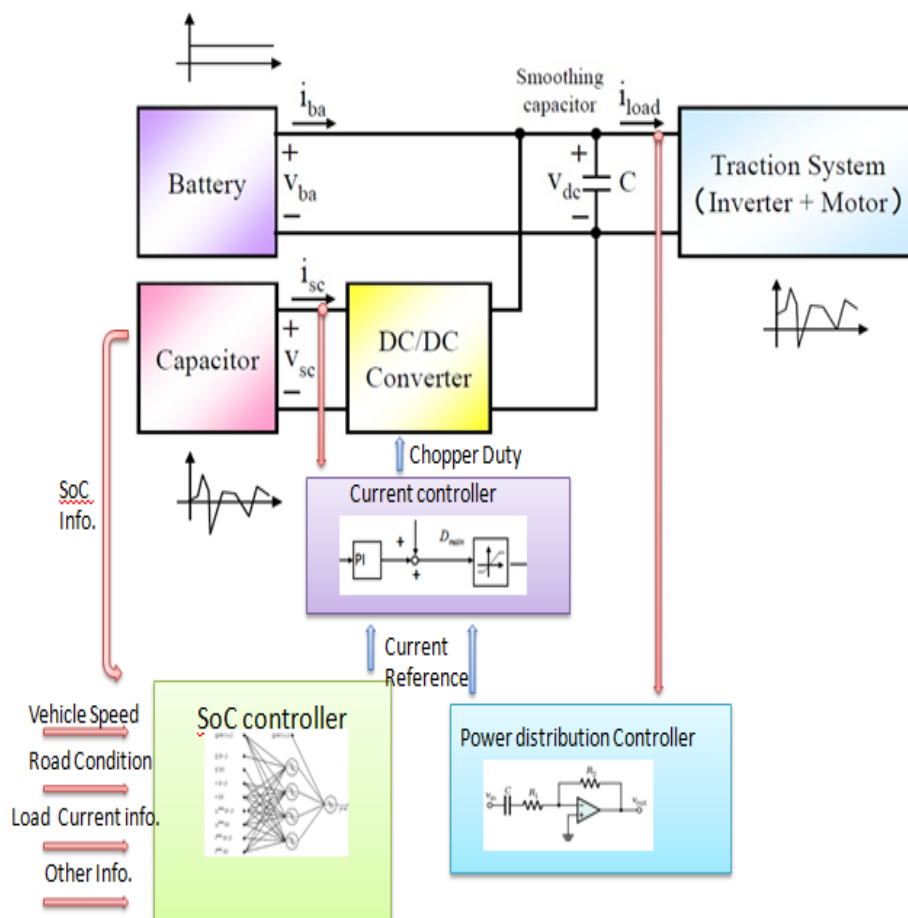


Figure 4.2 Control strategy block frame

The hardware is separated into two parts. The first part is focusing on the HESS control and the converter control. The second part is motor motion control with drive and load motor. The two parts are dependent to each other, and two control DSP chips TMS320F28335 are used in our system. The separation of the system in two parts reduces the noise from the drive motor and the control circuit for HESS.

The basic idea of power sharing method is separating the power requirement from load into two part in real-time. The high frequency part is provided by the SC bank and the low frequency part is from the battery bank. The battery stress can be release because some part of the required power is transfer to SC bank. Also peak power is remarkably decrease if the power from the battery is low frequency part. The battery life cycle is therefore can be extended. The principle is shown in Figure 4.6.

Also during regenerative braking, all the power is recovered to the SC bank by the current control algorithm. The efficiency of SC for peak power charging is higher than Lead-acid battery. Therefore the efficiency of the HESS is increased by control the recovery current flow.

Frequency-varying filter is applied in our system. The cut-off frequency can be changed based on different driving cycles. The aim for frequency varying is maximizing the efficiency of the SC bank utilization. For example, in the urban driving cycle, we increase the cut-off frequency of the power filter. So the SC can be charged and discharged with less energy every time. As we know the frequency of acceleration and deceleration cycle is high. It is good for the SC bank to provide energy assistance in a long period without returning to the charging mode.

On the other hand, during the highway driving cycle, there is a long distance between every acceleration and deceleration cycle. We can increase the cut-off frequency of the power filter to use the SC bank in deep state of charge during every speed up.

The choice of the cut-off frequency is made by the high layer controller in our system.

For the next step, the high layer controller can identify the different driving conditions, and then the decoupling frequency can be decided to optimize the energy consumptions of the whole energy system.

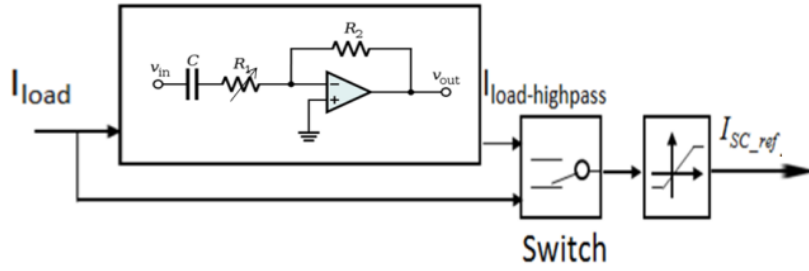


Figure 4.3 Power filter strategy block

A simple one order filter was selected for the sharing principle. As the DC bus voltage is constant, the power sharing is the current control problem.

$$\begin{cases} I_{sc(ref)}(s) = \frac{\tau s}{\tau s + 1} I_{load}(s) \\ I_{dc}(s) = \frac{1}{\tau s + 1} I_{load}(s) \end{cases} \quad \text{when } I_{load} \geq 0 \quad (4.1)$$

$$\begin{cases} I_{sc(ref)} = I_{load} \\ I_{dc} = 0 \end{cases} \quad \text{when } I_{load} \leq 0 \quad (4.2)$$

The cutoff frequency can be calculated by the equation as below.

$$f = \frac{1}{2\pi RC} = 0.1Hz$$

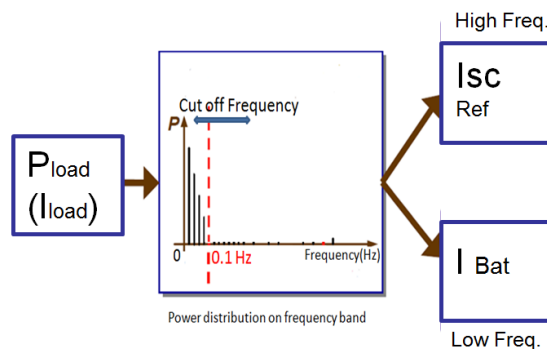


Figure 4.4 Power filter strategy description

Frequency decoupling method is a suitable solution for the power sharing in MES. The decoupling frequency is applied to the power distribution control. By modifying

the decoupling frequency based on different driving conditions, both SC and battery output power is changed to satisfy the requirement from the vehicle power train. The system behavior for different driving cycles can be analyzed using different decoupling frequencies.

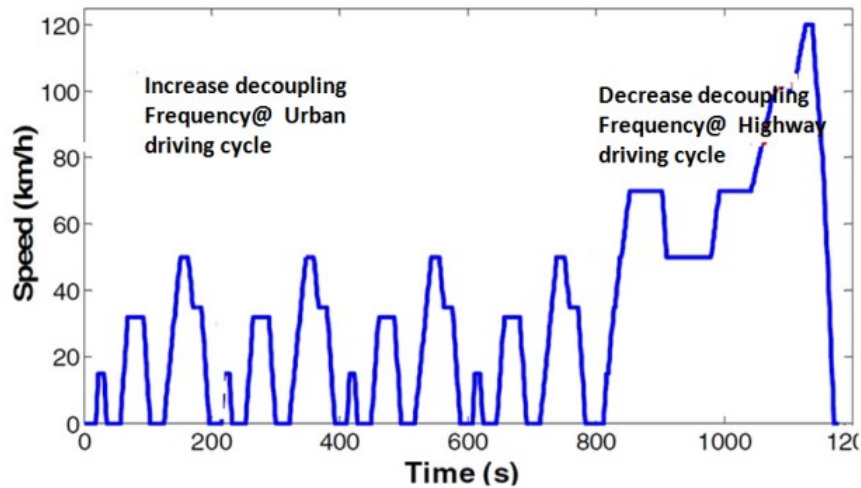


Figure 4.5 NEDC speed profiles from reference [54]

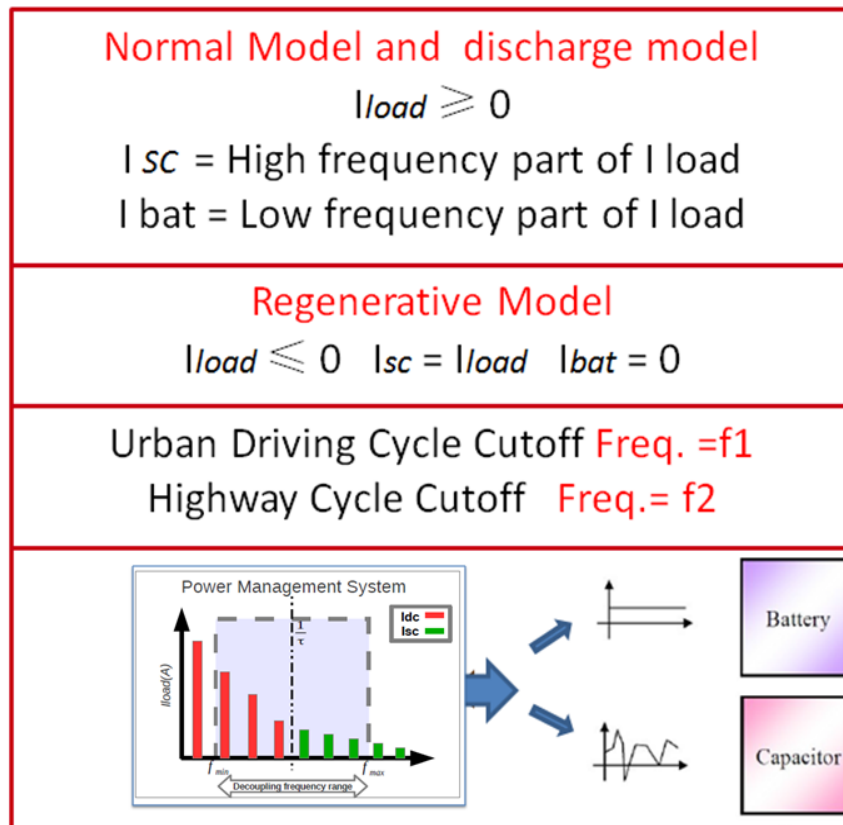


Figure 4.6 Frequency-varying filter for power sharing

The power distribution control is based on modes of operation of the hybrid structure. For regenerative braking the cut off frequency is equal to zero. frequency-varying filter works for power sharing in real-time.

4.3 Super capacitor state of charge control

SC SoC control includes two parts. The aim of first part is to keep the total energy in suitable level to ensure the SC bank work continually. It means the energy recovery of SC bank from the load or battery bank must be operated in some condition. Much information can be used to adjust the energy recovery such as real-time load power requirement and power output evolution in the next period. The second part is the SoC balance between the controlled and uncontrolled SC bank.

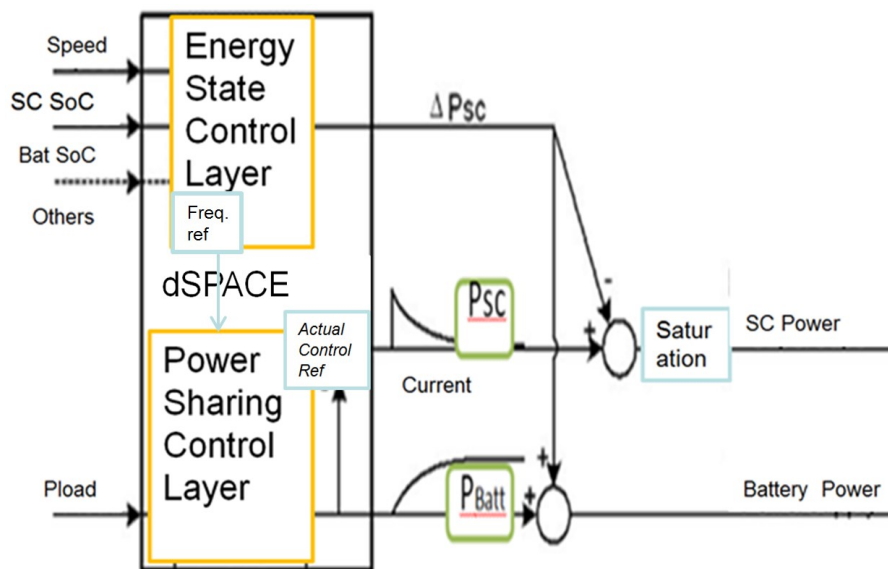


Figure 4.7 SC bank state of charge control

The algorithm of power sharing is introduced in the Figure. 4.6. The basic principle is based on the frequency decoupling of the powertrain current requirement. The high frequency section is provided by SC bank, and the left section is from battery passively. As shown in Figure 4.7, the power reference from the energy state control layer of the management system is used for control the state of charge of supercapacitor based on vehicular information input.

In our actual system, the finite-state machine principle is used for the continuous working of the HESS in a real long time driving cycle. The State of Charge of super capacitor is adjusted at the top levels, by measuring the voltage of the SC banks. I_{charge}

is set in the control system as a constant current reference I_{SC} in order to keep the state of charge of SC bank in an acceptable level.

4.4 Experimental setup and analysis

A traditional two-loop close-loop control is used to control the drive motor and the current loop control can be realized automatically by the motor driven board and the speed loop is realized by control DSP. The speed signal is used from the taco-generator and the current signal is obtained from the current sensor.

Table 4.1 Drive and load motor specification

Drive/Load Motor Specification		Output power	0.4 kW
Poles	4	Armature resistance	1.4 Ω
Rotational speed	1200 rpm	Armature inductance	3.98 mH
Voltage	60 V	Torque factor	0.35 Nm/A
Current	8.7 A	Rotor inertia	$5.88 \times 10^3 \text{ kgm}^2$

The battery used was a lead-acid GSYUASA (60 V) battery, which is composed of 6 cells and has a nominal power of 100 W. The transient auxiliary source consists of three Nisshinbo SC modules: SC0 is achieved with the connection of two individual elements in parallel (100 V and 29 F), and SC1 consist of a single module (100 V and 25 F).

As known from the basic knowledge of vehicle dynamics in textbook, the power load specification is mainly due to speed variation, tire friction dissipation, aerodynamics dissipation and mass elevation. This power, P_{motor} , can be expressed as:

$$P_{motor} = V(C_r Mg \cos(\alpha) + Mg \sin(\alpha) + M \frac{dv}{dt} + \frac{1}{2} \rho SC_x V^2) \quad (4.3)$$

Where V and M are the vehicle speed and mass, α is the road angle with a

horizontal line (in rad), C_r and C_x are the friction and aerodynamic coefficients, ρ is the air density, S is the front surface area. This equation can be obtained easily by vehicle dynamic analysis simply.

European light duty vehicles have to face the New European Driving Cycle (NEDC) which permits to evaluate and compare the different cars' performances in Europe. The NEDC consists of repeated urban cycles (called ECE-15 driving cycle) and an Extend-Urban driving cycle [54]. Figure 4.5 shows the ECE-15 cycle with the speed and the power demand of a car following a flat road. Also sudden power changes can be noticed each time the driver requires a speed change.

The proposed control strategy is mainly based on power filter strategy in the frequency domain of the power source of the load. This energy-management strategy fulfills the fast energy demands of the load and respects the integrity of each source. Precisely, the main idea is to assign the load power demands to the appropriate source.

The experimental results reveal and confirm the efficiency of the control strategy of the one-converter structure. In particular, the following key points can be observed.

- 1) The SCs' supplies most of the transient power required by the load.
- 2) The SCs' power has the fastest dynamics. The battery power has the slowest dynamics and both are well tuned.
- 3) The load requirements are always satisfied on the whole driving cycle.

A small scale test platform is designed before the HESS is setup to electric vehicle. A 400 W Motor Generator System is used for simulating the driving cycle pattern. The energy share between battery and capacitor, and the regenerative braking recovery can be compared using different decoupling frequencies, to verify the applicability of the proposed control system.

For the HC converter, the controlled SC bank is interconnected to the dc bus using a chopper built with 500 V 50 A power MOSFET modules. The switching frequency of the PWM is set up to 20 kHz. The inductor has a value of 1.8 mH with a rated current of 12 A.

Table 4.2 Half-controlled converter specification

Main circuit of HC converter	
Inductor	1.8 mH 12 A
Output capacitor	560 mF 350 V
Power MOSFET	Fuji 2MI50F-050
Working frequency	Up to 20 kHz
Balancing Circuit	
Inductor	3.9 mH, 2.8 A
Power MOSFET	IRF740LC
Working frequency	40 kHz

For the experiment, TI DSP32028355 is used as the low level controller linked together with the HC converter. And dSPACE DS1005 is used as high level controller of the HESS. At the battery bank, five GS Yuasa Lead acid batteries are connected in series to DC bus. The SC bank is built with two modules, and also connected in series to DC bus. The system hardware verified in Figure 4.8.

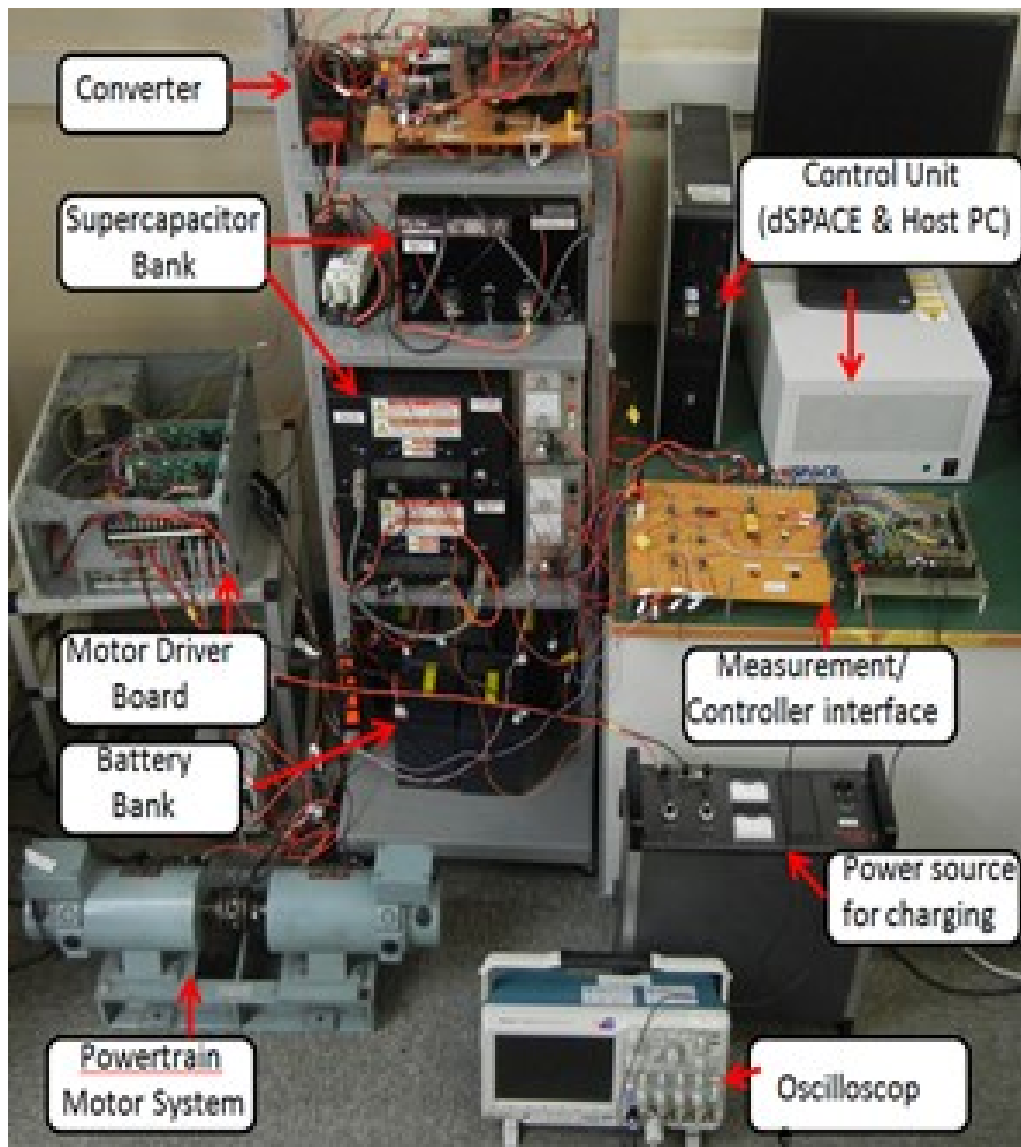


Figure 4.8 Reduced scale test platform for hybrid energy system.

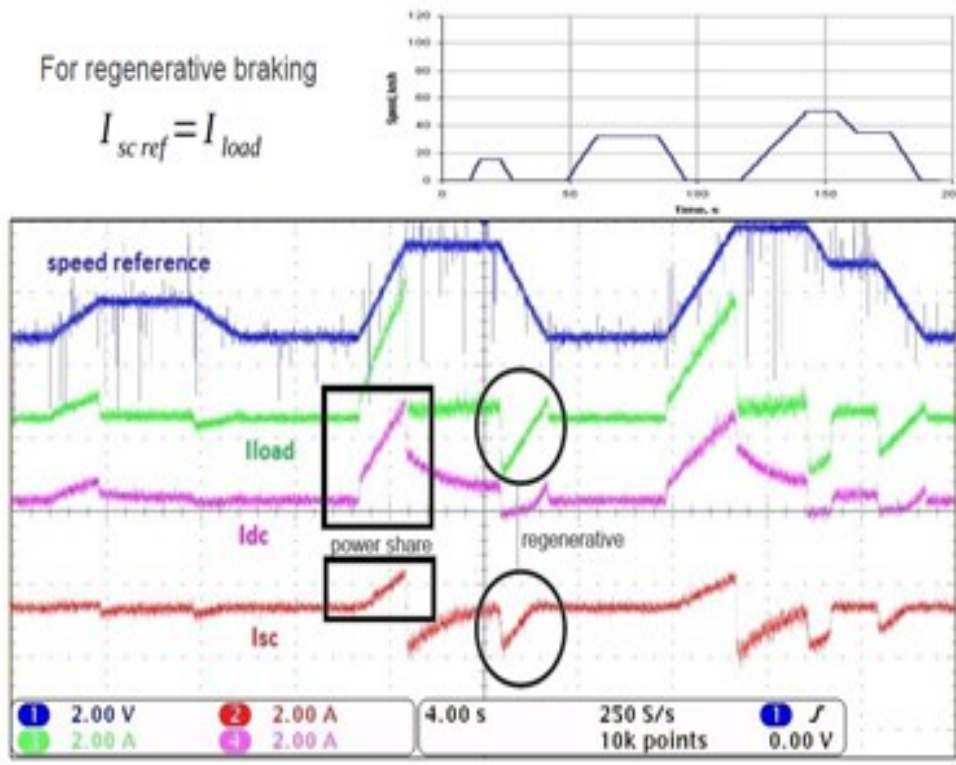


Figure 4.9 Power sharing and regenerative brake in simulated ECE15 driving cycle

A simulated ECE15 drive cycle for the DC motor powertrain is generated by the speed reference. In Figure 4.9, the output power is shared by the battery bank and SC bank, with the principle of frequency decoupling strategy. Also all the power is recovered to the SC bank when regenerative brake during the motor deceleration.

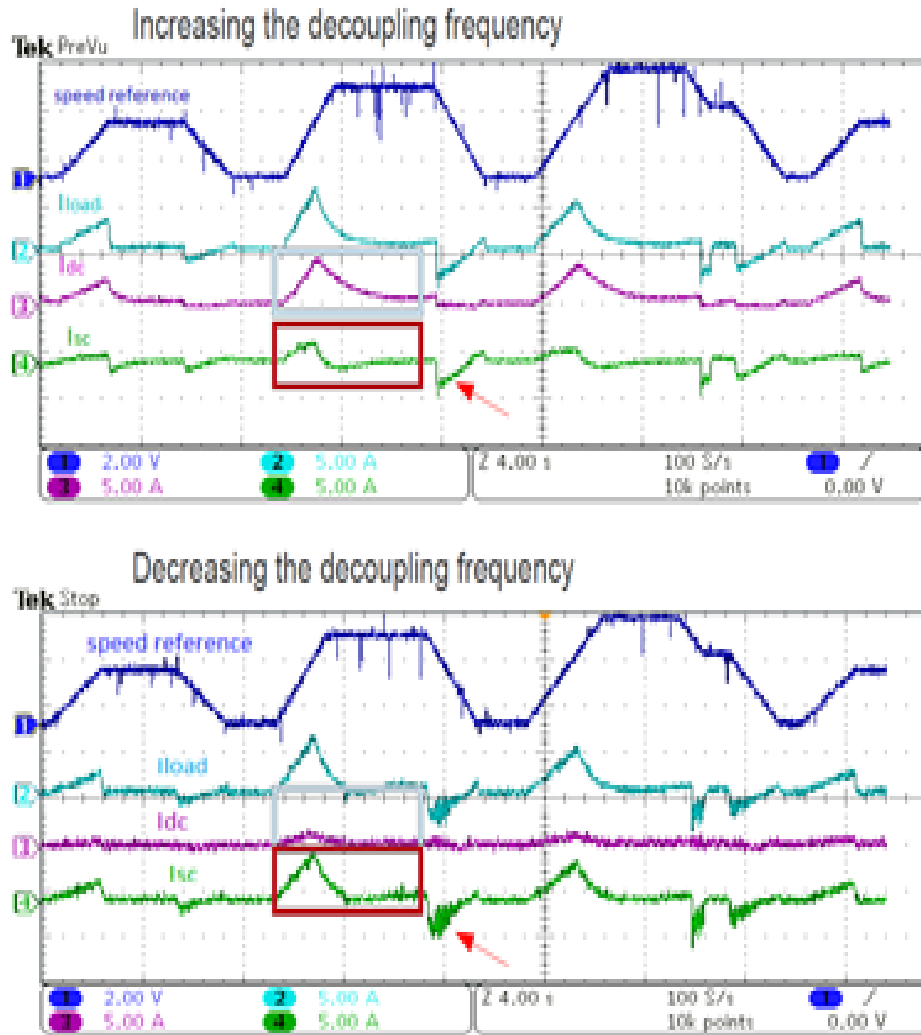


Figure 4.10 Test of HESS with variable frequency decoupling strategy [53]

With different decoupling frequencies, the energy sharing between battery and super capacitor, and the regenerative braking recovery can be compared as shown in Figure 4.10. At lower decoupling frequencies, the SC bank will provide more energy to the DC bank. As shown in the second part of Figure 4.10, the current from battery is limited to less than 1 A when the cutoff frequency is less than 0.01 Hz.

4.5 Summary

In this chapter, a three-layer control system is proposed as the energy management system of HESS after the power interface design. Variable frequency decoupling method is applied as the basic power sharing strategy between battery and super capacitor. The structure of the whole energy management strategy is discussed, and

the state of charge of SC bank is considered for vehicular energy system operation. The laboratory-scale test platform tests and experiments are introduced in this chapter.

5 Design of EV Prototype with HESS and Onboard Experiment Results

5.1 Introduction of experimental platform

The hybrid electric vehicle prototype for our research is given as Figure 5.2. The original EV is named CMOS, manufactured by Toyota Auto body Co., Ltd. Here we mounted the hybrid energy system to this vehicle body frame, as shown in Figure 5.3. Firstly, the motion control ECU is added and the inverters of the two in-wheel motors are modified, aiming to satisfy the requirement of vehicle advanced motion control research. For the hybrid energy system research, the energy management processor, converter system, and SC energy banks are installed in this EV.



Figure 5.1 Sections of hybrid energy EV CMOS

The main parameters are listed in Table 5.1.

Table 5.1 Main parameters of Hybrid EV

EV body	Toyota autobody COMS
In wheel motor	Peak power 2 kW X 2
Maximum speed	50 km/h
Weight	430 kg
DC bus voltage	72cV
Battery bank	Lead-acid 12 V 42 Ah X 6
SC bank X 3	90 V 64 F module
DC bus converter	Peak current 100A

As we designed, the HESS in the EV will be operated in different models, listed below:

- Normal model: SC and battery both provide energy to load following the energy management principle;
- Charge model: the EV SC bank is in low SoC. The system should charge the SC form battery or from load power regeneration;
- Regenerative model: the motor recover energy to energy storage device;
- Error model: the SC or battery, one energy source does not work or over load happened.

So our energy management system and control principle should be designed based on this four basic operation models.

5.2 Prototype design and experiments of converters for HESS

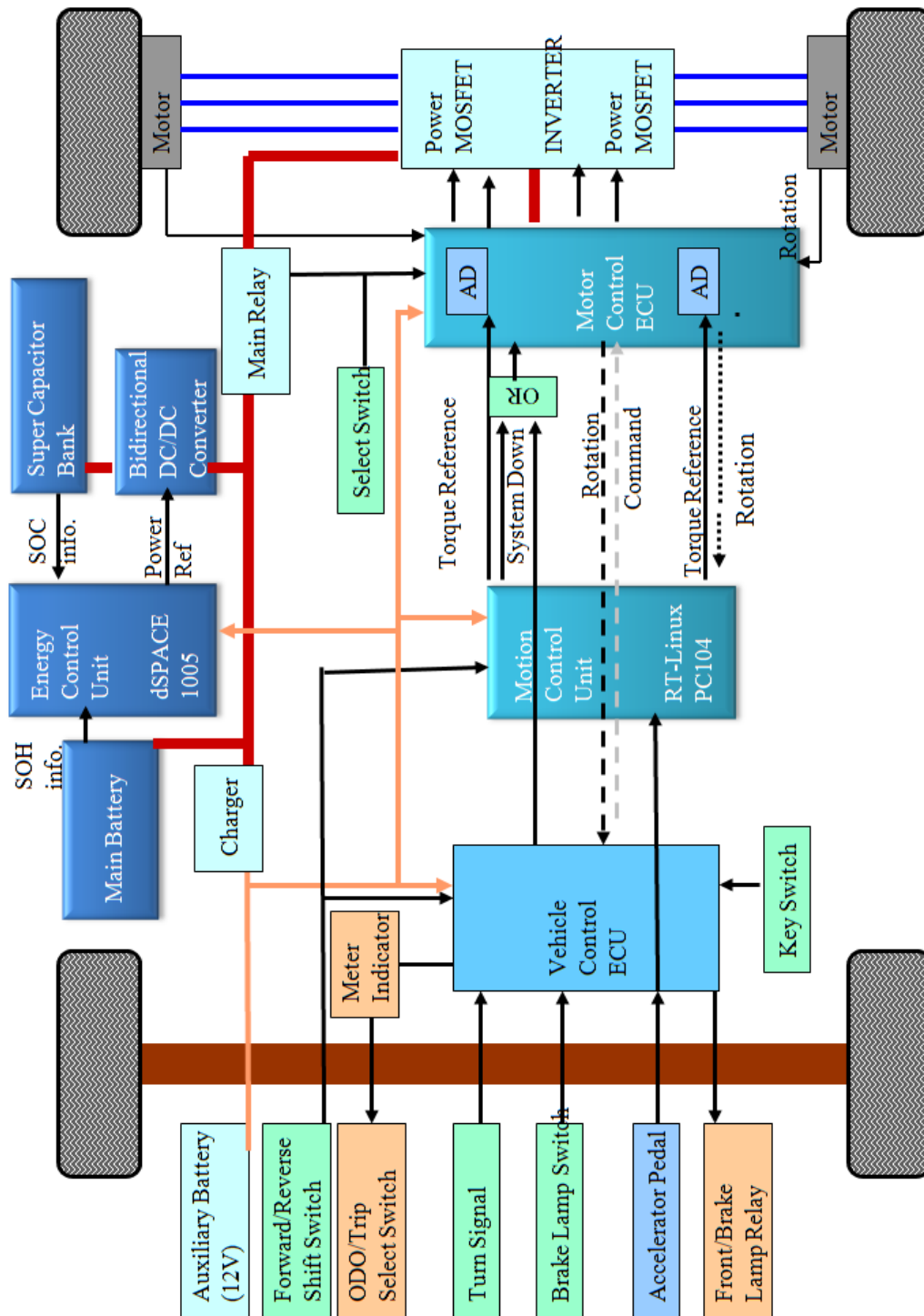


Figure 5.2 System structure of our EV with HESS

The prototype of EV with battery and super-capacitor hybrid energy system and driven by in-wheel motor system is shown in Figure 5.3, for our experiments and further research. The EV prototype is based on the Toyota EV COMS. The hybrid energy system with SC bank and converter control system is designed. The parameters of the hybrid EV prototype are shown in Table 1. The DC bus voltage of the energy system is 72 V, which is hold by the Lead-acid battery modules group. The maximum current output from SC bank is designed to be up to 100 A, considering the chopper size and the control algorithm.



Figure 5.3 Arranged hybrid energy systems for EV prototype

We can obtain the limiting duty of the main and balance PWM control and realize them in the algorithm.

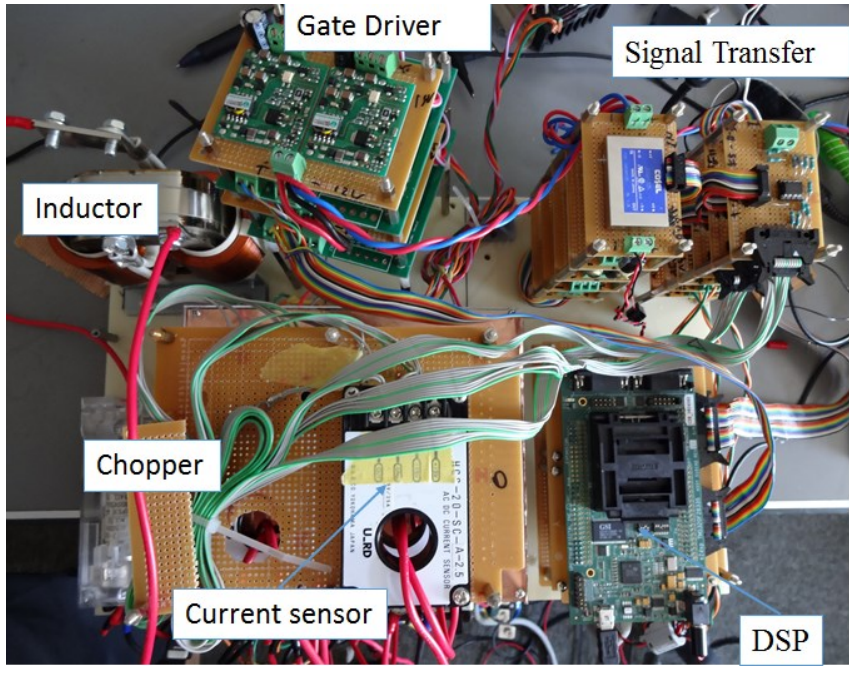


Figure 5.4 Converter structure setup to vehicle prototype

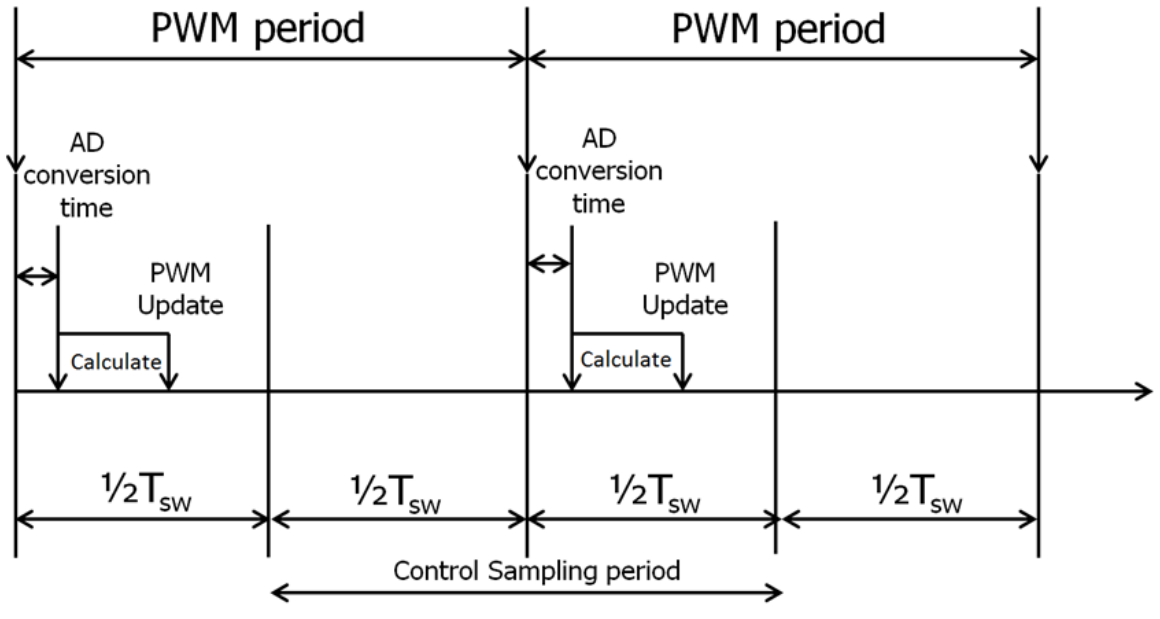


Figure 5.5 Program in the sampling period in converter controller DSP

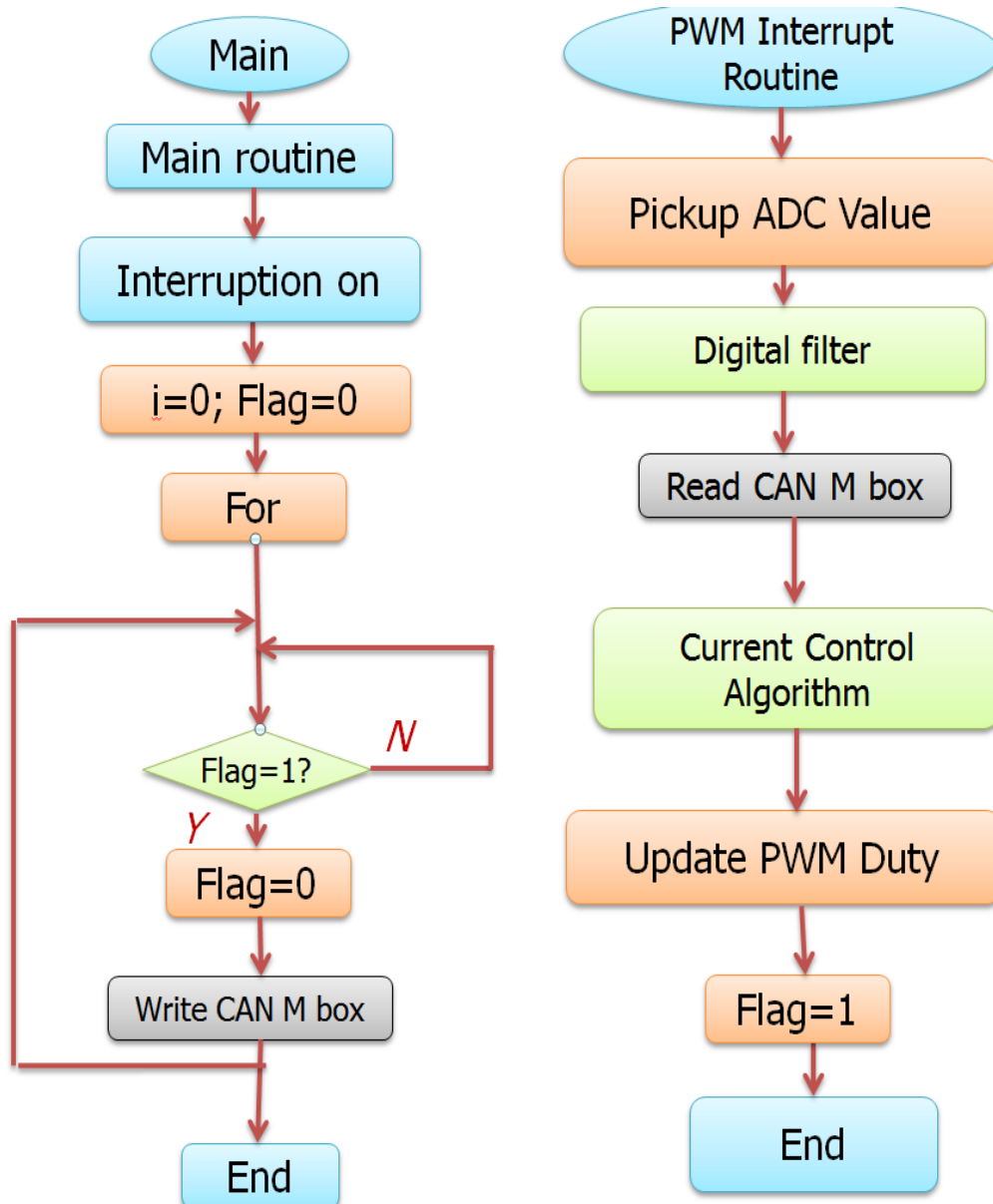


Figure 5.6 Simple flow chart of DSP program with high level controller communication

The tests and experiments is realized in a reduced scale powertrain system before implementing the HESS with converter prototype to the electric vehicle COMS. The 200 seconds simulated driving cycle is applied to test the HESS power sharing and converter control. The load and the powertrain system is realized with the 600 W DC motor- generator system.

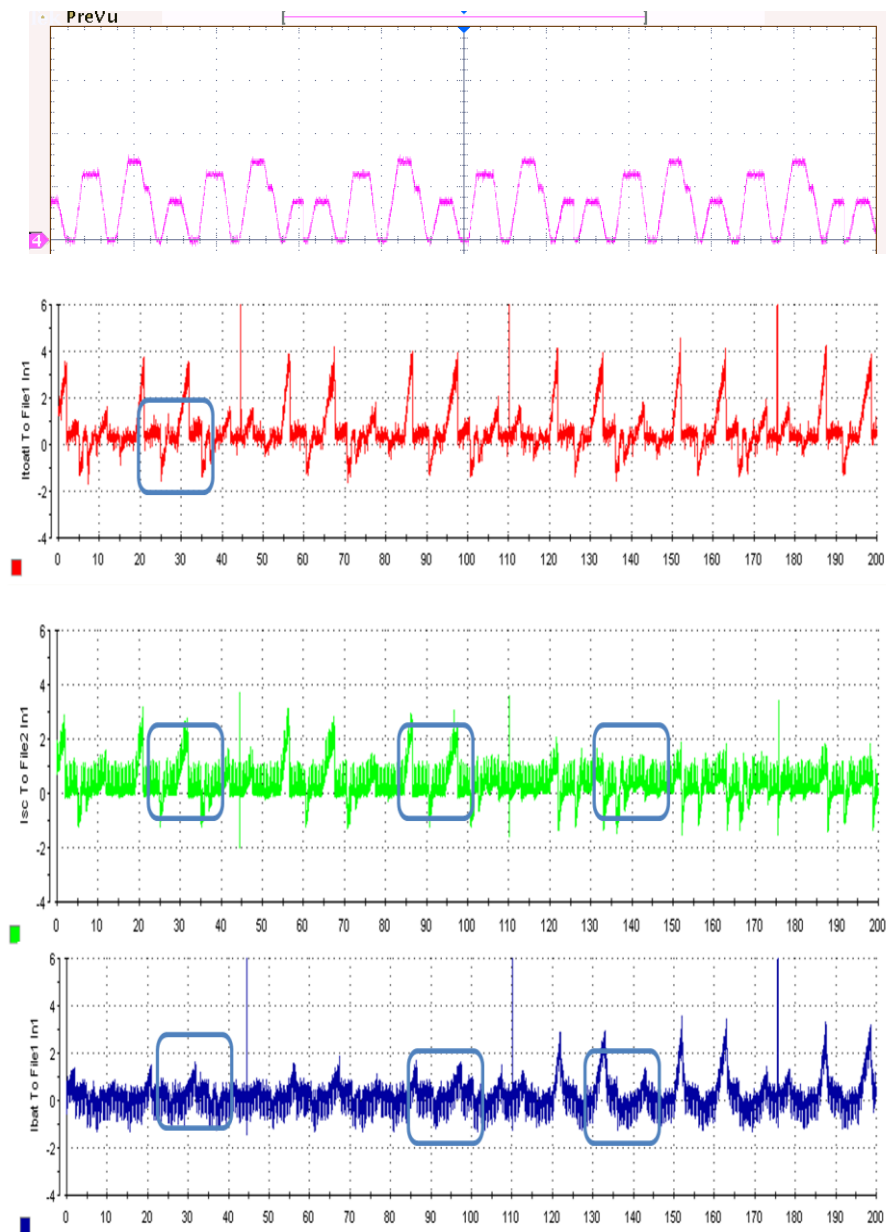


Figure 5.7 Experiment result in simulated urban drive cycle

In Figure 5.7 and Figure 5.8, it can be seen that the power for load can be separated to two sections. High frequency part is from SC, while low frequency part from battery. All the recovered energy returns to SC bank, improving the energy efficiency of the whole system.

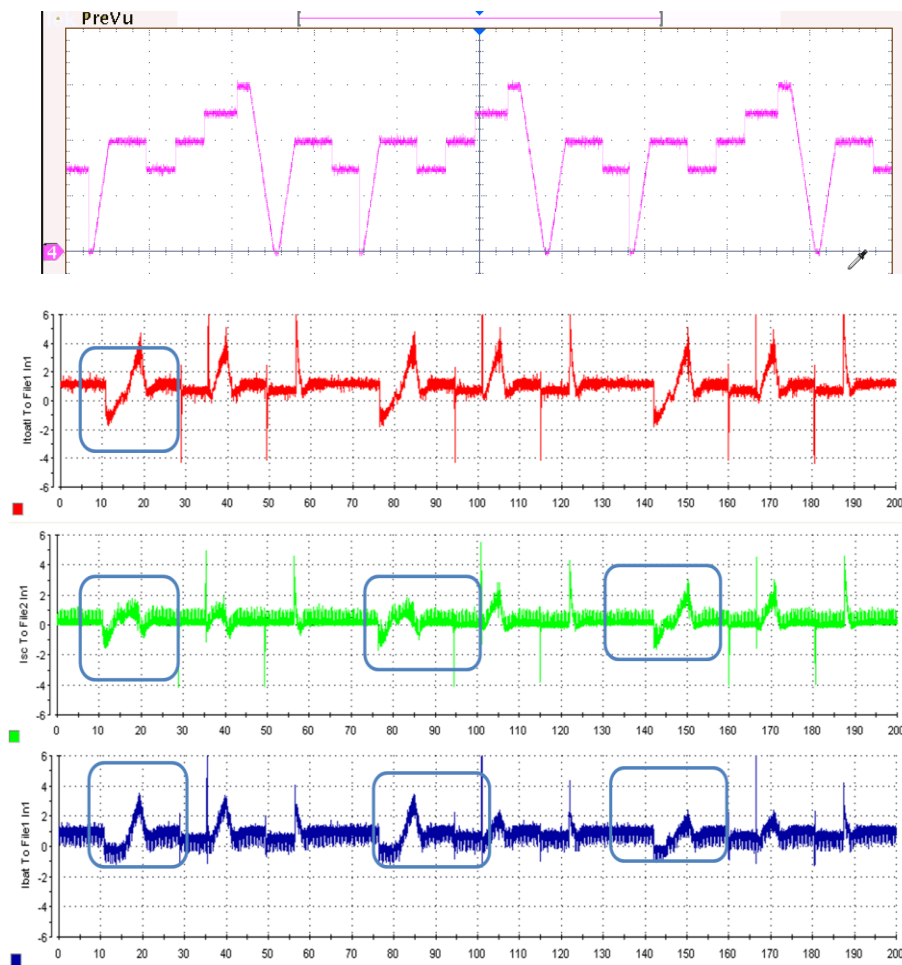


Figure 5.8 Experiment results in simulated highway driving cycle

Frequency-varying filter strategy can be used in different driving cycle to maximize the use of SC. The range of the cutoff frequency is from 0.01 Hz to 2 Hz. The energy from SC and battery is nearly the same in one driving cycle when the cutoff frequency is near to 0.09 and nearly 30% of the energy is recovered to SC bank in every drive cycle.

Table 5.2 Analysis of energy sharing and decoupling frequency

Energy (kJ) in test cycle	Defined decoupling frequency			
	0.012	0.122	0.56	2.20
Required from motor load	1.67	1.91	1.92	1.90
Provided by SC	0.43	1.15	1.47	1.54
Proportion of energy from SC (%)	25.7	60.2	76.6	81.1
Energy from regeneration	0.31	0.29	0.29	0.30
Recovered to SC	0.24	0.24	0.24	0.25
Proportion of recovered energy (%)	14.4	12.6	12.5	13.2

Proportion of energy sharing in test cycle (%)

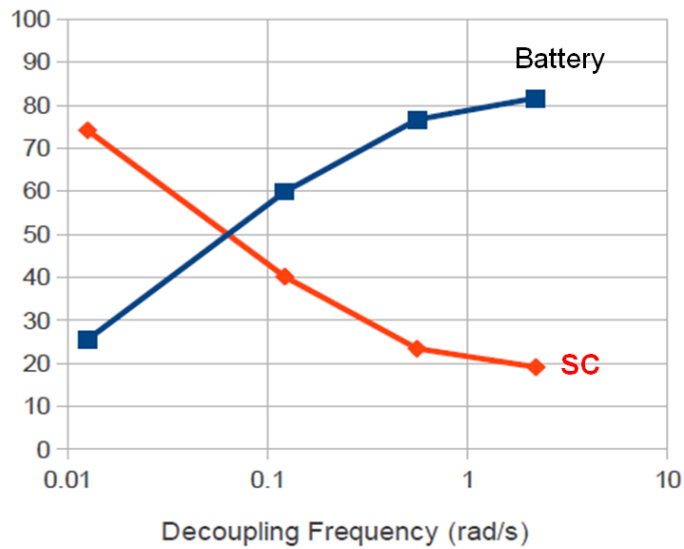


Figure 5.9 Relationship between decoupling frequency and output energy proportion of batter and SC

Based on the experiment results analysis, the decoupling frequency can be selected between 0.01 Hz to 2Hz, which can realize the 20%-80% of total energy provided from SC bank in our test driving cycle. It can be the reference of the SC bank capacity selection in the prototype design.

6 Conclusions and Future Works

This research focuses on the electrical power hybridization of battery and super capacitors. Battery/SC hybrid architecture has been proposed to minimize the number of power converters. Half-controlled converter is used to the transient source (SCs). A three-layer control structure has been developed and successfully implemented. It has been shown that the hybrid source is able to provide any load demand and to satisfy the sources inherent characteristics: battery and SC voltage and current limitations, are considered, as well as slow battery dynamics. Despite of the single degree of freedom, this innovative control strategy is proved to be simple and effective.

The three-layer control strategy for battery and super capacitor hybrid energy system is proposed. The HESS test platform with whole control system is also introduced. Half-controlled converter topology as the optimized power interface is successfully applied to the system. Also SC State of Charge management is considered for the continuous working of HESS. Frequency decoupling approach for powering sharing between the two energy banks is introduced. The test with the powertrain of the DC motor generator system under the simulated ECE drive cycle proved the effectiveness of the system.

The advantages of this system are the following: the power can be distributed by high level controller with the consideration of vehicular information. The battery stress will be decreased when the peak power is provided by SC bank. The efficiency of the whole system will be increased by power sharing principle and regenerative brake. The recharging of the SC by battery can be realized for management the state of charge for SC bank.

HESS with half-controlled converter is implemented to the small scale electric vehicle, COMS. The powertrain system is two in wheel motor with peak power of 2 kW. The DC bus voltage will be 72 V and the converter designed in this paper satisfies the requirement of the SC output power in EV system. This power sharing and energy management strategy is tested and analyzed in reduced scale driving environment.

The main future works includes two aspects. The HESS and converter test platform has been constructed, and the vehicle prototype is setting up. One aspect is to further ground test for HESS control using EV prototype. The second aspect is combining

hybrid energy system with wireless charging for electric vehicles. Dynamic charging while driving and charging power control are the two challenges for wireless power transfer technology application to EV hybrid energy system

Appendix

Advanced Charging System for HESS using Wireless Power Transfer

A.1 Requirement analysis HESS charging using WPT

Energy capacity of electric energy system is much lower than combustion engine. In order to improve the cruising range of EV, HESS should be charged repetitively. On the other hand, Wireless Power Transfer (WPT) via magnetic resonant coupling is suitable for repetitive charge and moving cars [55, 56, 57]. WPT via magnetic resonant coupling was first introduced in 2007, realizing high transmission efficiency over relatively larger gap compared to the induction method. Based on this, it is suitable for the application of EV contactless charging. Figure A.1 shows the characteristics and relationships of battery, SC and WPT as energy sources for electric vehicles. Figure A.2 shows the conception of Choco-Choco charging to future EV system.

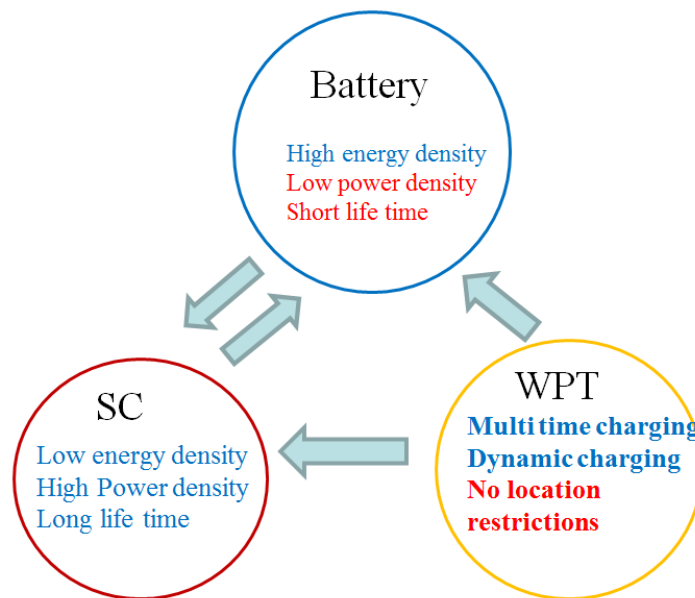


Figure A.1 Characteristics of battery, SC, and WPT as EV energy sources

The whole EV charging system using WPT via magnetic resonant with converter face to EV DC bus is shown in Figure A.3. The main sections are power source,

transmitter antenna, receiver antenna, and the rectifier. DC-DC converter is necessary for the charging system linked to battery and super capacitor energy banks.

For high transmission efficiency, load impedance control with DC-DC converter is proposed [58, 59]. The control of the power sources side is also necessary for wireless station charging. Moreover, due to energy capacity of HESS is limited, charging power should be taken into consideration and controlled according to SoC information.



Figure A.2 Conception of Choco-Choco charging to EV [58]

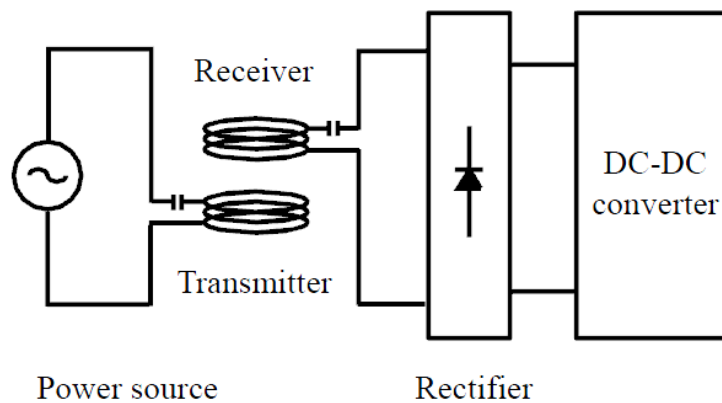


Figure A.3 WPT charging system with converter interface for HESS [59]

A.2 HESS Capacity design method with WPT charging

EV prototype powered by HESS and WPT charger is shown in Figure A.4. The topology of the energy system is in Figure A.5. All the energy devices are linked to DC bus. For prototype design, the charging mode should be defined, and the capacity

decision of battery and super capacitor energy banks is necessary for HESS design. In this section, the principle of HESS design with WPT charging mode description is proposed. The converter efficiency and power loss will not be considered in this part, and more accurate estimation method should be based on special converter and power interface. The optimized capacity of HESS considering WPT frequent charging can be obtained by the proposed method as below.

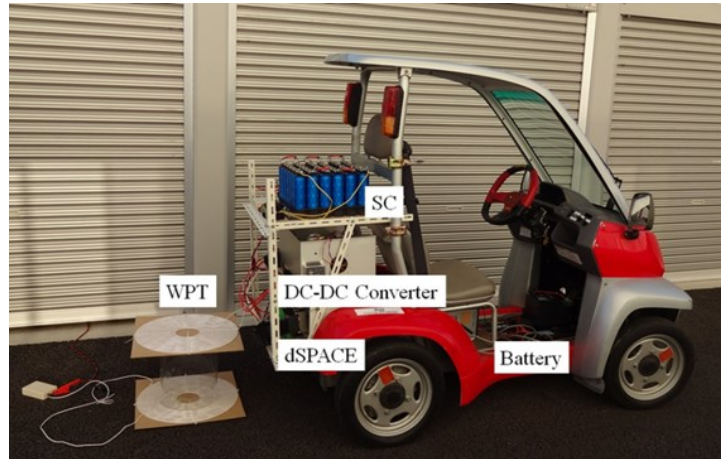


Figure A.4 EV prototype with HESS and WPT charger

As shown in Figure A.5, all parameters for describing the performance of battery and SC in HESS are given in Table A.1. The weight rate of SC determines the proportion of SC and battery. Then the total energy in HESS can be calculated if the total weight of HESS can be obtained. So the optimization and design of the total weight of HESS M_{HESS} should be done.

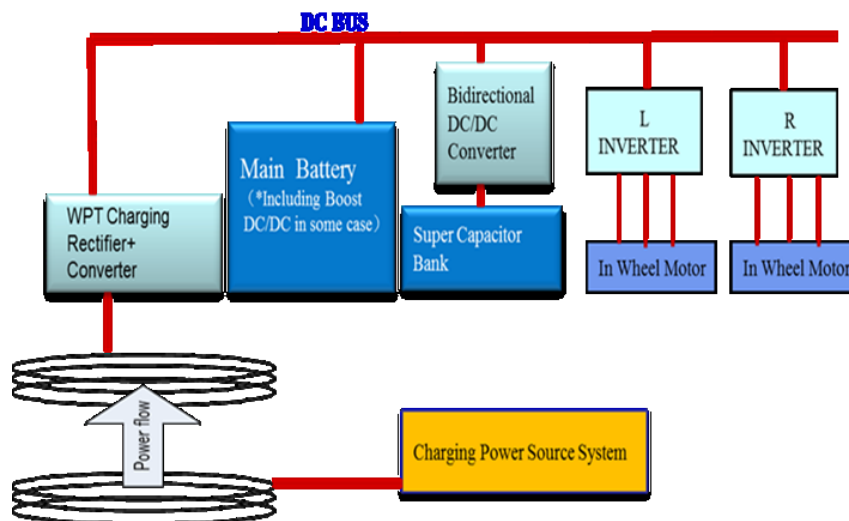


Figure A.5 Energy system topology of Hybrid CMOS with WPT charger

Table A.1 Performance parameters for EV HESS

Discharge density battery	P_{Bdis} [W/kg]
Energy density of battery	e_{Bat} [Wh/kg]
Energy in battery bank	E_{Bat} [Wh]
Charge power of battery	P_{Bch} [W]
Discharge power of battery	P_{Bdis} [W]
SC power density	p_{SC} [W/kg]
SC bank total energy	E_{SC} [Wh/kg]
SC bank total power	P_{SC} [W/kg]
SC energy density	e_{SC} [Wh/kg]
HESS charge power	P_{charge} [W]
HESS discharge power	P_{dis} [W]
Weight rate of SC in HESS	α
Total Weight of HESS	M_{HESS} [kg]

The EV driving condition and WPT charging strategy can be defined in Figure A.6. There are several charging times in one driving cycle, following Choco-Choco charging mode. The parameters for describing WPT charging and energy consumption for EV power train are given in Table A.2 and Table A.3 respectively.

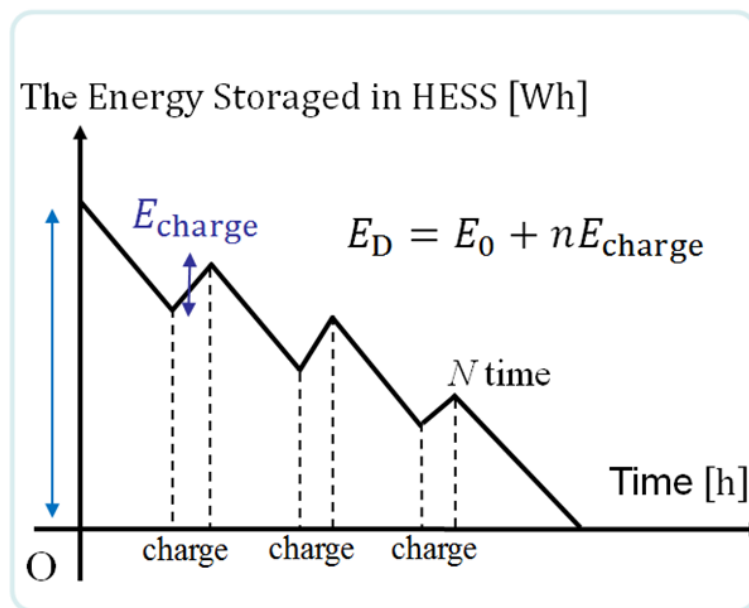


Figure A.6 WPT charging mode for HESS in one driving cycle

Table A.2 Parameters for EV HESS in driving test

Energy after driving cycle	E_D [Wh]
Energy before driving cycle	E_0 [Wh]
Average power to powertrain	P_D [W]
Discharge density Battery	P_{Bdis} [W/kg]
HESS discharge power	P_{dis} [W]

Table A.3 Parameters for WPT charging system

HESS charge power	P_{charge} [W]
HESS charge energy	E_{charge} [Wh]
Charging times	n
Charge degree	Q
Wireless charging power	P_{WPT} [W]

Here the charge degree should be explained clearly. Our principle of HESS charging using WPT is that super capacitor modules should be charged with priority, which can increase the whole system efficiency, just like the same principle in regenerative braking. So the Charge degree Q means the proportion of charged energy and total energy of battery bank, after the super capacitor is fully charged, during one charging time.

The HESS capacity can be designed by the optimization constraints, shown in Figure A.7. An example with equation description is given in Figure A.8 in detail.

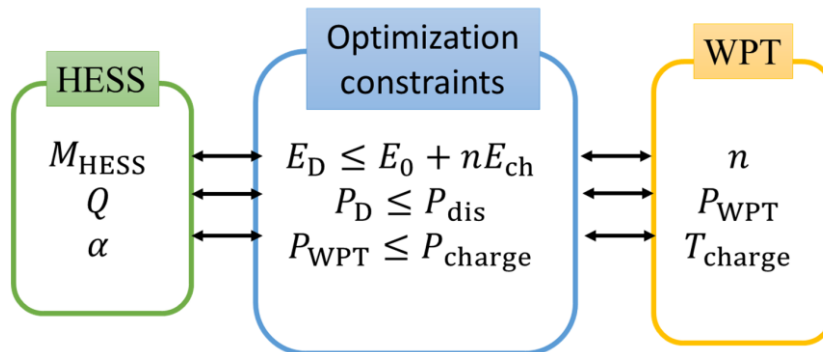


Figure A.7 Optimization constraints for HESS charging using WPT

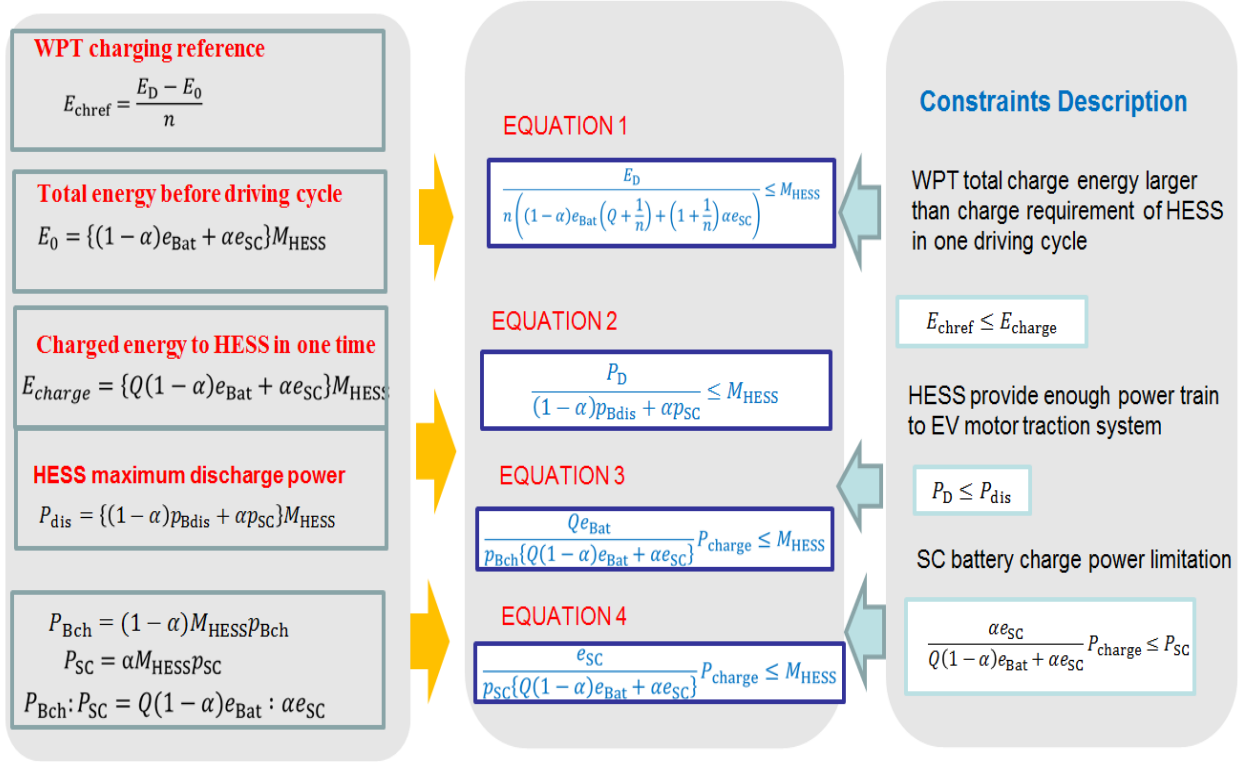


Figure A.8 Example of HESS capacity design with WPT charging

In summary, M_{HESS} can be designed in minimum size based on calculating Equation 1, 2, 3, and 4 in Figure A.8. When there is no charging in driving cycle, the parameter Charging time is equal to zero. The method is also suitable for the HESS capacity design without WPT charging, which is introduced in Chapter 2.

The capacity design method has already been applied to calculate the energy size of electric agricultural machinery powered by hybrid energy system with WPT charging for future industrial applications. The results are shown in [60].

Bibliography

1. Chan, C.C., "The state of the art of electric and hybrid vehicles," Proceedings of the IEEE, vol.90, no.2, pp.247-275, Feb. 2002.
2. Khaligh, A, Zhihao Li, "Battery, Ultra capacitor, Fuel Cell, and Hybrid Energy Storage Systems for Electric, Hybrid Electric, Fuel Cell, and Plug-In Hybrid Electric Vehicles: State of the Art," IEEE Trans. on Vehicular Technology, vol.59, no.6, pp.2806-2814, July 2010.
3. Hori, Y., "Future vehicle society based on electric motor, capacitor and wireless power supply," Power Electronics Conference (IPEC 2010), pp.2930-2934, 21-24 June 2010.
4. Kawashima, K., Uchida, T., Hori, Y., "Development of a novel ultra capacitor electric vehicle and methods to cope with voltage variation," Vehicle Power and Propulsion Conference, 2009. VPPC '09, pp.724-729, 7-10 Sept. 2009.
5. Kawashima, K., Hori, Y., Uchida, T., "Stabilizing control of vehicle motion using small EV driven by ultra-capacitor," 31st Annual Conference of IEEE, IECON 2005, 6-10 Nov. 2005.
6. Ortuzar, M., Moreno, J., Dixon, J., "Ultracapacitor-Based Auxiliary Energy System for an Electric Vehicle: Implementation and Evaluation," IEEE Trans. on Industrial Electronics, vol.54, no.4, pp.2147-2156, Aug. 2007.
7. Dixon, J., Nakashima, I., Arcos, E.F., Ortuzar, M., "Electric Vehicle Using a Combination of Ultracapacitors and ZEBRA Battery," IEEE Trans. on Industrial Electronics, vol.57, no.3, pp.943-949, March 2010.
8. Moreno, J., Ortuzar, M.E., Dixon, J.W., "Energy-management system for a hybrid electric vehicle, using ultracapacitors and neural networks," IEEE Trans. on Industrial Electronics, vol.53, no.2, pp. 614- 623, April 2006.
9. Martinez, J.S., Hissel, D., Pera, M.-C., Amiet, M., "Practical Control Structure and Energy Management of a Testbed Hybrid Electric Vehicle," IEEE Trans. on Vehicular Technology, vol.60, no.9, pp.4139-4152, Nov. 2011.
10. Tae-Suk Kwon, Seon-Woo Lee, Seung-Ki Sul, Cheol-Gyu Park, Nag-In Kim, Byung-il Kang, Min-seok Hong, "Power Control Algorithm for Hybrid Excavator With Supercapacitor," IEEE Trans. on Industry Applications, vol.46, no.4, pp.1447-1455, July-Aug. 2010.

11. Yee-Pien Yang, Jieng-Jang Liu, Tsan-Jen Wang, Kun-Chang Kuo, Pu-En Hsu, "An Electric Gearshift With Ultra capacitors for the Power Train of an Electric Vehicle With a Directly Driven Wheel Motor," IEEE Trans. on Vehicular Technology, vol.56, no.5, pp.2421-2431, Sept. 2007.
12. Emadi, A, Rajashekara, K., Williamson, S.S., Lukic, S.M., "Topological overview of hybrid electric and fuel cell vehicular power system architectures and configurations," IEEE Trans. on Vehicular Technology, vol.54, no.3, pp.763-770, May 2005.
13. Colton, S.; "A Simple SerieBattery/Ultracapacitor Drive System for Light Vehicles and Educational Demonstration," Massachusetts Institute of Techology Edgerton Center, Summer Engineering Workshop 2008.
14. Engineering Workshop 2008.Greenwell, W., Vahidi, A., "Predictive Control of Voltage and Current in a Fuel Cell–Supercapacitor Hybrid," IEEE Trans. on Industrial Electronics, vol.57, no.6, pp.1954-1963, June 2010.
15. Zandi, M., Payman, A., Martin, J.-P., Pierfederici, S., Davat, B., Meibody-Tabar, F., "Energy Management of a Fuel Cell/Supercapacitor/Battery Power Source for Electric Vehicular Applications," IEEE Trans. on Vehicular Technology, vol.60, no.2, pp.433-443, Feb. 2011.
16. Azib, T., Bethoux, O., Remy, G., Marchand, C., Berthelot, E., "An Innovative Control Strategy of a Single Converter for Hybrid Fuel Cell/Supercapacitor Power Source," IEEE Trans. on Industrial Electronics, vol.57, no.12, pp.4024-4031, Dec. 2010.
17. Haihua Zhou, Bhattacharya, T., Duong Tran, Siew, T.S.T., Khambadkone, A.M., "Composite Energy Storage System Involving Battery and Supercapacitor With Dynamic Energy Management in Microgrid Applications," IEEE Trans. on Power Electronics, vol.26, no.3, pp.923-930, March 2011.
18. 高橋正好: “減速回生システム i-ELOOP のデバイス開発”, マツダ技報 No.30, pp.43-50, 2012 (in Japanese).
19. 小谷和也: “i-ELOOP 制御技術の開発”, マツダ技報 No.30, pp.51-55, 2012 (in Japanese).
20. 高橋佑典: “FIT3 キャパシタ電源アイドルストップシステム”, 電気学会研究会資料, VT-14-001, pp.1-4, 2014 (in Japanese).
21. <http://ms.toyota.co.jp/jp/wec/ts040-hybrid-2014-spec.html>.

22. O. Garcia, P. Zumel, A. de Castro, and A. Cobos, "Automotive dc-dc bidirectional converter made with many interleaved buck stages," *IEEE Trans. on Power Electronics*, vol. 21, no 3, pp. 578 - 586. May 2006.
23. Liqin Ni; Patterson, D.J.; Hudgins, J.L., "A high power, current sensorless, bi-directional, 16-phase interleaved, DC-DC converter for hybrid vehicle application," *IEEE Energy Conversion Congress and Exposition (ECCE)*, 2010, pp.3611-3617, Sept. 2010.
24. K. Jin, M. Yang, X. Ruan, M. Xu, "Three-level bi-directional converter for fuel cell/battery hybrid power system," *IEEE Trans. on Industrial Electronics*, vol.57, no.12, pp.404-413, Dec. 2009.
25. Maneiro, J.; Hassan, F., "A flexible modular multi-level converter for DC microgrids with EV charging stations," *IEEE Applied Power Electronics Conference and Exposition (APEC)*, 2013, pp.1316,1320, March 2013.
26. Zhang, J.-S. Lai, R.-Y. Kim, and W. Yu, "High-power density design of a soft-switching high-power bidirectional dc-dc converters," *IEEE Trans. on Power Electronics*, vol.22, no.4, pp. 1145-1153, July 2007.
27. S. Inoue and H. Akagi, "A bidirectional dc-dc converter for an energy storage system with galvanic isolation," *IEEE Trans. on Power Electronics*, vol.22, no.6, pp. 2299-2306, December 2007.
28. G. Ma, W. Qu, G.Yu, Y. Liu, N. Liang and W. Li, "A zero-voltage-switching bidirectional dc-dc converter with state analysis and soft-switching-oriented design consideration," *IEEE Trans. on Industrial Electronics*, vol.56, no.6, pp.2174-2184, June 2009.
29. L. Gao, R. A. Dougal and S. Liu, "Power enhancement of an actively controlled battery/ultracapacitor hybrid," *IEEE Trans. on Power Electronics*, vol.20, no.1, pp.236-243, January 2005.
30. Emadi, A, Khaligh, A, Rivetta, C.H., Williamson, G.A, "Constant power loads and negative impedance instability in automotive systems: definition, modeling, stability, and control of power electronic converters and motor drives," *IEEE Trans. on Vehicular Technology*, vol.55, no.4, pp.1112-1125, July 2006.
31. Rahimi, AM., Emadi, A, "Active Damping in DC/DC Power Electronic Converters: A Novel Method to Overcome the Problems of Constant Power Loads," *IEEE Trans. on Industrial Electronics*, vol.56, no.5, pp.1428-1439, May 2009.

32. Guidi, G., Undeland, T.M., Hori, Y., "An Optimized Converter for Battery-Supercapacitor Interface," Power Electronics Specialists Conference, 2007. PESC 2007. IEEE, pp.2976-2981, June 2007.
33. Guidi, Giuseppe, Undeland, T.M., Hori, Y., "An Interface Converter with Reduced VA Ratings for Battery-Supercapacitor Mixed Systems," Power Conversion Conference - Nagoya, 2007. PCC '07, pp.936-941, 2-5 April 2007.
34. G. Guidi, "Energy Management Systems on Board of Electric Vehicles Based on Power Electronics," Doctoral theses at NTNU, 2009.
35. M. Takahashi, "Development of the "i-ELOOP" Device," Mazda Tech view, no.30, pp.43-50, 2012.
36. S. Buller, E. Karden, D. Kok, and R. W. Doncker, "Modeling the dynamic behavior of supercapacitors using impedance spectroscopy," IEEE Trans. on Industry Application, vol.38, no. 6, pp.1622-1626, Nov./Dec. 2002.
37. A. Schneuwly and R. Gallay, "Properties and applications of super capacitors: From the state-of-the-art to future trends," Proc. of PCIM 2000.
38. P. J. Grbovic, "Ultra-capacitor in power conversion system," Wiley Press, 2013.
39. www.chemi-con.co.jp/e/catalog/index.html.
40. B. E. Conway, "Electrochemical super capacitors, scientific fundamentals and technological applications," Kluwer Academic/Plenum Publisher, New York 1999.
41. Lukic, S.M., Jian Cao, Bansal, R.C., Rodriguez, F., Emadi, A., "Energy Storage Systems for Automotive Applications," IEEE Trans. on Industrial Electronics, vol.55, no.6, pp.2258-2267, June 2008.
42. Cao, J.; Emadi, A.; "A New Battery/Ultra-Capacitor Hybrid Energy Storage System for Electric, Hybrid and Plug-in Hybrid Electric Vehicles," IEEE Vehicle Power and Propulsion Conference 2009.(VPPC 09) , pp.941-946, Sept. 2009.
43. Shuai Lu, Corzine, K.A., Ferdowsi, M., "A New Battery/Ultracapacitor Energy Storage System Design and Its Motor Drive Integration for Hybrid Electric Vehicles," IEEE Trans. on Vehicular Technology, vol.56, no.4, pp.1516-1523, July 2007.
44. M. Marchesoni and C. Vacca, "New DC-DC converter for energy storage system interfacing in fuel cell hybrid electric vehicles," IEEE Trans. on Power Electron., vol. 22, no. 1, pp. 301-308, Jan. 2007.

45. M. Marchesoni and C. Vacca, "New DC–DC converter for energy storage system interfacing in fuel cell hybrid electric vehicles," *IEEE Trans. on Power Electron.*, vol. 22, no. 1, pp. 301–308, Jan. 2007.
46. Junhong Zhang; Rae-Young Kim; Jih-Sheng Lai, "High-Power Density Design of a Soft-Switching High-Power Bidirectional DC-DC Converter," *IEEE Power Electronics Specialists Conference, 2006. (PESC06). 37th*, pp.1,7, 18-22, June 2006.
47. X.Huang, T.Hiramatsu, Y.Hori, "Optimized Topology and Converter Control for Supercapacitor Based Energy Storage System of Electric Vehicles", *EVTec and APE Japan*, May 2014.
48. Thounthong, P., "Control of a Three-Level Boost Converter Based on a Differential Flatness Approach for Fuel Cell Vehicle Applications," *IEEE Trans. on Vehicular Technology*, vol.61, no.3, pp.1467-1472, March 2012.
49. Dusmez, S., Hasanzadeh, A, Khaligh, A, "Comparative Analysis of Bidirectional Three-Level DC-DC Converter for Battery/Ultracapacitor Automotive Applications," *IEEE Trans. on Industrial Electronics*, vol.61, no.9, May 2014.
50. P. J. Grbovic, P. Delarue, P. L. Moigne, and P. Bartholomeus, "A Bidirectional Three-Level DC-DC Converter for the Ultracapacitor Applications," *IEEE Trans. on Ind. Electron.*, vol. 57, no. 10, pp. 3415–3430, Oct. 2010.
51. X.Huang, T Hiramatsu, Y Hori, "Energy Management Strategy Based on Frequency-Varying Filter for the Battery Supercapacitor Hybrid System of Electric Vehicles", *27th Electric Vehicle Symposium and Exhibition, EVS-27*, Nov. 2013.
52. Curti, J.M.A., Huang, X., Minaki, R., Hori, Y., "A Simplified Power Management Strategy for a Supercapacitor/Battery Hybrid Energy Storage System using the Half-Controlled Converter", *IECON 2012*, Oct. 2012.
53. Huang Xiaoliang, Curti, J.M.A, Hori, Y., "Energy management strategy with optimized power interface for the battery supercapacitor hybrid system of Electric Vehicles," *Industrial Electronics Society, 39th Annual Conference of the IEEE, IECON 2013*, pp.4635-4640, Nov. 2013.
54. http://en.wikipedia.org/wiki/New_European_Driving_Cycle.
55. Hori, Y., "Novel EV society based on motor/ capacitor/ wireless — Application of electric motor, supercapacitors, and wireless power transfer to enhance operation of future vehicles," *Microwave Workshop Series on Innovative Wireless Power Transmission: Technologies, Systems, and Applications (IMWS), 2012 IEEE MTT-S International*, pp.3-8, 10-11 May 2012.

56. Li, S., Mi, C., "Wireless Power Transfer for Electric Vehicle Applications," IEEE Journal of Emerging and Selected Topics in Power Electronics, 2014.
57. Chopra, S., Bauer, P., "Driving Range Extension of EV With On-Road Contactless Power Transfer—A Case Study," IEEE Trans. on Industrial Electronics, vol.60, no.1, pp.329-338, Jan. 2013.
58. Y. Moriwaki, T. Imura, and Y. Hori, "Basic study on reduction of reflected power using DC/DC converters in wireless power transfer system via magnetic resonant coupling," in 2011 IEEE 33rd International Telecommunications Energy Conference (INTELEC), 2011.
59. M. Kato, T. Imura, and Y. Hori, "Study on Maximize Efficiency by Secondary Side Control Using DC-DC Converter in Wireless Power Transfer via Magnetic Resonant Coupling," 27th Electric Vehicle Symposium and Exhibition, EVS-27, Nov. 2013.
60. T.Hiramatsu, X.Huang, Y.Hori, "Capacity design of super capacitor battery hybrid energy system with repetitive charging via wireless power transfer", 2014 IEEJ Technical Meetings of Vehicle Technology (IEEJ-VT-14-006), Feb. 2014. (in Japanese).

Publications

Journal papers

1. Huang Xiaoliang, Hori Yoichi, “Power flow control of supercapacitor battery hybrid energy system with half-controlled power interface for EV application”, *Journal of Power Electronics*, (submitted)
2. Huang Xiaoliang, Yoichi Hori, “Controllable power maximum efficiency wireless charging Interface for EV hybrid energy system”, to be submitted to *IEEE trans. on Power Electronics*, (in preparation)

Conference papers

1. Huang Xiaoliang, J. Marcus Curti, Yoichi Hori, “Energy management strategy with optimized power interface for the battery supercapacitor hybrid system of electric vehicles”, The 39th Annual Conference of IEEE Industrial Electronics Society (IECON2013), 2013.11
2. Huang Xiaoliang, Toshiyuki Hiramatsu, Yoichi Hori: “Energy management strategy based on frequency-varying filter for the battery supercapacitor hybrid system of electric vehicles”, The 27th Electric Vehicle Symposium and Exhibition (EVS27), 2013.11
3. Huang Xiaoliang, Toshiyuki Hiramatsu, Yoichi Hori, “Optimized topology and converter control for supercapacitor based energy storage system of electric vehicles”, EVTeC & APE Japan 2014, 2014.7
4. Huang Xiaoliang, Yoichi Hori, “System design and converter control for supercapacitor and battery hybrid energy system of compact electric vehicles”, The 16th Conference on Power Electronics and Applications, EPE’14-ECCE Europe (EPE14), 2014.8
5. Huang Xiaoliang, Yoichi Hori, “Bidirectional power flow control for battery supercapacitor hybrid energy system for electric vehicles with in-wheel motors”, The 16th International Power Electronics and Motion Control Conference and Exposition (PEMC 2014). 2014.9

Proceeding papers

1. Huang Xiaoliang, J. Marcus Curti, Yoichi Hori, “Power management of hybrid energy system for electric vehicles by converter control of super capacitor bank,” Proc. the 13th SNU-UT Joint Seminar, 2013.3

Co-authored papers

1. J.M.A Curti, X. Huang, R. Minaki, Y. Hori, “A simplified power management strategy for a supercapacitor/ battery hybrid energy storage system using the half-controlled converter”, The 38th Annual Conference of IEEE Industrial Electronics Society (IECON 2012), 2012.10
2. Rached Dhaouadi, Yoichi Hori, Huang Xiaoliang, “Robust control of an ultracapacitor-based hybrid energy storage system for electric vehicles”, The 13th International Workshop on Advanced Motion Control (AMC 2014), 2014.3
3. Toshiyuki Hiramatsu, Huang Xiaoliang, Yoichi Hori, “Capacity design of supercapacitor battery hybrid energy system with repetitive charging via wireless power transfer”, The 16th International Power Electronics and Motion Control Conference and Exposition (PEMC 2014), 2014.9
4. Toshiyuki Hiramatsu, Huang Xiaoliang, Yoichi Hori, “Capacity design of supercapacitor battery hybrid energy system with repetitive charging via wireless power transfer”, 2014 IEEJ Technical Meetings of Vehicle Technology (IEEJ-VT-14-006), 2014.2 (in Japanese)
5. J.M.A Curti, X. Huang, Y. Hori, “Applying Sliding Mode Control for Half-Controlled Converter”, 2013 Proc. IEEJ Technical Meeting (IEEJ-IIC-13-140), 2013.3 (in Japanese)

- THE END -

A BEGINNING...